U.S.NRC

United States Nuclear Regulatory Commission

Protecting People and the Environment

MELCOR Best Practices as Applied in the State-of-the-Art Reactor Consequence Analyses (SOARCA) Project

Office of Nuclear Regulatory Research

AVAILABILITY OF REFERENCE MATERIALS
IN NRC PUBLICATIONS

NRC Reference Material

As of November 1999, you may electronically access NUREG-series publications and other NRC records at NRC's Public Electronic Reading Room at http://www.nrc.gov/reading-rm.html. Publicly released records include, to name a few, NUREG-series publications; *Federal Register* notices; applicant, licensee, and vendor documents and correspondence; NRC correspondence and internal memoranda; bulletins and information notices; inspection and investigative reports; licensee event reports; and Commission papers and their attachments.

NRC publications in the NUREG series, NRC regulations, and Title 10, "Energy," in the *Code of Federal Regulations* may also be purchased from one of these two sources.
1. The Superintendent of Documents
   U.S. Government Printing Office
   Mail Stop SSOP
   Washington, DC 20402–0001
   Internet: bookstore.gpo.gov
   Telephone: 202-512-1800
   Fax: 202-512-2250
2. The National Technical Information Service
   Springfield, VA 22161–0002
   www.ntis.gov
   1–800–553–6847 or, locally, 703–605–6000

A single copy of each NRC draft report for comment is available free, to the extent of supply, upon written request as follows:
Address: U.S. Nuclear Regulatory Commission
         Office of Administration
         Publications Branch
         Washington, DC 20555-0001
E-mail: DISTRIBUTION.RESOURCE@NRC.GOV
Facsimile: 301–415–2289

Some publications in the NUREG series that are posted at NRC's Web site address http://www.nrc.gov/reading-rm/doc-collections/nuregs are updated periodically and may differ from the last printed version. Although references to material found on a Web site bear the date the material was accessed, the material available on the date cited may subsequently be removed from the site.

Non-NRC Reference Material

Documents available from public and special technical libraries include all open literature items, such as books, journal articles, transactions, *Federal Register* notices, Federal and State legislation, and congressional reports. Such documents as theses, dissertations, foreign reports and translations, and non-NRC conference proceedings may be purchased from their sponsoring organization.

Copies of industry codes and standards used in a substantive manner in the NRC regulatory process are maintained at—
         The NRC Technical Library
         Two White Flint North
         11545 Rockville Pike
         Rockville, MD 20852–2738

These standards are available in the library for reference use by the public. Codes and standards are usually copyrighted and may be purchased from the originating organization or, if they are American National Standards, from—
         American National Standards Institute
         11 West 42nd Street
         New York, NY 10036–8002
         www.ansi.org
         212–642–4900

MELCOR Best Practices as Applied in the State-of-the-Art Reactor Consequence Analyses (SOARCA) Project

Prepared by:
Kyle Ross*, Jesse Phillips*, Randall O. Gauntt*,
Kenneth C. Wagner**

*Sandia National Laboratories
 Albuquerque, New Mexico 87185
 Operated for the U.S. Department of Energy

**dycoda, LLC

ABSTRACT

The modeling approach used in the State-of-the-Art Reactor Consequence Analyses (SOARCA) project to characterize the release of radionuclides to the environment accompanying a postulated severe (core damage) accident is based on plant-specific applications of the MELCOR computer code. MELCOR is a state-of-the-art computational model developed by Sandia National Laboratories for the U.S. Nuclear Regulatory Commission. Due to large uncertainties in many aspects of severe accident behavior, MELCOR provides the code user a wide spectrum of options for modeling uncertain physical phenomena and characterizing plant response to beyond design basis accident conditions. The selection and exercise of the available modeling capabilities are an important aspect of the overall modeling approach.

This document describes the specific manner in which MELCOR modeling capabilities were used to represent important, and in some cases uncertain, aspects of severe accident behavior in the SOARCA project. This description includes choices made among alternate modeling options offered through code input, changes to selected input parameters from those offered as 'default' values, and in some cases, user-generated 'models' to represent features of plant response to a severe accident that are not directly available in MELCOR. Collectively, these features represent the "SOARCA best practice" guidance for using MELCOR to calculate severe accident behavior in operating nuclear power plants.

TABLE OF CONTENTS

LIST OF FIGURES

LIST OF TABLES

EXECUTIVE SUMMARY

The purpose of this report is to describe best practices for the MELCOR severe accident analysis code, as implemented in the State-of-the-Art Reactor Consequence Analyses (SOARCA) project for the Peach Bottom Atomic Power Station and Surry Power Station. By applying modern analysis tools and techniques in the SOARCA project, a body of knowledge regarding the realistic outcomes of severe reactor accidents has been developed through the integrated modeling of accident progression and offsite consequences. The SOARCA project provides analyses that use state-of-the-art source term and consequence modeling together with consideration of current operational practices and procedures. Collectively, this information represents the "best practice" modeling approach for MELCOR accident progression and source term analyses.

The objective of this report is to describe the best practices, which are comprised of the model improvements, modeling approach, and parameter selections, that support the best-estimate analyses in NUREG-1935 [1], NUREG/CR-7110 Volume 1 [62], and NUREG/CR-7110 Volume 2 [63]. This best practices document provides a compilation of the parameters and inputs used in the SOARCA documents. It also includes additional detail on the approach to developing some of the input values and methodologies applied in the SOARCA studies. This document explains the significance of key modeling improvements and presents a review of the validation and phenomena modeling to support the application of MELCOR. This report is intended to provide guidance and insights for developers and users of MELCOR.

An accumulation of various efforts, including an expert review panel conducted in August 2006 and peer review committee meetings during 2009-2011 as well as 25 years of research into severe accident phenomenology and security related mitigation improvements, has been utilized in codifying both the depiction of the facilities investigated and the current knowledge of severe accident phenomena. The entire body of code input reflects the informed judgment on how a MELCOR model should be configured to generate a realistic estimate of plant response to a severe accident. This information as well as its implementation represents the best practice modeling approach used in the SOARCA project for the severe accident progression and radionuclide source term calculations.

The best practice modeling features, described herein, fall into two broad categories, input controls impacted by the user and modifications and enhancements made to MELCOR in support of the SOARCA project.

1. General user input categorizes all input options exercised by the user to perform the following functions:

    a. Specification of parameters which are not equivalent to the default value, typically performed for sensitivity coefficients;

    b. Model selection from the available models within MELCOR; and

    c. Development of model logic to characterize systems and procedures whereby an internal MELCOR model does not exist or is replaced.

2. MELCOR modifications categorize advanced modeling features incorporated into the MELCOR source code to accommodate necessary enhancements for the SOARCA project.

In addition to the best practices detailed within this document, the continued improvement in computing resources permits improved fidelity in the physical representation of nuclear power reactors and their associated systems. The spatial nodalization of the reactor pressure vessel, primary coolant system, and containment in the MELCOR models developed for pressurized water reactors (PWRs) and boiling water reactors (BWRs) recognizes much more geometric detail. For example, the entire PWR reactor coolant system (RCS) was represented by four spatial regions in the NUREG-0772, "Technical Bases for Estimating Fission Product Behavior During LWR Accidents," calculations. The MELCOR model of the same 3-loop Westinghouse PWR used in the SOARCA analysis uses 25 control volumes for the core region alone; over 100 control volumes are used to represent the entire RCS. This dramatic increase in detail provides much greater resolution of the driving forces governing fission product transport and deposition and establishes a best practice with regard to model detail.

The SOARCA project evaluated plant improvements and changes not reflected in earlier NRC publications including system improvements, improvements in training, emergency procedures, offsite emergency response, security-related improvements, and plant changes such as power uprates and higher core burnup. Given the advancement in severe accident analyses afforded by conducting the SOARCA project, an opportunity to investigate accident phenomena at a much greater level of detail was available than analyses performed in the past, which has promoted recognition of various insights which benefit the probabilistic risk assessment (PRA) community. As these insights can be contributed to the implementation of best practices in the SOARCA project, they are presented as well; a select few are presented below. A more detailed listing is provided in the body of this document.

1. In the Surry station blackout (SBO) scenarios, the most likely first RCS failure occurs at the hot leg nozzle prior to significant in-vessel fuel damage. This leads to vessel depressurization, accumulator discharge, fuel cooling, and an interruption to the core heat-up. A new release pathway for radionuclides is established at the failed hot leg. The response of a thermally-induced steam generator tube rupture (TISGTR) is also impacted by hot leg failure. The hot leg failure substantially decreases TISGTR flow due to the RCS depressurization and the introduction of the larger failure location as the primary fission product pathway from the vessel.

2. With regard to the interfacing systems loss of coolant accident (ISLOCA) modeling and the magnitude of predicted radionuclide releases to the environment, a key insight is the large amount of deposition of aerosolized radionuclides in the low head safety injection (LHSI) piping by means of turbulent deposition. Sustained high velocities in the LHSI piping during core degradation drive the importance of this phenomenon. A thorough representation of the LHSI piping is necessary to address turbulent deposition of fission product aerosols in the piping and revaporization of deposits.

3. The improvements to fuel degradation modeling and 2-dimensional core modeling show a delayed heat-up followed by accelerated oxidation. The accelerated oxidation phase ends following molten Zircaloy breakout. Without molten Zircaloy breakout, the subsequent heat-up is primarily controlled by decay heat. The best practice modeling of Zircaloy-oxide collapse creates a debris bed similar to Three Mile Island Unit 2 (TMI-2). The debris bed slows oxidation by creating blockages and inhibiting natural circulation. The debris bed gradually grows axially and radially, which eventually leads to core plate failure.

ACKNOWLEDGMENTS

ABBREVIATIONS AND ACRONYMS

ABCOVE	Aerosol Behavior Code Validation and Evaluation
ACRR	Annular Core Research Reactor
AHMED	Aerosol and Heat Transfer Measurement Device
ANL	Argonne National Laboratory
BWR	Boiling Water Reactor
CCFL	Counter-Current Flow Limitation
CFD	Computational Fluid Dynamics
COR	Core (or Core Package)
CSARP	Cooperative Severe Accident Research Program
CSE	Containment Systems Experiment
CVTR	Carolinas-Virginia Tube Reactor
CWTI	Corium-Water Thermal Interactions
DCH	Direct Containment Heating
DEMONA	Demonstration of Nuclear Aerosol Behavior
DOE	U.S. Department of Energy
EMUG	European MELCOR User Group
EPRI	Electric Power Research Institute
FLECHT	Full-Length Emergency Cooling Heat Transfer
FP	Fission Product
GE	General Electric
GRS	Gesellschaft fur Anlagen- und Reaktorsicherheit mbH
HDR	Heissdampfreaktor
HHSI	High Head Safety Injection
HI	Horizontal Induction
HPME	High Pressure Melt Ejection
IBRAE	Nuclear Safety Institute of the Russian Federation
IET	Integral Effects Test
IPEEE	Individual Plant Examination for External Events
ISLOCA	Interfacing Systems Loss of Coolant Accident
ISP	International Standard Problem
JAERI	Japan Atomic Energy Research Institute
LACE	Light Water Reactor Aerosol Containment Experiment
LHF	Lower Head Failure
LHSI	Low Head Safety Injection
LPRM	Local Power Range Monitor
LOCA	Loss of Coolant Accident
LOFT	Loss-of-Fluid Test
LTSBO	Long-Term Station Blackout
LWR	Light Water Reactor
MAAP	Modular Accident Analysis Program
MACCS	MELCOR Accident Consequence Code System
MACE	Melt Attack and Coolability Experiments
MAEROS	Multi-Component Aerosol Module for CONTAIN
MCAP	MELCOR Code Assessment Program
MCCI	Molten Core Concrete Interaction
MEI	Moscow Power Engineering Institute
MSLB	Main Steam-Line Break
NRC	U.S. Nuclear Regulatory Commission
NTS	Nevada Test Site

NUPEC	Nuclear Power Engineering Corporation
OECD	Organization for Economic Co-operation and Development
ORNL	Oak Ridge National Laboratory
PBF	Power Burst Facility
PNL	Pacific Northwest National Laboratory
PORV	Power-Operated Relief Valve
PRA	Probabilistic Risk Assessment
PRC	Peer Review Committee
PWR	Pressurized Water Reactor
RAMCAP	Risk Analysis and Management for Critical Asset Protection
RAS	Russian Academy of Science
RCS	Reactor Coolant System
RHR	Residual Heat Removal system
RN	Radionuclide Package
RPV	Reactor Pressure Vessel
RTF	Radioiodine Test Facility
RWST	Refueling Water Storage Tank
SBO	Station Blackout
SEASET	Systems Effects And Separate Effects Test
SFD	Severe Fuel Damage
SFP	Sandia Fuel Project
SG	Steam Generator
SNAP	Symbolic Nuclear Analysis Package
SNL	Sandia National Laboratories
SOARCA	State-of-the-Art Reactor Consequence Analyses
SPARC	Suppression Pool Aerosol Removal Code
SQA	Software Qualification Assurance
SST	Siting Source Term
STCP	Source Term Code Package
SURC	Sustained Urania-Concrete
SV	Safety Valve
TISGTR	Thermally-Induced Steam Generator Tube Rupture
TIP	Traversing In-core Probe
TMI-2	Three Mile Island Unit 2
VANAM	Experiments on the Aerosol Behavior within a Multi-Compartment Containment (German translation)
VI	Vertical Induction

1. INTRODUCTION

The evaluation of accident phenomena and the offsite consequences of severe reactor accidents has been the subject of considerable research by the U.S. Nuclear Regulatory Commission (NRC) and others over the last several decades. As a result of this research focus, analyses of severe accidents at nuclear power reactors are more detailed, integrated, and realistic than at any time in the past. A desire to leverage this capability to reexamine significantly less realistic aspects of previous reactor accident analysis efforts was a major motivating factor in the genesis of the State-of-the-Art Reactor Consequence Analyses (SOARCA) project. By applying modern analysis tools and techniques, the SOARCA project seeks to provide a body of knowledge that will support an informed public understanding of the likely outcomes of selected severe nuclear reactor accidents.

The overall objective of the SOARCA project was to develop a body of knowledge regarding the realistic outcomes of severe reactor accidents. To accomplish this objective the SOARCA project has utilized state-of-the-art computational analysis tools, which incorporate knowledge gained from the past 25 years of research. These tools require a large amount of input data by the code user to describe the physical configuration of the plant and to describe user preferences among alternate modeling options for uncertain severe accident phenomena. Furthermore, the code also accepts certain types of user input that adds new modeling features to a MELCOR calculation. For example, user defined functions, which operate on specific time-dependent variables exposed to the user, and which can be used to specify boundary conditions or to control the operation of various objects defined in the user model; the results of these logic and arithmetic operations can be included to define the response of specific plant components or systems to changes in thermodynamic or other environmental conditions that might occur during a particular calculation. The entire body of code input reflects the informed judgment of the code user on how a MELCOR model should be configured to generate a realistic estimate of plant response to a severe accident. Collectively, this information represents the "best practice" modeling approach for using MELCOR in performing severe accident progression and radionuclide source term calculations.

This report documents the best practice approach for performing MELCOR calculations for the SOARCA project. Section 2 describes the overall technical approach used in the current analysis and compares it to the technical approach used in the analyses documented in NUREG/CR-2239, "Technical Guidance for Siting Criteria Development" [45]. Section 3 describes the specific modeling practices used to develop and exercise the MELCOR models of pressurized water reactor (PWR) and boiling water reactor (BWR) plants examined in this study. Section 4 presents a discussion on MELCOR validation. Finally, Section 5 presents an accounting of several insights realized from analyses utilizing the best practices.

1.1   Background

MELCOR [2] is a fully integrated, engineering-level computer code that models the progression of severe accidents in light-water reactor nuclear power plants. MELCOR is developed at Sandia National Laboratories (SNL) for the NRC as a second-generation plant risk assessment tool and the successor to the Source Term Code Package. A broad spectrum of severe accident phenomena in both boiling and pressurized water reactors is treated in MELCOR in a unified framework. These include thermal-hydraulic response in the reactor coolant system (RCS), reactor cavity, containment, and confinement buildings; core heat-up, degradation, and relocation; core-concrete attack; hydrogen production, transport, and combustion; fission product release and transport behavior.

Modifications were made to the code throughout the SOARCA studies leading to enhanced user options. To take advantage of the modifications discussed throughout the report, MELCOR version 1.8.6 subversion 3870 or later will be required. Many of the code modifications and the inclusion of new models were available in versions prior to subversion 3870; however, subversion 3870 was employed for the last SOARCA simulations. Continual code development is ongoing; therefore, confirmation of default user input and models should be performed by analysts hoping to employ the practices discussed herein.

1.2 Objective

The objective of this report is to describe the best practices, which are comprised of the model improvements, modeling approach, and parameter selections, that support the analyses in NUREG-1935 [1], NUREG/CR-7110 Volume 1 [62], and NUREG/CR-7110 Volume 2 [63]. This document also explains the significance of key modeling improvements and presents a review of the validation and phenomena modeling to support the application of MELCOR.

1.3 Independent Peer Review

Two independent review groups were established for the SOARCA project. The first group was an expert panel convened in a public meeting forum August 21-24, 2006. The purpose of the meeting was to determine whether the MELCOR and MELCOR Accident Consequence Code System (MACCS) modeling approaches were consistent with the project objectives to use state-of-the-art modeling with emphasis on realism in phenomenological and system treatments. The review was conducted by two panels drawn from the nuclear industry, the U.S. Department of Energy (DOE) national laboratory complex, and Gesellschaft fur Anlagen- und Reaktorsicherheit mbH (GRS), with recognized expertise in the MELCOR and MACCS numerical simulation tools. Observations and recommendations specific to each model were provided. The experts found the MELCOR code and the proposed approach for application of the codes (i.e., best practices) to be generally appropriate for performing realistic predictions of accident progression and source term for the SOARCA project. A summary of the expert review panel's findings may be found in "State-of-the Art Reactor Consequence Analyses (SOARCA) Project MELCOR Modeling Practices Review" [4].

The second review was conducted by a formal peer review committee (PRC) of internationally renowned experts established in 2009-2011 to evaluate and suggest improvements to the SOARCA project. The PRC evaluated the project approach, assumptions, results, and conclusions. To support the peer review, a series of PRC meetings were held where NRC and SNL staff presented technical details regarding the MELCOR accident progression modeling and MACCS consequence modeling. The PRC was provided draft documents for review prior to the meetings. Technical discussions were conducted on all major topics such as the accident sequence selection and screening process, seismic analysis, emergency response, offsite consequences, and code validation.

The PRC reviewed the modeling approach, parameter development, parameter selection, and consequence results. The PRC provided insights and identified gaps and issues for consideration throughout the project. The final letter of each PRC member is provided in Appendix B to NUREG-1935 [1]. This MELCOR best practices document was not included in the PRC review because it was completed after the publication of the SOARCA project primary documentation: NUREG-1935 and NUREG/CR-7110 Volumes 1 and 2.

2. TECHNICAL APPROACH

The technical approach used to calculate radionuclide release to the environment (i.e., the "source term") accompanying credible, but very low frequency accident scenarios relies on the application of the MELCOR computer code [2], which was specifically designed to calculate reactor and containment system response to postulated severe accidents. The technical approach for evaluating the consequences arising from the release of radioactive material to the environment involves a separate computer code (i.e., MACCS), which is described in a separate report [3]. Key differences in the approach used in the SOARCA project from those used in past nuclear reactor radiological consequence calculations are described in Section 2.2.

2.1 Analytical Models

The technical approach that was adopted to define the quantitative characteristics of radiological release to the environment was to calculate temporal changes in reactor and containment conditions using MELCOR Version 1.8.6. MELCOR is a large, integrated computer code developed at SNL under the direction of the NRC and the joint sponsorship of international members of the Cooperative Severe Accident Research Program (CSARP). The code is "integrated" in the sense that it combines analytical models for a wide-spectrum of physical processes (previously evaluated as separate disciplines) into a single, numerically-coupled simulation. Among the technical disciplines addressed by MELCOR are:

- thermal-hydraulic response of the RCS and containment to the postulated accident scenario,

- fuel (core) heat-up and physical degradation due to melting and loss of mechanical strength,

- fission product release from fuel, and

- transport of fission products (in vapor or aerosol form) away from the core, through the RCS and containment, to the environment.

Critical to quantitative evaluation of these disciplines are mathematical models for complex physical processes, such as: changes in the physical state (morphology) of core materials, generation and combustion of hydrogen as a byproduct of the oxidation of metallic components in the core, the erosion of concrete in regions of the containment under the reactor pressure vessel due to chemical decomposition by molten core debris, and mechanical failure of major structural barriers to fission product release (such as the reactor pressure vessel and containment). The MELCOR Reference Manual [64] provides a detailed accounting and description of these models. The information contained in this document is designed as a companion to the MELCOR code manuals, and provides a brief description of the way in which MELCOR models were used to represent aspects of nuclear power plant behavior during a severe accident that are (a) difficult to predict with high confidence due to uncertainties in their governing phenomena and (b) whose outcome is important to calculated results. Major uncertainties in MELCOR models for accident progression were addressed in two steps. First, the accident progression analysts developed a list of uncertain phenomena that can have a significant effect on the progression of the accident. Second, alternate ways of addressing each phenomenon were considered and a 'best-estimate' approach was developed by applying appropriate and available modeling tools in MELCOR. Calculations performed using the best-estimate approach are referred to in this document as the 'base case' analysis, and the manner

in which MELCOR models and input parameters were configured to represent uncertain and important events and processes is described in Section 3.

2.2   Important Differences in Approach from Prior Work

Radiological source terms to the environment used in NUREG/CR-2239, "Technical Guidance for Siting Criteria Development," were developed from early research on severe accident behavior that followed the publication of WASH-1400 in 1975 and the accident at Three Mile Island Unit 2 (TMI-2) in 1979. This research was initiated to develop predictive methods for calculating fission product release and transport during a wide spectrum of postulated accident sequences involving substantial damage to fuel in the reactor core. Results of this work were documented in NUREG-0772 [5], which was published in 1981.

The analysis methods used to generate the 'Siting Source Terms' (SSTs) used in NUREG/CR-2239 involved the manual integration of calculations from several computer codes, as illustrated in Figure 2-1. Each code examined a particular portion of the overall analysis, such as RCS thermal-hydraulic response, core heat-up and 'meltdown' (MARCH), fission product transport and deposition in the RCS (TRAP-MELT) and fission product retention in the containment before release to the environment (CORRAL, NAUA, etc.)[1]. The central element of this calculation scheme was the TRAP computer code, which used estimates of fluid velocities and RCS surface temperatures calculated by MARCH, combined with formulas for vapor and aerosol deposition rates, to characterize the extent to which fission products 'plate out' on RCS surfaces before being carried to the containment. Similar information regarding flow rates and temperatures in the containment were used to estimate deposition on containment surfaces[2].

Several major simplifications were involved in the NUREG-0772 calculations that have been eliminated in the current approach. Among the most important of these are the following:

- The source term analysis tools illustrated in Figure 2-1 represent a linear progression of calculations, in which results of one calculation become 'input' to a subsequent calculation. As a result, physical dependencies between processes modeled in different codes can only be represented in one direction. Feedback mechanisms are not directly treated. For example, decay heating of surfaces in the RCS or containment due to deposited radionuclides was not addressed in the MARCH calculation of RCS thermal-hydraulic response. As a result, long-term revaporization of fission products from surfaces was not addressed as a late release mechanism.

  In contrast, models for the processes governing severe accident progression and radionuclide release/transport are arranged into an integrated set of computational modules in MELCOR, which are solved in a single computational framework. Interdependencies among diverse phenomena are captured directly in the numerical solution.

- In the early NUREG-0772 approach, the release of fission products from fuel was not integrally linked to the calculation of time-dependent changes in fuel temperatures by the MARCH code. Results of the MARCH calculations were used to inform the analysts

---

[1] A description of these codes can be found in references cited in NUREG-0772.
[2] The code system used to perform the calculations documented in NUREG-0772 developed later into the 'Source Term Code Package' (STCP), which was the predecessor of MELCOR as the NRC's principal tool for severe accident analysis.

about the time at which fuel failure would be expected to begin for a particular accident sequence, but fission product release rates were not explicitly (numerically) coupled to the calculated fuel temperature history. Rather, an average (constant) release rate was defined as input to the TRAP-MELT calculations based on limited data from early experimental measurements. Distinct release rates were defined for iodine, cesium, and (collectively) all other particulate matter.

In contrast to this simplified approach, MELCOR calculates time-dependent release rates for fission products from the core, based on a validated correlation of fission product release rate and the temperature history calculated at 50 distinct regions of fuel assemblies (five radial rings and ten axial levels).[3]

```
                                    ┌─────────────────────┐
                                    │      ORIGEN         │
                                    │                     │
                                    │  Core Inventory of  │
                                    │ Radioactive Material│
                                    └─────────────────────┘
                                              │
                    ┌─────────────────┐   ┌ ─ ─ ─ ─ ─ ─ ─ ─ ─ ─┐
                    │     MARCH       │     Fission Product Release
                    │                 │   │  Rate from Fuel     │
                    │Thermal Response │     ─ ─ ─ ─ ─ ─ ─ ─ ─ ─ 
                    │of Reactor &     │   └ ─ ─ ─ ─ ─ ─ ─ ─ ─ ─ ┘
                    │Containment      │              │
                    └─────────────────┘   ┌─────────────────────┐
                                          │     TRAP-MELT       │
                                          │                     │
                                          │Primary Coolant System│
                                          │ Transport & Retention│
                                          └─────────────────────┘
                                                     │
                                          ┌─────────────────────┐
                                          │   CORRAL, NAUA,     │
                                          │  HAARM-3, QUICK     │
                                          │                     │
                                          │Transport of Vapor & Aerosols│
                                          │in the Containment Atmosphere│
                                          └─────────────────────┘
                                                     │
                                          Release of Radioactive
                                          Aerosol & Vapor to the
                                                Environment
                                              (Source Term)
```
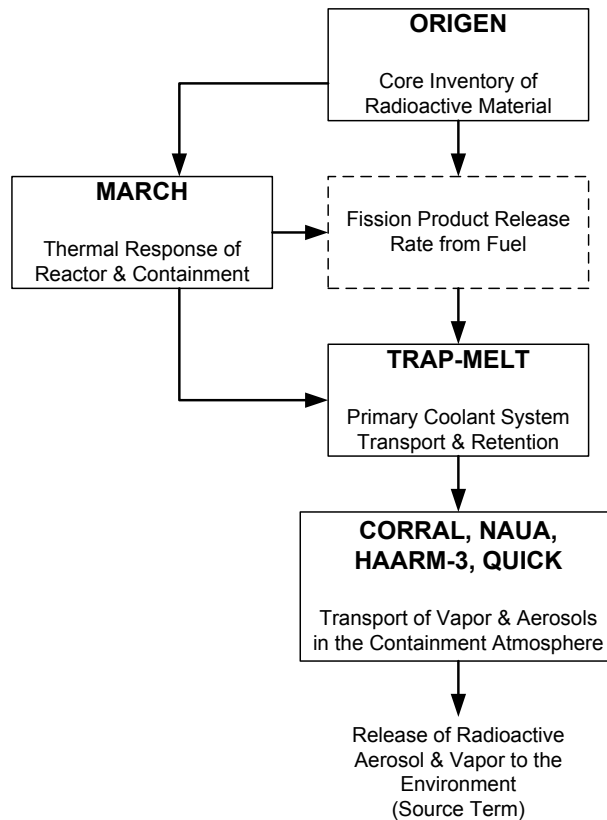
Figure 2-1   Computational methods used to derive source terms in NUREG-0772

- For the NUREG-0772 analyses, a linear series of control volumes (each with internal surfaces) was used to represent fission product transport and deposition within the primary coolant system. Fission product retention in the containment was calculated by applying a variety of computational models to the entire containment free volume, which account for various aerosol and vapor deposition and attenuation mechanisms. An illustration of a typical nodalization scheme used for the TRAP-MELT calculation of RCS retention is shown in Figure 2-2.

---

[3] Previous MARCH results were limited to fewer nodes and a one-dimensional thermal-hydraulic representation of the core because of storage and computer runtime limitations.   It led to a more coherent melt, which was contrary to the end-state of the TMI-2 accident.

In contrast, the spatial nodalization of the reactor pressure vessel, primary coolant system, and containment in the MELCOR models developed for the SOARCA project recognizes much more geometric detail. For example, the entire PWR RCS was represented by four spatial regions in the NUREG-0772 calculations. The MELCOR model of the same 3-loop Westinghouse PWR used in the current Surry analysis uses 25 control volumes for the core region alone; over 100 control volumes are used to represent the entire RCS. This dramatic increase in detail provides much greater resolution of the driving forces governing fission product transport and deposition. In particular, local fluid velocities and temperatures, structural surface temperatures and associated temperature gradients are all calculated in greater detail than was available or practical at the time of the analyses supporting NUREG/CR-2239.

Release Pathway for
PWR Cold Leg LOCA

Release Pathway for
BWR ATWS
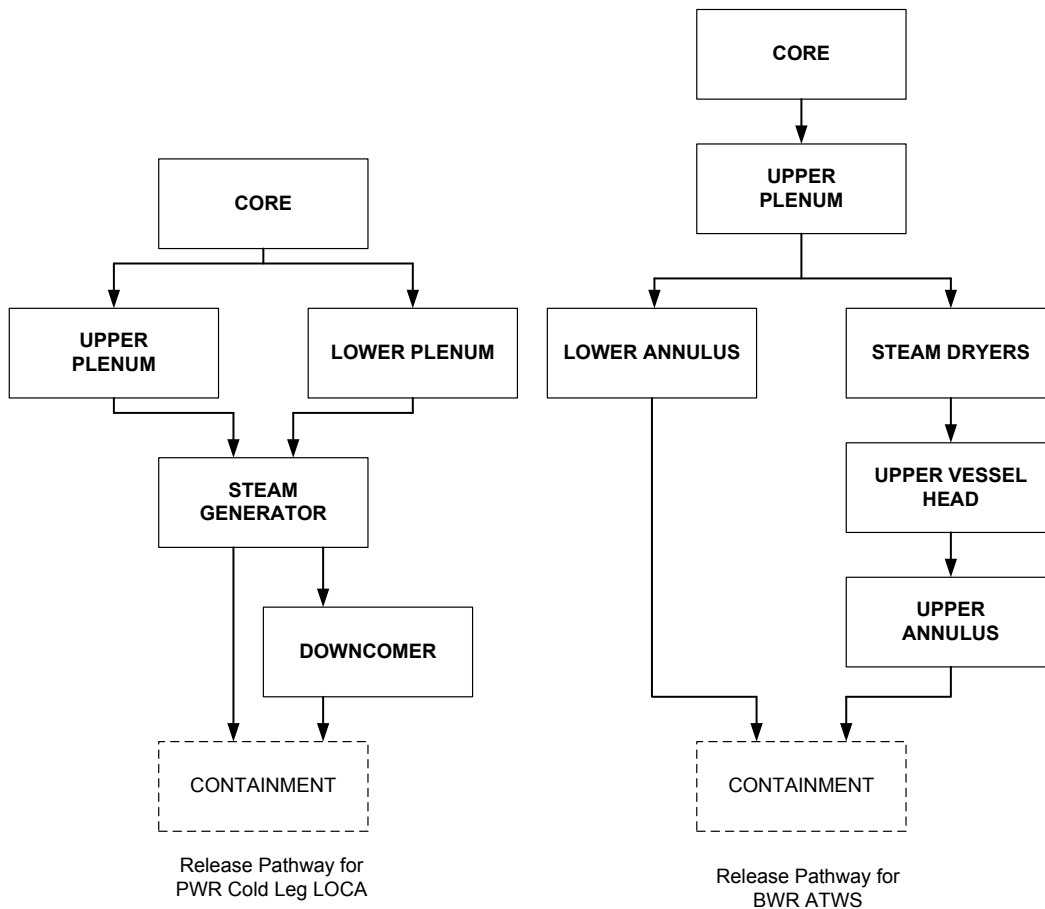
Figure 2-2   Typical spatial nodalization of RCS in the NUREG-0772 methodology

3.   MELCOR BEST PRACTICES FOR SEVERE ACCIDENT ANALYSIS

This section describes the MELCOR best practices used in the SOARCA scenarios selected for the Peach Bottom and Surry Nuclear Power Stations. The detailed approach to modeling all phenomena governing fuel damage, fission product release, and other aspects of plant response to postulated severe accident is not provided here. Rather, a small subset, focused on the best practices of the large body of important phenomena, is addressed. The basic selection criteria applied to determine which phenomena or modeling practices were included in the discussion were the following:

- was the phenomenon or event an important contributor to the progression of the accident,

- was uncertainty perceived in the system response to the phenomenon or event, and

- was the phenomenon or event addressed in the calculation by user generated models or input that differed from the default input parameters.

Although many of the practices described in this section are expressed in terms of their implementation into MELCOR models specifically developed for the SOARCA project, they involve phenomenological considerations and uncertainties that have broader applicability.

The best practice modeling features described in this chapter fall into two primary categories, user input and hard-coded modifications to the MELCOR source code.

1.   User input is a broad category encompassing severe accident modeling features that are controlled or influenced by the user through input file modifications. Modeling practices within this category can take several forms depending on the specific type of user input used to influence or define a MELCOR model. The best practice user input guidance is documented in Section 3.1.

   a.   Sensitivity coefficients are an inherent form of user input, native to MELCOR, which permit a large variety of modifications which establish the methodology for performing the simulation. These parameters span a wide spectrum from coefficients of heat transfer correlations to numerical convergence criteria. In general, the default values for the sensitivity coefficients represent best-estimate settings and are not typically changed.

   b.   Model selection is an additional form of user input. The user input identifies the desired model among the available MELCOR options. An example of this form of user influenced modeling practice is the correlation used to calculate the release rate of fission products from over-heated fuel. MELCOR offers several types of correlations, and the user must select one.

   c.   A third form of user influence on a MELCOR calculation is an analytical expression or implementation logic developed by the user (typically via control functions) to represent an aspect of severe accident progression that is not directly represented as a 'model' within MELCOR. An example of this type of modeling practice is a user-specified correlation or condition that determines if, and when, a particular component would fail to function. Failure of a safety/relief

valve to reclose due to repeated cycles, or enhanced leakage through an over-heated reactor coolant pump seal would fall into this category.

2.   A second broad category of changes to MELCOR modeling practices involve changes to the MELCOR source code (Fortran) to accommodate advanced modeling needs for the SOARCA project. In some cases, these changes codified modeling practices that had been implemented through user input in many past NRC applications of MELCOR. Incorporating the user generated input directly into the code simplified user input and enhanced the fidelity of the modeling practice among MELCOR models for various nuclear power plants. Enhancements to the MELCOR source code that were implemented as part of the SOARCA project are described in Section 3.2.

The best practices documented within this report typify general user input methodologies for which the reader must appropriately incorporate for their specific application. The implementation of these modeling practices in a plant-specific MELCOR model depends on the details of that model and is not described in this report. Important modeling details, including possible deviations from best practice, are provided in the documentation associated with the plant-specific MELCOR models developed for use in the SOARCA project.

3.1   Best Modeling Practices

Several of the modeling practices that are defined or controlled by user input are applied in calculations of severe accident progression for a PWR or BWR. Others are specific to one design or the other. Generic modeling practices (i.e., those applicable to both designs) are described in Section 3.1.1. PWR- and BWR-specific modeling practices are then described in Sections 3.1.2 and 3.1.3, respectively. The recommended best modeling practices described in Sections 3.1.1 through 3.1.3 were presented and reviewed by an independent expert panel. In addition to the best modeling practices described in Sections 3.1.1 through 3.1.3, other best modeling practices that were less important or had less uncertainty in their implementation are simply outlined in Appendix A.

3.1.1   Generic Light Water Reactor Best Practices

Modeling practices discussed in this section are applied generically to both MELCOR models of the SOARCA project Surry Power Station and Peach Bottom Atomic Power Station. The specific manner in which they are implemented can vary slightly between the two, but the physical processes that are represented in these models are consistent between the two designs.

3.1.1.1   Fuel Degradation and Relocation Treatment

As a reactor core overheats in a severe accident, fuel cladding ruptures would occur at relatively low temperatures releasing fission product gases from the fuel-cladding gaps. As temperatures continue to rise, fuel cladding would oxidize and the fuel rods would form outer oxide shells. The oxide shells would have a high melting temperature relative to that of unoxidized cladding (Zircaloy) and, as evidenced in the Phebus tests, would maintain fuel geometry as Zircaloy, interior to the shell, melts and drains away. This configuration is illustrated in Figure 3-1. In maintaining fuel geometry, the oxide shells would be susceptible to thermal-mechanical weakening over time. Modeling was added to the MELCOR code during the course of the SOARCA project that acknowledges this thermal-mechanical weakening as a function of time and temperature. Prior to the modeling addition, an oxide shell could maintain fuel geometry at very high temperatures for a long period of time after interior Zircaloy drains away (ending

oxidation and the associated heat generation). An oxide shell would not fail until its temperature reaches the eutectic temperature for the UO_2/ZrO_2 system (2500 K); and with oxidation heat generation gone, this could take a long time. The new modeling eliminates this threshold temperature failure requirement. The modeling is functionally similar to what is accomplished in the Modular Accident Analysis Program (MAAP) [59]. In the new modeling, as cladding oxide temperature increases from the melting temperature of Zircaloy (2099 K by default in MELCOR), a thermal lifetime function accumulates fractional damage towards an inferred thermal-mechanical failure. The cumulative fractional damage is incrementally increased each time step by the fractional damage incurred during the timestep considering the current cladding temperature and lifetime associated with that temperature, i.e.:

$$D_{i+1} = D_i + \left[\frac{dt}{TtF(T)} \right]$$

Equation 1

where,

D_{i+1} is the fractional damage accrued through the current timestep
D_i is the fractional damage accrued up to the current timestep
dt is the duration of the current timestep
$TtF(T)$ is the time at the current temperature (T) required to fail oxidized cladding

Fractional damage is accrued in this way locally by axial level and radial ring throughout the core. The best practice dependence of time-to-failure as a function of temperature, enforced through user input, is presented in Table 3-1[4].

Table 3-1   Best-estimate time to fuel rod collapse versus cladding oxide temperature

Cladding Temperature	Time to Failure
2090 K	Infinite
2100 K	10 hrs
2500 K	1 hr
2600 K	5 min

Times to failure intermediate to entries in Table 3-1 are linearly interpolated. Infinite lifetime is assumed at cladding oxide temperatures below the melting point of Zircaloy. The relatively short time associated with 2500 K and the even shorter time associated with 2600 K reflect the melting tendencies of irradiated fuel inferred from the Phebus experiments. Damage function accumulation does not begin until unoxidized cladding thickness drops below 10% of nominal values.

---

[4] Sandia National Laboratories conducted an expert review of severe accident progression modeling for the SOARCA project in Albuquerque, NM on August 21-22, 2006 [4]. The expert review was conducted by five panelists with demonstrated expertise in the analysis of severe accidents at commercial nuclear power plants. The time-to-failure dependencies in Table 3-1 were presented to the panelists as one of the several uncertain modeling practices presented. The panelists provided written comments and suggestions, which were incorporated into the subsequent analyses.
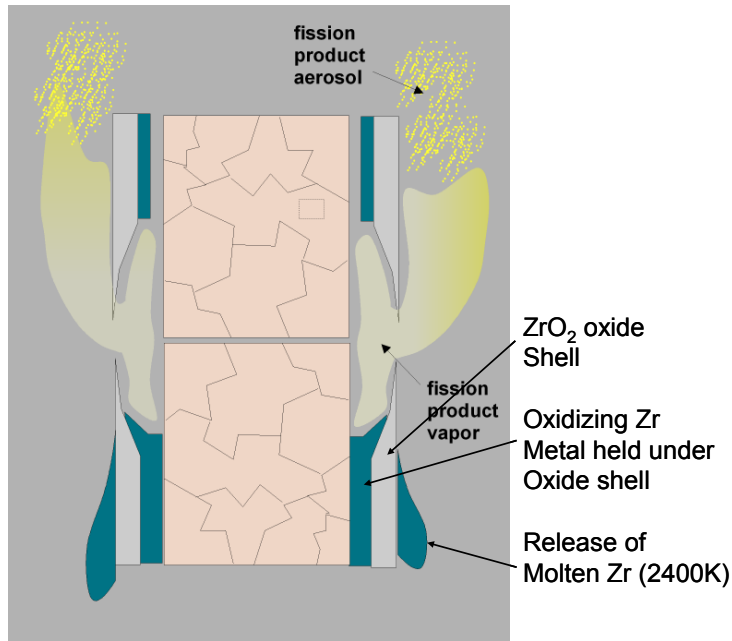
Figure 3-1   MELCOR depiction of fuel rod degradation

3.1.1.2   Lower Plenum Debris/Coolant Heat Transfer

Direct interaction between over-heated (possibly molten) core debris and a pool of water can occur at two key junctures in the chronology of a severe accident in a light water reactor (LWR). The first major juncture is when core debris relocates from a position above the lower core support structures; the second juncture is when the reactor vessel lower head fails and core debris relocates onto the floor of the containment. The thermo-mechanical interactions between core debris and water during these periods of debris relocation can be either benign or extremely energetic, depending on several factors:

- the thermodynamic state of the debris (temperature and morphology),
- composition of the debris (unoxidized metals, ferric oxides, ceramics, etc.),
- debris relocation geometry (coherent pour, massive slump, cascade of particulate, etc.),
- depth and temperature of water pool (saturated or subcooled), and
- initial pressure of the confining vessel.

Proper accounting for the interaction between fuel and coolant at these two junctures can have a significant effect on the prediction of severe accident chronology, challenges to containment integrity and the resulting source terms. For example, relocation of core debris into the lower head without significant interaction with residual water below the lower core support structure can result in rapid heating and early failure of lower head structures. Conversely, significant interaction between core debris and water can significantly delay the time of vessel breach, produce large quantities of steam (leading to enhanced oxidation of metallic components) and potentially result in a coolable debris bed in the lower head.

Ex-vessel interactions between core debris and water on the containment floor can be equally important to severe accident progression. The possibility of avoiding fission product release from fuel debris during corium-concrete interactions by quenching core debris upon release

from the reactor vessel is a significant enough reason for properly characterizing ex-vessel debris-coolant interactions.

Most studies of debris-coolant interactions have viewed the phenomenon as a precursor to steam explosion. However, most experiments involving molten debris-coolant interactions do not result in a steam explosion. These less energetic events are of equal (perhaps greater) value to the analysis of severe accident progression as they provide valuable information on debris quenching and long-term coolability. Published literature describing these studies was reviewed to determine the depth of water required to sufficiently fragment and cool molten core debris. This depth of water could then be applied to typical in-vessel or ex-vessel situations in which the coolability of relocating debris needs to be evaluated in MELCOR. Data from five different test series and a total of 29 different experiments were examined. Key measurements from these tests are listed in Table 3-2.

Analysis of hydrodynamic breakup behavior in these tests resulted in estimates of the vertical distance a molten jet must travel in a pool of water to fully quench the molten debris. This distance (referred to as the molten jet breakup length) was estimated to be between 20 and 50 jet diameters for melts without unoxidized metals, and between 10 and 20 diameters for melts with unoxidized melts. Test results indicate that molten jet breakup occurs at both the leading edge and along the trailing column. Steam production at the leading edge leads to jet breakup. Steam moving through the pool alongside the molten jet also contributes to jet breakup. When unoxidized metals are present, steam oxidizes metals at the jet surface releasing additional energy to the steam/water mixture and enhancing breakup along the trailing jet column.

If these figures are applied to full-scale reactor conditions, and one can postulate a representative diameter of the jet of molten core debris that would emerge from the reactor vessel lower head after failure, the minimum depth of water required to quench the debris can be estimated. For example, if one assumes the characteristic diameter of the molten jet is roughly the diameter of a single 'unit cell' of a reactor fuel assembly (i.e., approx. 10 cm), fragmentation and quenching of the molten material would be achieved in 2 to 5 m of water (for oxidic melts) and 1 to 2 m of water for metallic melts. This distance is well within the range of water depth in the lower plenum of a typical BWR at the time lower core support plate failure would first occur, initiating large scale in-vessel debris relocation. Therefore, a best-estimate characterization of debris behavior operates under the assumption of efficient debris cooling provided a sufficiently deep pool of water remains in the lower plenum.

Default MELCOR code user input parameters for the 'falling debris quench' model were, therefore, changed to effect efficient heat transfer. In particular, the debris hydraulic diameter was defined to correspond to the average end-state conditions observed in the FARO tests and the average 'fall velocity' was set to a value that caused the temperature of falling debris to decrease by an amount that ensured debris temperatures in the lower head were below the film boiling limit. In addition, the one-dimensional counter-current flow limitation (CCFL) was removed, through user input, from the overlying debris heat transfer model to represent water penetration into the debris bed, perhaps through 2- or 3-dimensional circulation flow patterns. This modeling approach resulted in debris cooling if there was a pool of water in the lower plenum and delayed heat-up of the vessel lower head until the overlying water had evaporated.

Table 3-2   Summary of data from molten debris-coolant interactions experiments.

Experiment	Melt Composition (w/o)	Melt Mass (kg)	Melt Superheat (K)	Melt Jet Diameter (cm)	Pool Mass (kg)	Pool Surface Area (cm2)	Pool Depth (m)	Pool Subcooling (K)	Pool/Melt Ratios Mass (-)	Pool/Melt Ratios Cross-Sectional Area (-)	Initial Pressure (MPa)	Melt free fall in gas (m)	Free Volume (m3)	FCI Trigger	FCI Event	Debris Oxidation (%)	Debris MMD (mm)	Debris Energy Release (MW/kg)
FARO L-06	80% UO2 20% ZrO2	18		10	120	1735	0.87	Saturated	7	22	5	1.66	0.464	No	B	na	4.5	
FARO L-08#	80% UO2 20% ZrO2	44		10	255	3959	1	Saturated	6	50	5	1.53	0.875	No	B	na	3.8	0.8
FARO L-11	76.7% UO2 19.2% ZrO2 4.1% Zr	151		10		3959	2	Saturated		50	5	1.09	1.28	No	B	100	3.5	
FARO L-14#	80% UO2 20% ZrO2	125	200	10		3959	2.05	Saturated		50	5	1.04	1.26	No	B	na	4.8	0.8
FARO L-19	80% UO2 20% ZrO2	157	200	10		3959	1.1	Saturated		50	5	1.99	1.635	No	B	na	3.7	
FARO L-20	80% UO2 20% ZrO2	96	300	10		3959	1.97	Saturated		50	2	1.12	1.291	No	B	na	4.4	
FARO L-24	80% UO2 20% ZrO2	176	150	10		3959	2.02	Saturated		50	0.5	1.07	1.266	No	E	na		
FARO L-29	80% UO2 20% ZrO2	39		5	492	3959	1.48	97	13	202	0.21	0.74	3.54	No	B	na		
FARO L-31	80% UO2 20% ZrO2	92	117	5	481	3959	1.54	104	5	202	0.22	0.77	3.53	No	B	na	3.2	
KROTOS-30	Al2O3	1.40	248	3	7.5	71	1.08	80	5	10	0.1	0.46		No	SE	na		
KROTOS-32	80% UO2 20% ZrO2	2.61	190	3	7.1	71	1.08	22	3	10	0.1	0.46		No	B	na	2.5	0.87
KROTOS-33	80% UO2 20% ZrO2	2.80	190	3	7.7	71	1.08	75	3	10	0.1	0.46		No	B	na	2	0.97
KROTOS-35	80% UO2 20% ZrO2	1.42	150	3	7.7	71	1.08	10	5	10	0.1	0.46		Yes	E	na		
KROTOS-36	80% UO2 20% ZrO2	2.8	152	3	7.7	71	1.08	79	3	10	0.1	0.46		Yes	B	na		
KROTOS-37	80% UO2 20% ZrO2	2.92	145	3	34.5	314	1.105	79	12	44	0.1	0.44		Yes	B	na	1.4	
KROTOS-38	Al2O3	1.52	340	3	34.5	314	1.105	79	23	44	0.1	0.44		Yes	SE	na		

Table 3-2 (continued)

Experiment	Melt Composition (w/o)	Mass (kg)	Superheat (K)	Jet Diameter (cm)	Pool Mass (kg)	Surface Area (cm2)	Depth (m)	Subcooling (K)	Pool/Melt Mass (-)	Cross-Sectional Area (-)	Initial Pressure (MPa)	Melt free fall in gas (m)	Free Volume (m3)	FCI Trigger	Event	Oxidation (%)	MMD (mm)	Energy Release (MW/kg)
TROI-1	ZrO2	5.00	400	3.7	283	4225	0.67	5	57	393	0.1	3.5	8.032	No	SE	na		
TROI-2	ZrO2	5.50	400	5.2	283	4225	0.67	8	51	199	0.1	3.5	8.032	No	B	na		
TROI-3	ZrO2	4.88	400	6	283	4225	0.67	50	58	149	0.1	3.5	8.032	No	B	na		
TROI-4	ZrO2	4.20	400	2.8	283	4225	0.67	81	67	686	0.1	3.5	8.032	No	SE	na		
TROI-5	ZrO2	2.90	400	3.8	283	4225	0.67	36	98	373	0.1	3.5	8.032	No	SE	na		
CWTI-9	60% UO2 16% ZrO2 24% SS	4.00	160	2.54			0.36	6			0.1	0.2		No	B	67%	0.78	
CWTI-10	60% UO2 16% ZrO2 24% SS	4.00	160	2.54			0.36	75			0.1	0.2		No	B	10%		
FITS-0D*	Thermite	17.8	375	5	182.9	3721	0.51	0	10	190	0.085	1.79	5.6	No	E	24%	4.6	
FITS-2D*	Thermite	19	375	5	95.3	1444	0.66	169	5	74	1.1	2.7	5.6	No	B	20%		
FITS-2DR*	Thermite	18.7	375	5	95.3	1444	0.66	158	5	74	1.1	2.7	5.6	No	B	25%		
FITS-3D*	Thermite	18.9	375	5	86.6	5776	0.15	37	5	294	0.7	1.6	5.6	No	B	82%		
FITS-5D*	Thermite	19.2	375	5	383	5776	0.66	83	20	294	0.083	1.6	5.6	No	SE	20%	0.5	
FITS-8D*	Thermite	19.5	375	5	21.3	1444	0.15	0	1	74	0.083	2.7	5.6	No	E	26%	3.4	

*FITS melt superheat value estimate based on alumina melting point, melt jet diameter is arbitrary

FARO melt energy released is provided in MJ/kg

3.1.1.3   Safety Relief Valve Cycling and Failure

Safety and relief valves are installed at BWR and PWR installations to provide over-pressure protection for the primary loop. The MELCOR user defined models of the valves provide a detailed accounting of these valves, including the actuation conditions, support system dependencies, and failure characteristics. The various types of safety and relief valves can be manually actuated if requisite support systems are available (e.g., electric power, control air, etc.). Pressurizer power-operate relief valve (PORV) and safety valves (SVs) as well as steam generator PORVs and SVs are included in PWR designs and in the general MELCOR models. Similarly safety relief valves (SRVs) are included in the BWR models. Failure, in this context means failure-to-reclose after successfully opening to relieve pressure.

Two modes of failure are represented in the MELCOR user defined models independently. The first failure mode represents stochastic failure of the valves to reclose when pressure reduces below the closure set point. Mechanisms for failure-to-reclose are identical to those incorporated in the random event captured in the probabilistic risk assessment (PRA) for most nuclear power plants. The second failure mode accounts for high temperature operation induced seizure in the open state.

Uncertain parameters are modeled as best-estimate values; therefore, stochastic failure is represented by the expected value, the mean. Mean failure-to-open and failure-to-reclose probabilities for the specific type(s) of valve(s) installed at a particular plant were obtained from plant data (if available) or from generic failure data documented in NUREG/CR-6928, "Industry-Average Performance for Components and Initiating Events at U.S. Commercial Nuclear Power Plants". In all cases examined thus far, the probability for failure-to-reclose was much greater than failure-to-open; therefore, failure-to-open is currently ignored in the MELCOR simulations.

Stochastic failure of the safety relief valve is determined from the failure-to-reclose rate, 3.7×10^{-3} per demand as presented in NUREG/CR-6928. (Other alternate sources for valve failure characteristics are available. The PWR simulations used data supplied by the utility.) The expected failure is calculated as the inverse of the failure rate, which corresponds to the 270th cycle or 63rd percentile of the cumulative distribution function.[(5)] The cumulative probability of failure is calculated with each valve cycle. When the maximum tolerable cumulative failure limit has been exceeded, the cycling valve remains in the failed open position.

Engineering judgment based on material properties of internal components was employed to determine an adequate failure criterion based on temperature. Periodic cycling of a safety or relief valve with very high internal gas temperatures will cause the valve body and internal components to slowly increase in temperature. At some temperature, thermal expansion or yielding of internal components will prevent the valve stem from moving and re-seating. No data or models are available that clearly identify the temperature at which seizure would occur. However, stainless steel loses its strength at temperatures above approximately 1000 F (811 K). Temperatures in excess of 900 K reduce the ultimate tensile strength and yield strength by 30 percent of the design temperature strengths. A reasonable maximum temperature limit of 900 K was chosen as an approximation for internal component failure [62]. A representative heat structure was implemented in the BWR simulations to calculate internal component

---

[5] The inverse of the failure rate or the harmonic mean was selected as the best-estimate value for the failure rate. The harmonic mean is characteristic of a best-estimate average for rate functions. Due to its importance on the BWR accident progression, SOARCA also performed sensitivity studies that examined the impact of alternate failure assumptions.

temperature with regard to the maximum temperature limit criterion. Additional temperature induced failure mechanisms were also considered and are discussed in [62].

3.1.1.4 Fission Product Release

Insights have been developed over the past decade as a result of experimental programs and have been used to update the recommended MELCOR specifications for modeling the release of fission products[6] from reactor fuel under severe accident conditions. The new models have been incorporated as new defaults in the MELCOR code. Separate specifications are provided for use in spent fuel pool release conditions owing to differences in the reduction/oxidation potential in air oxidizing conditions. Some review of the motivation for the new modeling approach follows with an assessment of the new model against fission product release experiments.

Past versions of MELCOR primarily used the CORSOR-M release model for calculating fission product release as described in the MELCOR Reference manuals and in a Battelle report by Ramamurthi and Kuhlman titled "Refinement of CORSOR – An Empirical In-Vessel Fission Product Release Model [6]." Also described in these references are the CORSOR and the Booth diffusion release model, implemented in MELCOR as the CORSOR-Booth optional release model. The CORSOR and CORSOR-M models are classified as *fractional release rate* models, differing only slightly in mathematical form, which specify the fractional release rate of the fission product inventory remaining unreleased up to that time. These are empirical models that are based largely on the small-scale horizontal induction (HI) and vertical induction (VI) experiments performed at Oak Ridge National Laboratory (ORNL).

The Booth diffusion model is by comparison a physics-based model, albeit oversimplified, that describes the transport of fission products within fuel grains to the grain surface as a diffusion process. In the MELCOR code implementation of the Booth diffusion treatment, an additional gas phase transport process is imposed in moving fission products from the grain surfaces to the atmosphere. Elements such as molybdenum that are modeled in MELCOR as having very low vapor pressures are ultimately released at a low rate regardless of the rate of diffusion within the grain. Once released from the fuel, fission product class combinations can be defined, such as CsI, in order to represent fission product chemistry and speciation. In the present code architecture, multiple combination assignments such as CsI and Cs_2MoO_4 were not foreseen and must be approximated. Once assigned to the chemical class on release, generally no additional chemistry is allowed, an exception being CsI chemisorption with subsequent revaporization of iodine, leaving the permanently chemisorbed Cs attached to a deposition surface.

Critical assessments of these models and their performance have been limited, partly owing to lack of additional quality data from which to render a judgment. One assessment performed by ORNL with MELCOR 1.8.2 evaluated the performance of the MELCOR default models when applied to the VI series of tests [7]. The report observed that while total releases could often be adequately predicted that the time-release signature was often not very good.

Recommendations were provided for code modeling improvements, including provision to vary release based on the H_2/H_2O environment. Recently however, additional experimental data are

---

[6] The recent modifications to Version 1.8.6 (Version YR) for the SOARCA project implemented the new ORNL-Booth fission product release model as the new default model. In Version 1.8.6, the new defaults are invoked with the Version "2.0" keyword. All subsequent 2.X code versions will automatically use the new ORNL-Booth model as the default fission product release model.

becoming increasingly available from international testing programs, in particular the French VERCORS program and the Phebus integral experiments, and user assessment of current MELCOR release models in the prediction of these tests has illuminated some deficiencies that are partly remedied in the recommendations of this report. The Phebus experiments in particular reveal shortcomings of the empirical CORSOR and CORSOR-M models with respect to release rates during the initial fuel heat-up, and those models have been found to significantly overestimate early release rates even though total integral releases might compare reasonably well. Additionally, the integral Phebus tests provide release data under conditions that are significantly less coherent (and more prototypic) in terms of temperature and oxidation/reduction conditions than in the small scale tests (HI, VI and VERCORS) where the fuel sample is small, temperatures are uniform and oxidation/reduction conditions controlled and constant. The Phebus experiments, we contend, provide conditions for release that are more representative of conditions expected in the full scale reactor accident case, and are used as the principal reference for judging the performance of the MELCOR release models.

MELCOR Release Models
The various release rate models available in the MELCOR code for user selection are briefly summarized as follows.

CORSOR
The original CORSOR model correlates the *fractional* release rate coefficient in exponential form,

$$k_i = A_i \ \exp(B_i \ T) \qquad for \ T \ge T_j \qquad \text{Equation 2}$$

where k_i is the fractional release rate per minute, A_i and B_i are empirical coefficients based on experimental data, T is the core cell component temperature in Kelvin, and i indicates the specific class. Different values for A_i and B_i are specified for three separate temperature ranges. The lowest temperature, T_j, for given range j, as well as the corresponding coefficient set, A_i and B_i, are defined in sensitivity coefficient array 7101. If the cell temperature is below the lowest temperature range limit specified, no release is calculated.

CORSOR-M
The CORSOR-M model correlates the same release data used for the CORSOR model using an Arrhenius form,

$$k_i = k_{o,i} \exp(-Q_i/RT) \qquad \text{Equation 3}$$

The values of $k_{o,i}$, Q_i, and T are in units of min^{-1}, kcal/mole, and K, respectively. The value of R is 1.987 x 10^{-3} in kcal/mole-K. The values of $k_{o,i}$ and Q_i for each class i are implemented in sensitivity coefficient array 7102.

CORSOR-Booth
The CORSOR-Booth model considers mass transport limitations to radionuclide releases and uses the Booth model for diffusion with empirical diffusion coefficients for cesium releases. Release fractions for other classes are calculated relative to that for cesium. The effective diffusion coefficient for cesium in the fuel matrix is given by:

$$D = D_o \exp(-Q/RT) \qquad \text{Equation 4}$$

where R is the universal gas constant (cal/mole-K), T is the temperature (K), Q is an activation energy (cal/mol), and the pre-exponential factor D_0 is a function of the fuel burn-up (m^2/s). The cesium release fraction f at time t is calculated from an approximate solution of the diffusion equation for fuel grains of spherical geometry [8],

$$f = 6 \sqrt{\frac{D't}{\pi}} - 3 \, D't \qquad \text{for } D't < 1/\pi^2 \qquad\qquad \text{Equation 5}$$

$$f = 1 - \frac{6}{\pi^2} \exp\left(-\pi^2 \, D't\right) \qquad \text{for } D't > 1/\pi^2 \qquad\qquad \text{Equation 6}$$

where

$D't$ = Dt/a^2 (dimensionless), and

a = equivalent sphere radius for the fuel grain.

The release rate (in mole/s) of Cs during a time interval t to $(t + \Delta t)$ from the fuel grain is calculated as:

$$\text{Release rate}_{Cs} = \frac{\left[f\left(\sum D'\Delta t\right)_{t+\Delta t} - f\left(\sum D'\Delta t\right)_t\right]V\rho}{F\Delta t} \qquad\qquad \text{Equation 7}$$

Where ρ is the molar density of UO$_2$ in the fuel, V is the fuel volume (m^3), F is the fraction of the Cs inventory remaining in the fuel grain, and the summations are done over the timesteps up to time, $(t + \Delta t)$ and t, respectively.

The release rate formulation in the CORSOR-Booth model is also limited by mass transfer through the gas phase. The gas phase mass transport release rate from the fuel rod for species i, $\dot{m}_k$ (in mole/s), is calculated using an analogy from heat transfer as:

$$\dot{m}_i = \left[\frac{A_{fuel} Nu \, D_{i,gas}}{D_{fuel} RT}\right] \cdot \left(P_{i,eq} - 0\right) \qquad\qquad \text{Equation 8}$$

where

D_{fuel} = diameter of fuel pellet (m)

A_{fuel} = fuel rod flow contact area (m^2)

$D_{i,gas}$ = diffusivity of class i in the gas mixture(m^2/s)

Nu = Nusselt number

R = Universal gas constant (J/mol-K)

$P_{i,eq}$ = equilibrium vapor pressure of class i at temperature T. (Pa)

In the mass transfer term the driving potential is the difference in pressure at the surface of the grain and the pressure in the free atmosphere, here assumed to be approximately zero.

The effective release rate for Cs given by Equation 7 is a combination of the rates given by diffusion and by gas phase mass transport. Therefore, the contribution from diffusion only is taken as:

$$DIFF_{Cs} = \left[\frac{1}{\text{Release rate}_{Cs}} - \frac{1}{\dot{m}_{Cs}} \right]^{-1}$$

<div align="right">Equation 9</div>

The diffusion release rate (in mole/s) for species i, other than cesium, is given by multiplying the cesium diffusion release rate by an appropriate scaling factor S_i for each RadioNuclide Package (RN) class i:

$$DIFF_i = DIFF_{Cs}S_i$$

<div align="right">Equation 10</div>

The combined mass transport and diffusion release rate $\dot{m}_{tot,i}$ (in mole/s) for class i is then

$$\dot{m}_{tot,i} = \frac{1}{DIFF_i^{-1} + \dot{m}_i^{-1}}$$

<div align="right">Equation 11</div>

Inspection of Equation 11 together with Equation 8 reveals that the release predicted by the MELCOR models can be mass transfer limited by low vapor pressures even if the diffusive transport is large.

Limitations of MELCOR Release Models
The fission product release models implemented in previous versions of MELCOR (i.e., before Version 1.8.6 (RO) and the code modifications) are quite simplified and are more than 10 years dated as indicated in the principal reference for the MELCOR models. The implemented models base the release of all radionuclide chemical classes on the release predicted for Cs, which in the Booth model is appropriately considered a diffusion process. Scaling factors are used to estimate release of other species based on the data fit to experimentally observed Cs release in spite of the fact that it is recognized that likely not all fission product classes diffuse at the same rate out of the fuel grains, nor are all principal release mechanisms well represented as a diffusion process. Consideration of speciation in MELCOR release models is crude and for the most part fixed at the time of release to represent the predominating speciation. The vapor pressures of the MELCOR release classes are defined to represent the presumed fission product speciation.

A better treatment would be to allow the vapor pressure to be adjusted to account for local speciation affected by oxidizing or reducing conditions and to then source these species into appropriate chemical classes. Such modifications are probably needed for Ba, Mo, UO_2 and Ru. Provision does exist to consider the extent of cladding oxidation to attempt to simulate retention of Te or Ba, but data are needed to use this provision effectively. Separate diffusion coefficients for each of the volatile classes would probably be appropriate, and a UO_2 oxidation model is needed to account for the effect of stoichiometry on diffusion and to predict fuel volatilization. UO_2 volatilization may be responsible for release of UO_3 as well as other non-volatile species owing to physical stripping of the fuel matrix containing the fission products. A number of more recently evolved release models consider the effect of fuel stoichiometry on the diffusion coefficient as well as the oxidizing/reducing potential of the environment [9][10][11][12]. The VICTORIA code considers a large number of potential fission product species in a thermodynamic equilibrium approach; some simplifications to this potentially numerically burdensome approach may be needed [13].

In the more recent models, often, with respect to release behavior, fission products are classified into three main groups, volatile (i.e., Xe, Cs, I, Te), semi-volatile (i.e., Ru, Ba, La, Ce), and non-volatile (i.e., UO_2 and actinides – Ce and La might belong here also). Volatile fission products are released based on the Booth diffusion model where the diffusion coefficient includes effects of UO_2 hyper-stoichiometry. The hyper-stoichiometry in turn is determined by a fuel oxidation model. Release of semi-volatile fission products are strongly affected by vapor pressure which in turn is affected strongly by speciation determined by the oxidizing/reducing conditions resulting from air/steam/hydrogen/Zr-metal in the release location. Non-volatile release may be dominated by UO_2 volatilization by formation of UO_3, producing fuel matrix degradation and fuel vaporization. The French Elsa code follows this approach, using models similar to those reported by Lewis et al. [9][10].

A more detailed (and flexible) release modeling was needed for the SOARCA project. The importance of accounting for speciation and the ensuing effect on specie volatility (vapor pressure) is clear. In the best practices approach, as described in the following section, the dominant speciation at the time of release is specified and used globally throughout the core region. A more elegant model would allow variation of release speciation as conditions in the core change locally and temporally with respect to steam and hydrogen concentrations. In the case of air exposure, such as in spent fuel pool accidents, different assumptions about speciation, especially concerning Ru release, are needed.

Assessment of MELCOR Default Release Models
Whereas the HI-VI ORNL tests provided the original basis for development of the MELCOR fission product release models, the Phebus FPT-1 integral experiment is used as the principal basis for evaluation of release modeling options. In previous assessment exercises, in particular the ISP-46 (International Standard Problem 46 [14]), while the MELCOR default CORSOR-M release model was found to predict reasonable total release fractions for many fission products, the empirical model was observed by many MELCOR ISP participants to over predict the initial release rates. Similar rapid early release is also observed for the CORSOR option. The Booth diffusion treatment for release was thought to be a potentially superior release model since it has some basis in a physical transport process, however, investigation of the MELCOR CORSOR-Booth option using the default Booth release parameters was found to produce inferior results, with total release of Cs and other fission products being significantly under predicted in test FPT-1. In view of this, review of the literature revealed numerous other, more recent parameter-fits to the Booth solution.

Modifications to MELCOR Booth Release Modeling
A number of these alternative models are reported in an ORNL report that recommends updated values for the previously discussed models [56]. Shown in Figure 3-2 are release fractions predicted at a constant temperature of 2000 K by the various release models discussed in the ORNL report. From this it can be seen that fractional releases predicted by CORSOR-M produce the largest total release of all of the models. This trend is consistent with observations from analyses considering measured releases from FPT-1. Similarly, the CORSOR-Booth diffusion model produces the lowest total release of all of the models. This too is consistent with MELCOR analyses of FPT-1 using these modeling parameters. Judging that a best fit might lie somewhere in between these extremes, the ORNL-Booth parameters were subsequently investigated in MELCOR analyses of FPT-1, wherein significantly improved release signatures were obtained. The ORNL-Booth parameters were recommended over the CORSOR-Booth parameters in the 1995 ORNL report. The ORNL-Booth model is specified by the parameters in Table 3-3. Figure 3-3 shows other comparisons between the ORNL-Booth and CORSOR-M release behaviors. The fractional release rate (%/min) for the two models obtained by differentiating the release fractions in Figure 3-3 are shown in Figure 3-4.
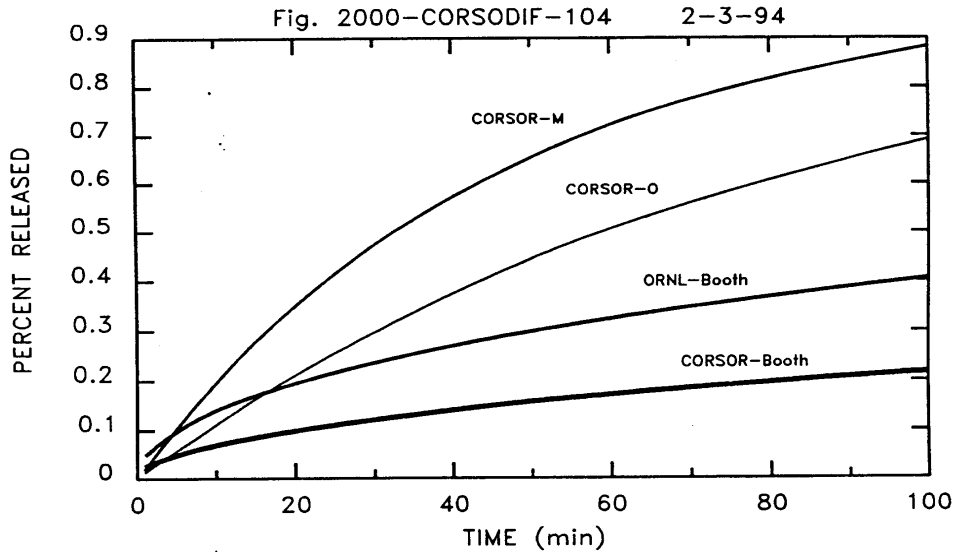
Figure 3-2   Release fractions for different release models – release temperature = 2000 K

[*Note: CORSOR-M produces largest release whereas CORSOR-Booth produces the smallest release.*]

Table 3-3   CORSOR-Booth, ORNL-Booth, and Modified ORNL-Booth parameters.

	CORSOR-Booth	ORNL-Booth	Modified ORNL-Booth
Diffusion coeff. D_o	2.5×10^{-7} m^2/sec	1×10^{-6} m^2/sec	1×10^{-6} m^2/sec
Activation Energy Q	3.814×10^5 joule/mole	3.814×10^5 joule/mole	3.814×10^5 joule/mole
Grain radius, a	6 μm	6 μm	6 μm
Class Scale Factors	---	---	---
Class 1 (Xe)	1	1	1
Class 2 (Cs)	1	1	1
Class 3 (Ba)	3.3×10^{-3}	4×10^{-4}	4×10^{-4}
Class 4 (I)	1	0.64	0.64
Class 5 (Te)	1	0.64	0.64
Class 6 (Ru)	1×10^{-4}	4×10^{-4}	0.0025
Class 7 (Mo)	0.001	0.0625	0.2
Class 8 (Ce)	3.34×10^{-5}	4×10^{-8}	4×10^{-8}
Class 9 (La)	1×10^{-4}	4×10^{-8}	4×10^{-8}
Class 10 (U)	1×10^{-4}	3.6×10^{-7}	3.2×10^{-4}
Class 11 (Cd)	0.05	0.25	0.25
Class 12 (Sn)	0.05	0.16	0.16

3-14
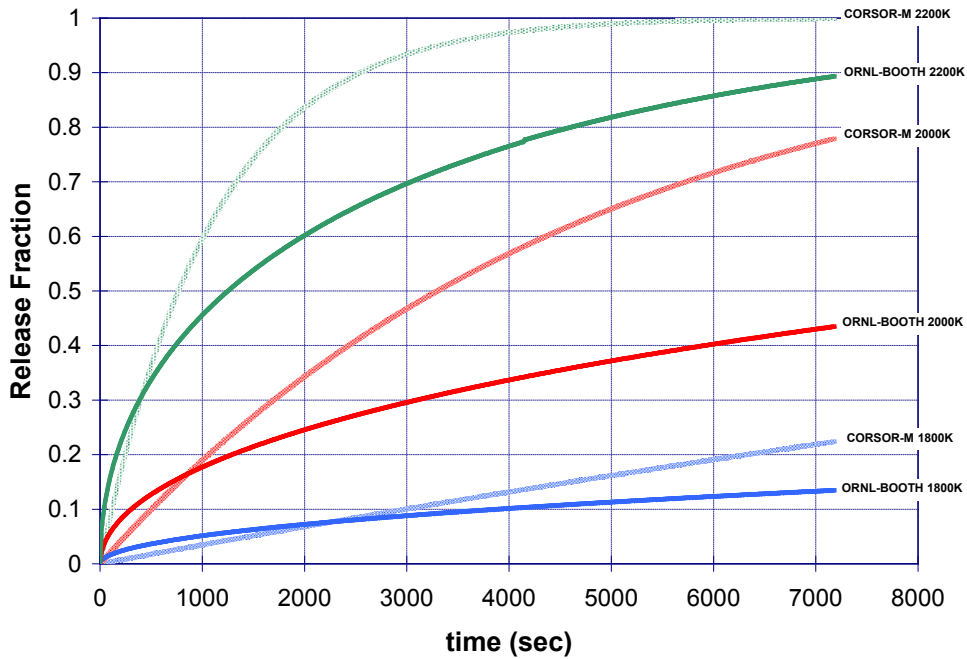
Figure 3-3   Release fractions at constant temperature for ORNL-Booth versus CORSOR-M
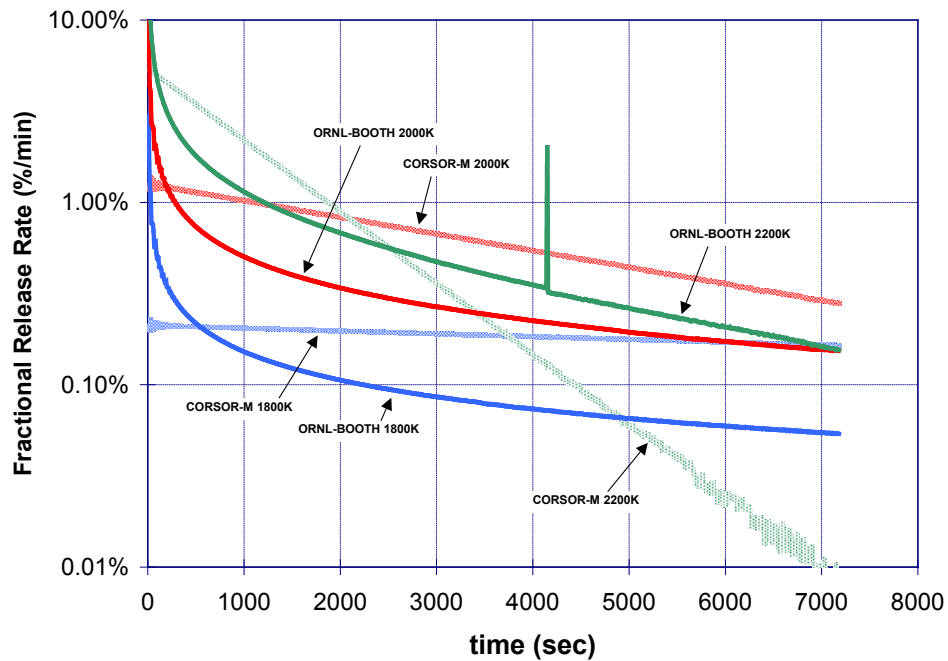
Figure 3-4   Fractional release rate (%/min) – the time derivative of release fraction
[*Note: The discontinuity when transitioning between Equation 5 and 6 results in the observed spike in the ORNL-Booth 2200K curve.*]

While significant improvements in release behavior were obtained for the analysis of the FPT-1 test with the as-reported ORNL-Booth parameters, an additional modification to the MELCOR release model was pursued. Evidence from the Phebus experiments increasingly indicates that the dominant chemical form of released Cs is that of cesium-molybdate, Cs_2MoO_4. This is based on deposition patterns in the Phebus experiment where Cs is judged to be in aerosol form at 700°C, explaining deposits in the hot upper plenum of the Phebus test section, and deposition patterns in the cooler steam generator tubes. In recognition of this, the vapor pressure of both Cs and Mo classes were defined to be that of Cs_2MoO_4. While having little effect on the net release of Cs, this change had a significant effect on the release of Mo. In MELCOR, by default the Mo vapor pressure is so exceedingly low that the net release is limited by the vapor transport term, as expressed in Equation 8 and Equation 9. Vapor pressures for selected fission product species are shown in Figure 3-5. Defining the Mo vapor pressure to be that of Cs_2MoO_4 produced significantly improved the predicted Mo release rate with respect to observed FPT-1 releases, as will be seen in the following section.

Fission Product Vapor Pressure
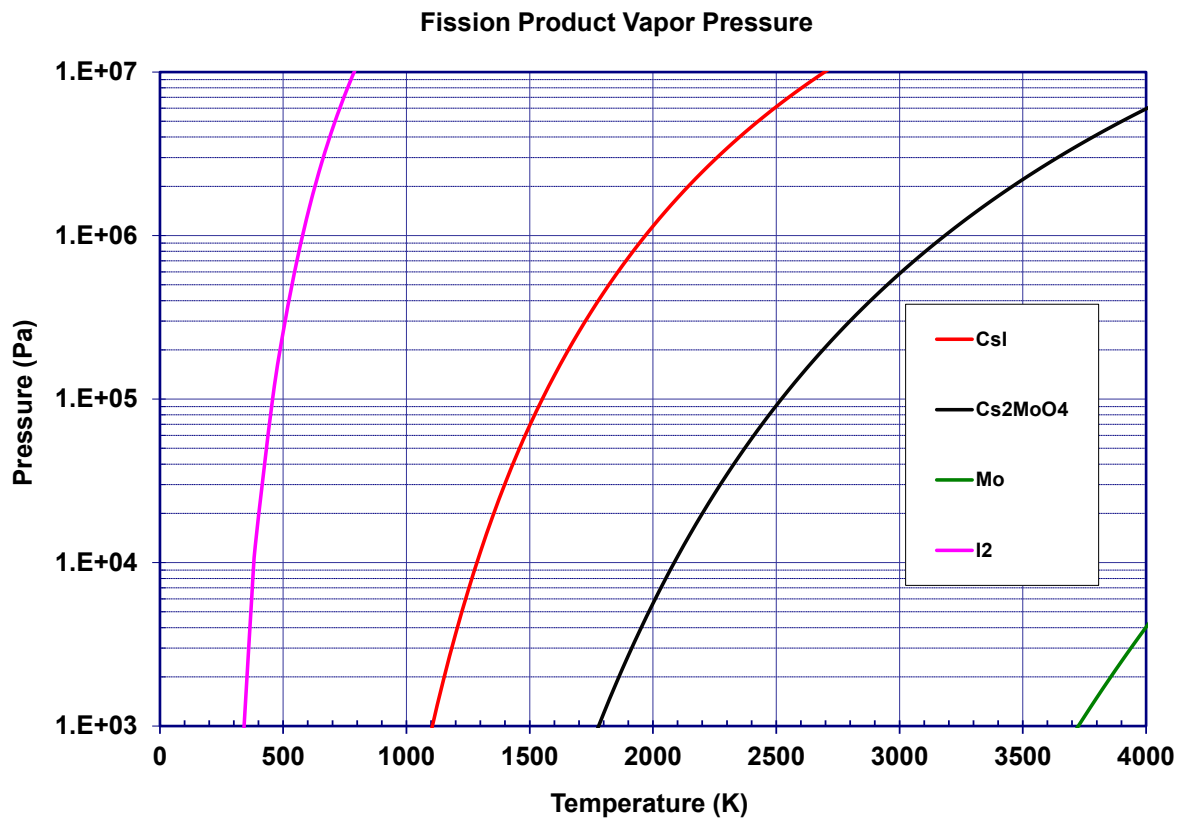
Figure 3-5   Vapor pressure of selected species

Assessment of Modified ORNL-Booth Model Against Phebus FPT-1
The Phebus program provides probably the best source of prototypic data on fission product release from irradiated fuel, benefiting from many lessons learned from earlier similar experimental efforts and from advances in testing technology, instrumentation, etc. A schematic of the Phebus test facility is shown in Figure 3-6. A previously irradiated fuel bundle of about a meter in length is situated in the irradiation cavity in the Phebus test reactor and caused to undergo severe damage from nuclear heating and oxidation by injected steam. Fission products released from the test bundle flow through a heated section representing the reactor

coolant system, through a simulated steam generator tube where strong deposition can occur, and into a simulated containment where fission product fallout occurs.

PHEBUS facility
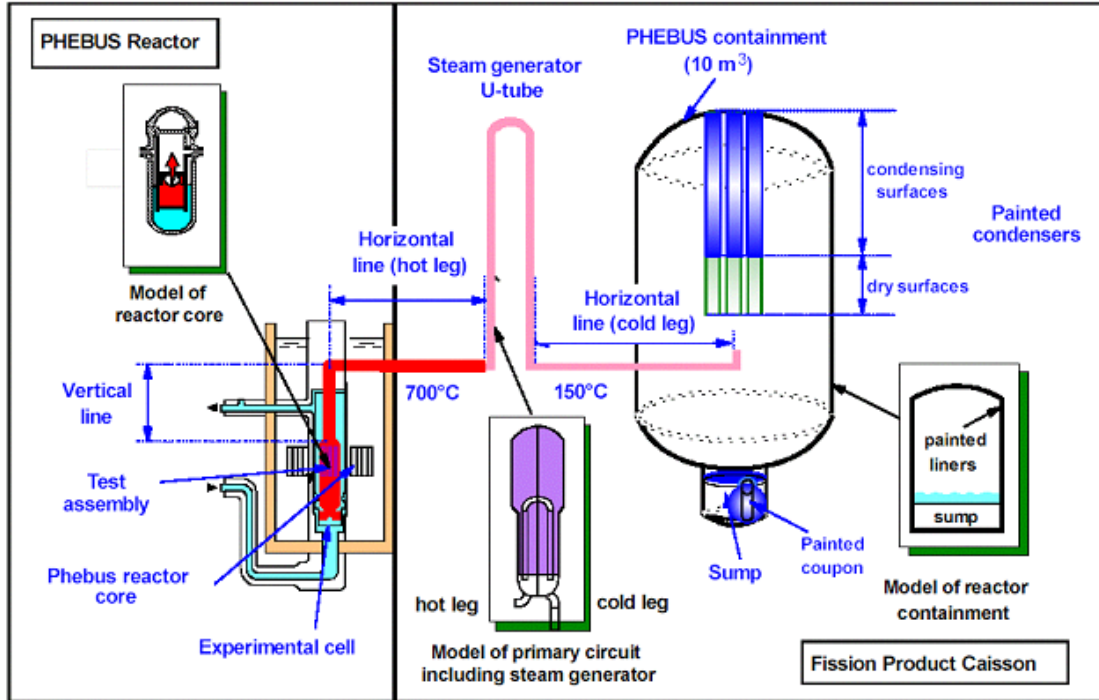
Figure 3-6   Schematic of the Phebus Test Facility showing test fuel bundle, heated lines, steam generator tube and simulated containment

Shown in Figure 3-7 is the nuclear heating history that was used in test FPT-1 to heat the bundle to simulate severe accident decay heating conditions. The chemical heating produced by steam-Zr oxidation is also shown in the figure. The temperature response of the test fuel is shown in Figure 3-8 where the temperature transient resulting from the additional oxidation heating is clearly evident. During this time, fission products are also released where oxidation conditions vary from oxidizing to reducing, depending on elevation in the test bundle. Figure 3-9 shows the end state of the test bundle following conclusion of the experiment.
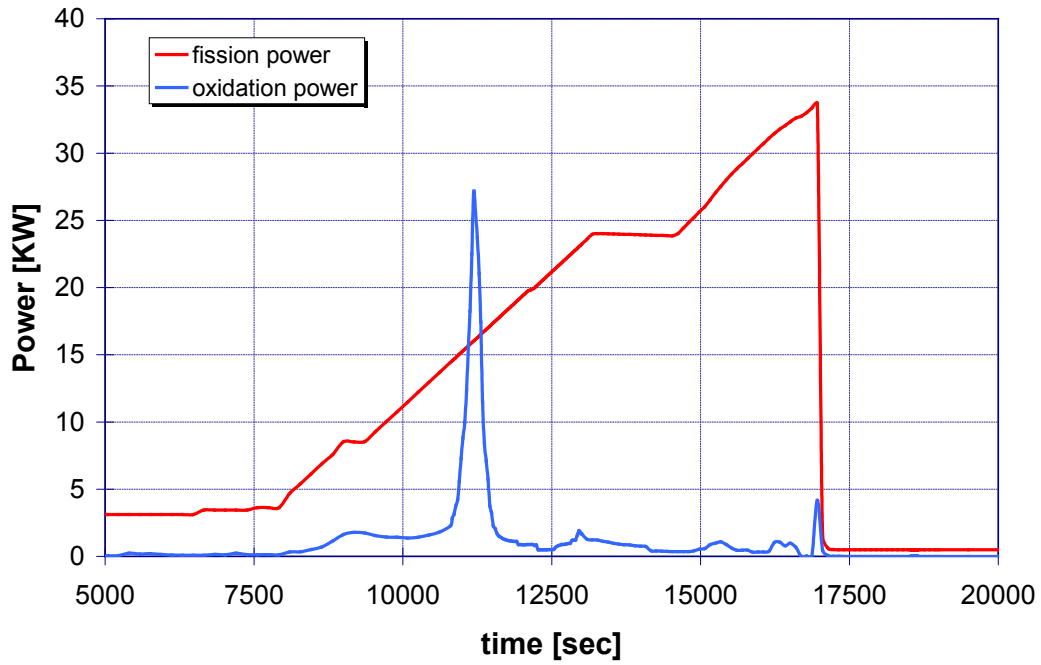
Figure 3-7   FPT-1 nuclear and chemical heating history
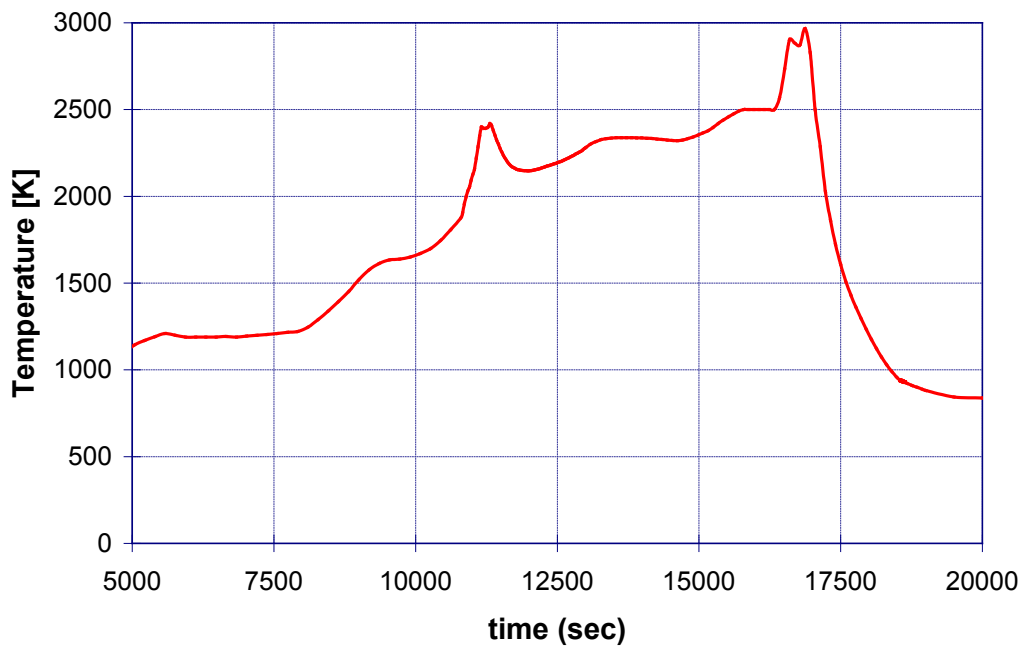
Figure 3-8   FPT-1 maximum bundle temperature history
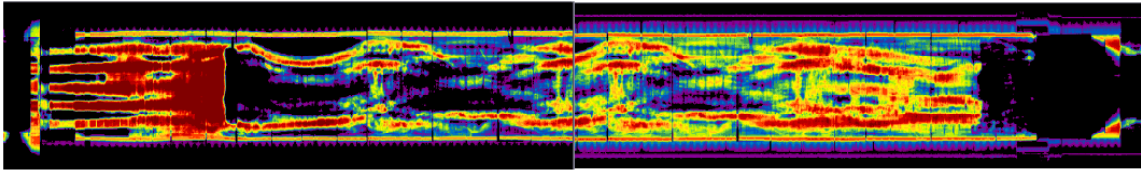
Figure 3-9   Emission gamma tomography of the end-state condition of test FPT-1

The following figures (Figure 3-10 through Figure 3-21) show the results of using the modified ORNL-Booth model for fission product release in the FPT-1 analysis. In most cases significant improvement is realized in both the early release time signature as well as for total predicted release. Where available, Phebus data is presented. The release for the barium class for the ORNL-Booth model is low relative to the data, whereas the release predicted using the CORSOR-M model is high. Improvement to this observed release proved elusive and it is believed that some adjustments to the vapor pressure for Ba to account for some not yet understood barium speciation could produce some improvement. Adjustments to both vapor pressure and scaling factors were rationalized for Mo release based on Phebus program findings, producing good agreement with experiment. The Ru vapor pressure was increased by a factor of 10 arbitrarily to account for some greater volatility attributed to formation of oxides under moderately oxidizing conditions, and the Booth scaling factor was adjusted to gain agreement with experimental observations. The Booth scaling factor for UO_2 was increased significantly in order to gain agreement with test observations. This also is rationalized as due to effects of fuel oxidation and greater volatility of fuel oxides. Ce and La release parameters were not adjusted owing to lack of experimental basis; however, one could reason that their releases ought to roughly follow UO_2 release if fuel matrix stripping follows from fuel volatilization. The following section presents comparisons of the modified ORNL-Booth model against ORNL VI tests and more recent VERCORS test data.
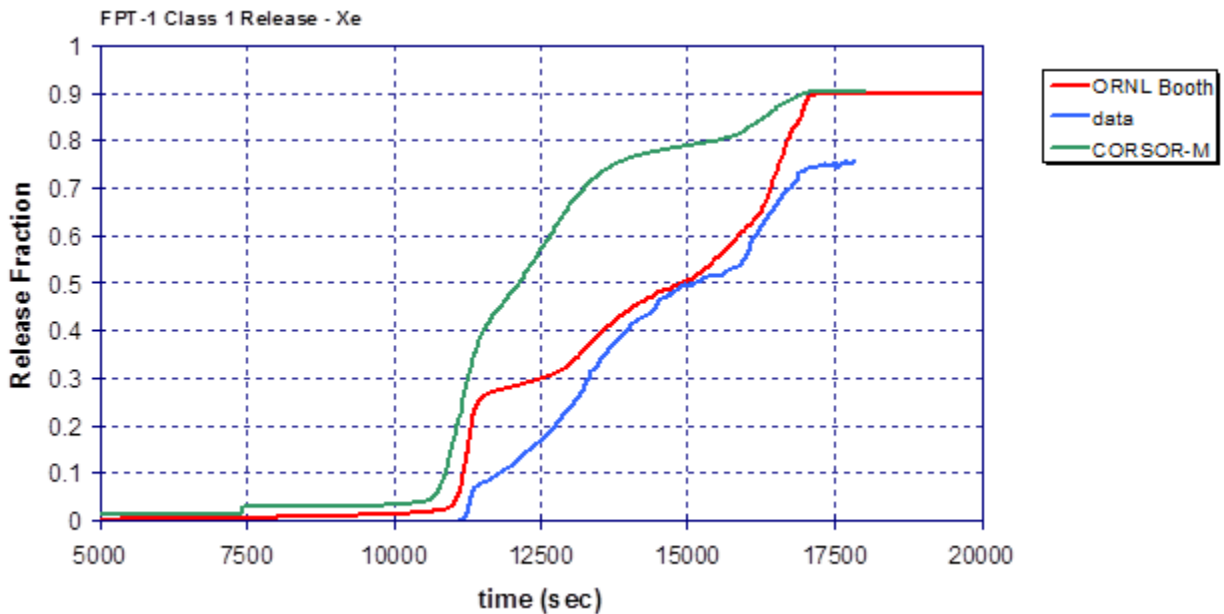
Figure 3-10   Comparison of ORNL-Booth versus CORSOR-M for Xe release (Class 1)
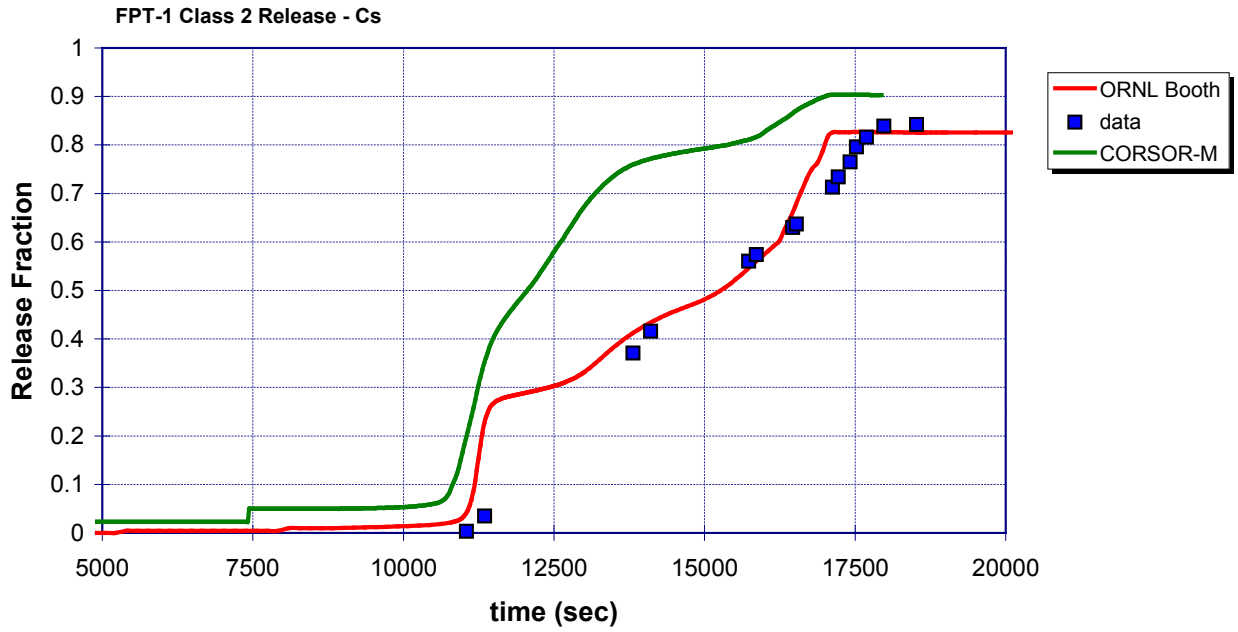
Figure 3-11   Comparison of ORNL-Booth versus CORSOR-M for Cs release (Class 2)
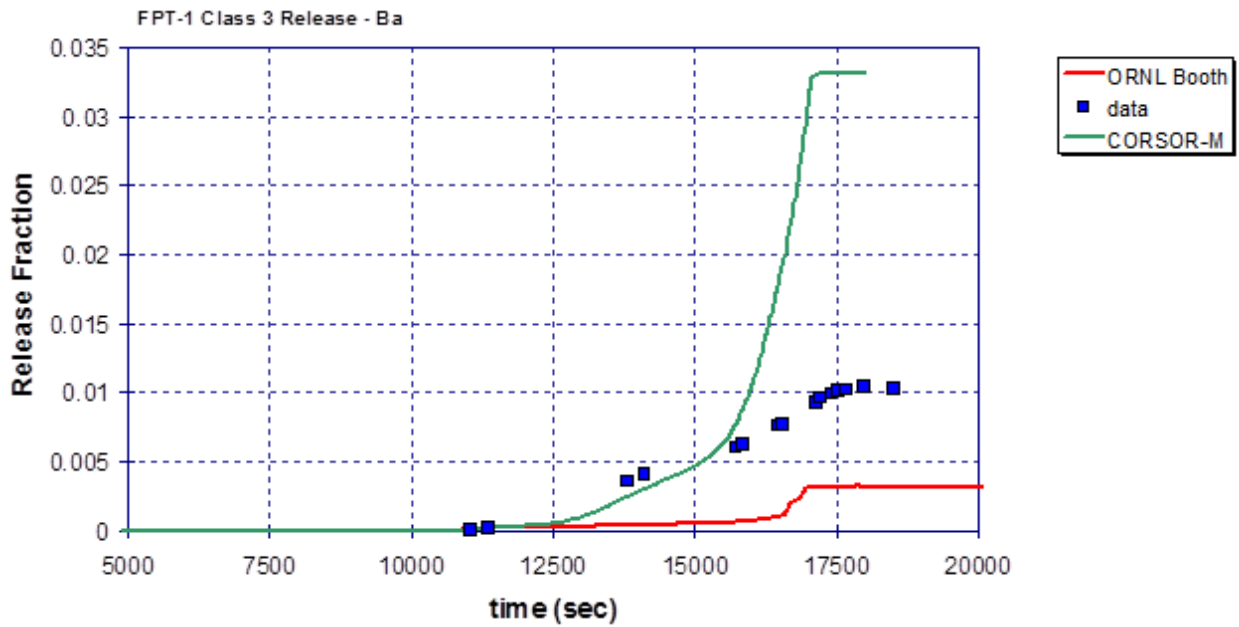
Figure 3-12   Comparison of ORNL-Booth versus CORSOR-M for Ba release (Class 3)
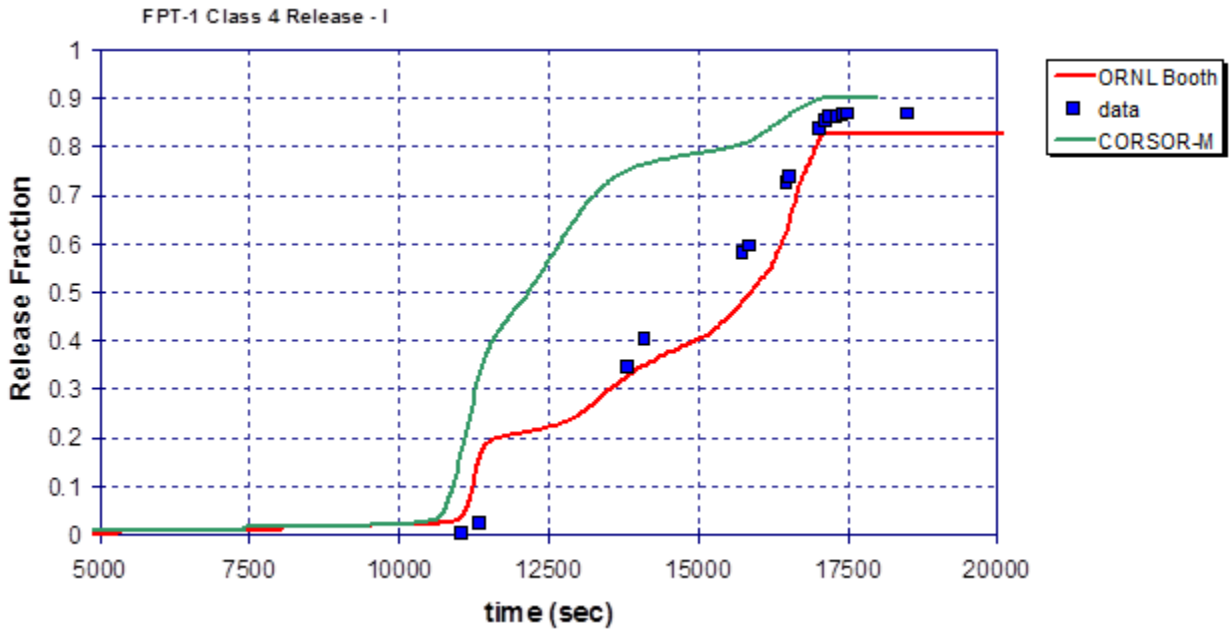
Figure 3-13   Comparison of ORNL-Booth versus CORSOR-M for I release (Class 4)
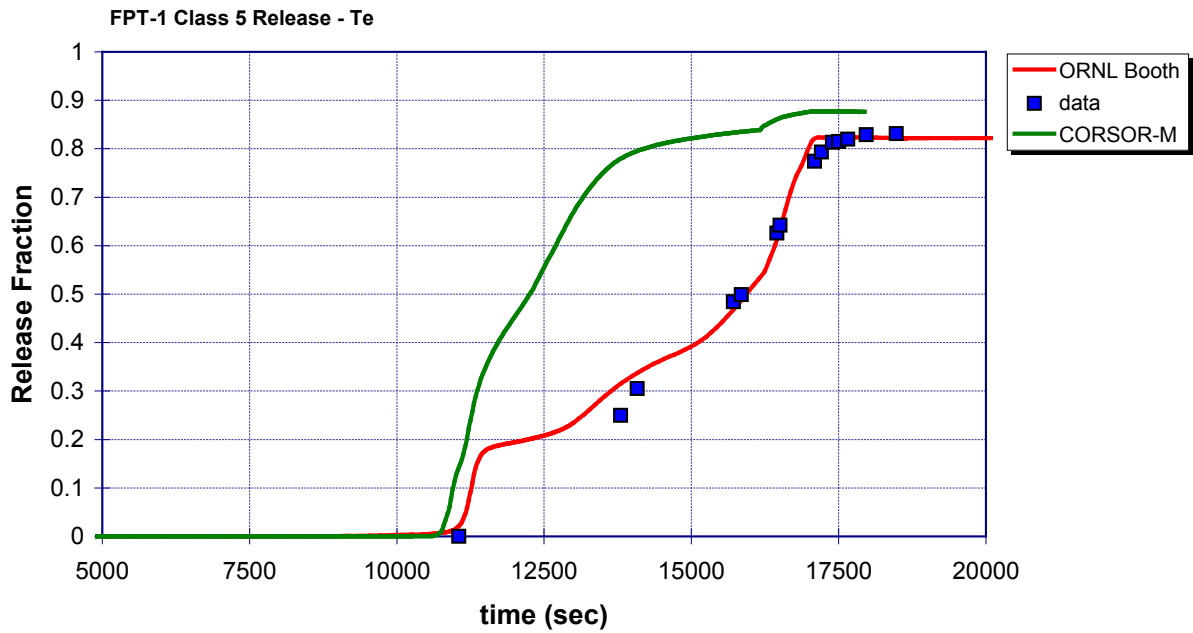
Figure 3-14   Comparison of ORNL-Booth versus CORSOR-M for Te release (Class 5)
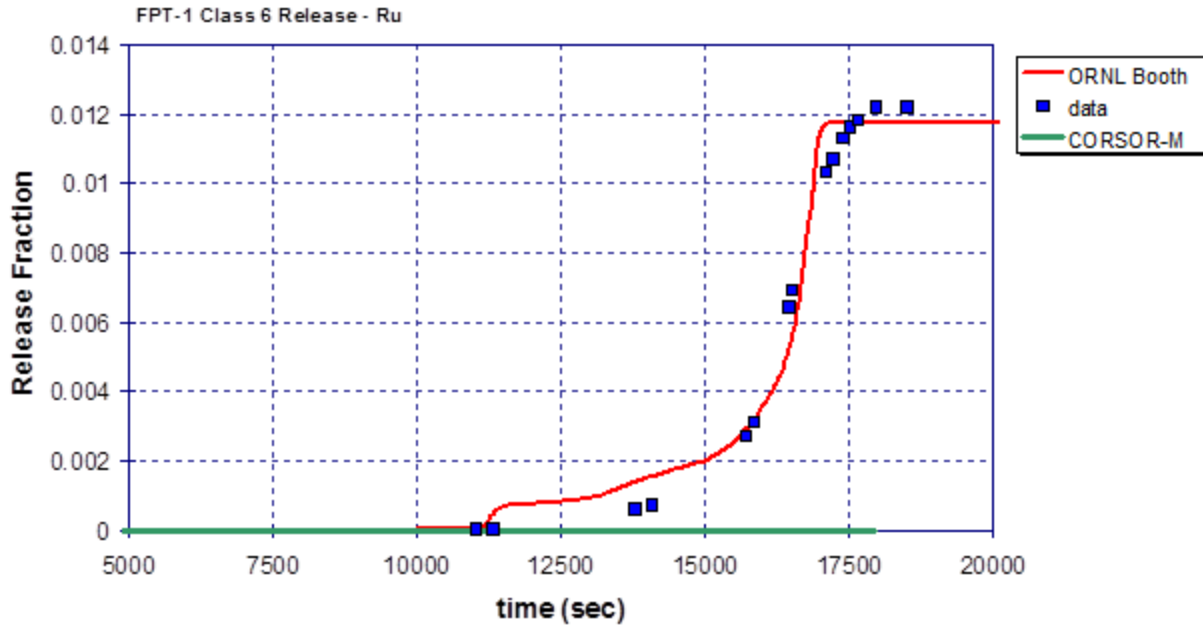
Figure 3-15   Comparison of ORNL-Booth versus CORSOR-M for Ru release (Class 6)
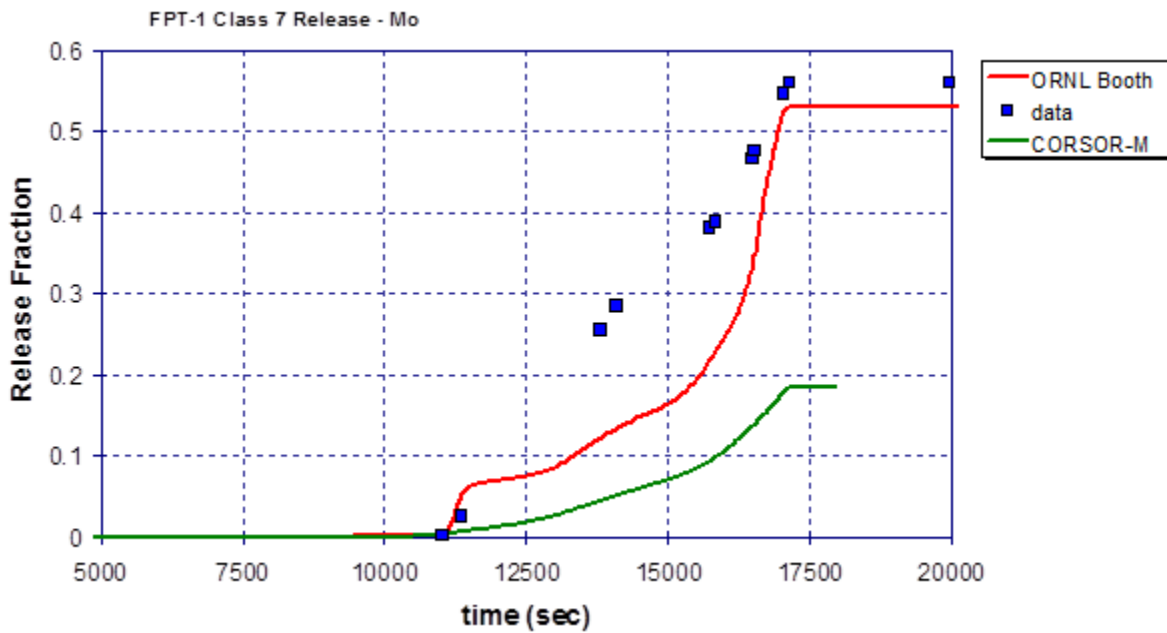
Figure 3-16   Comparison of ORNL-Booth versus CORSOR-M for Mo release (Class 7)
[Note: The Mo vapor pressure was set to correspond to Cs_2MoO_4.]
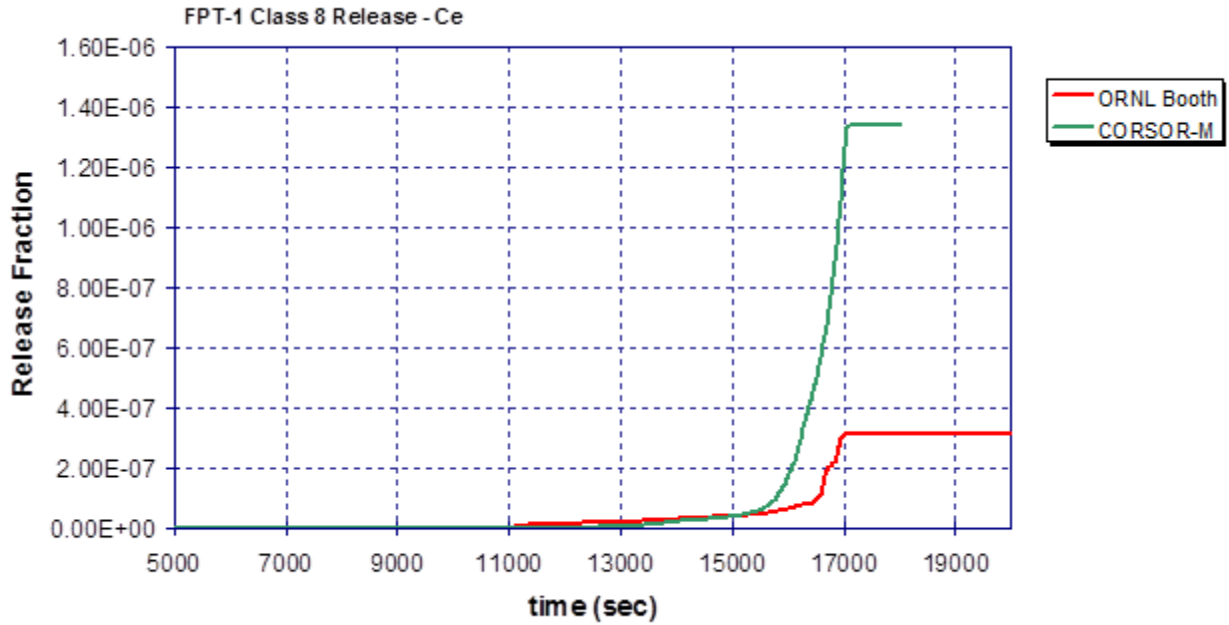
Figure 3-17   Comparison of ORNL-Booth versus CORSOR-M for Ce release (Class 8)
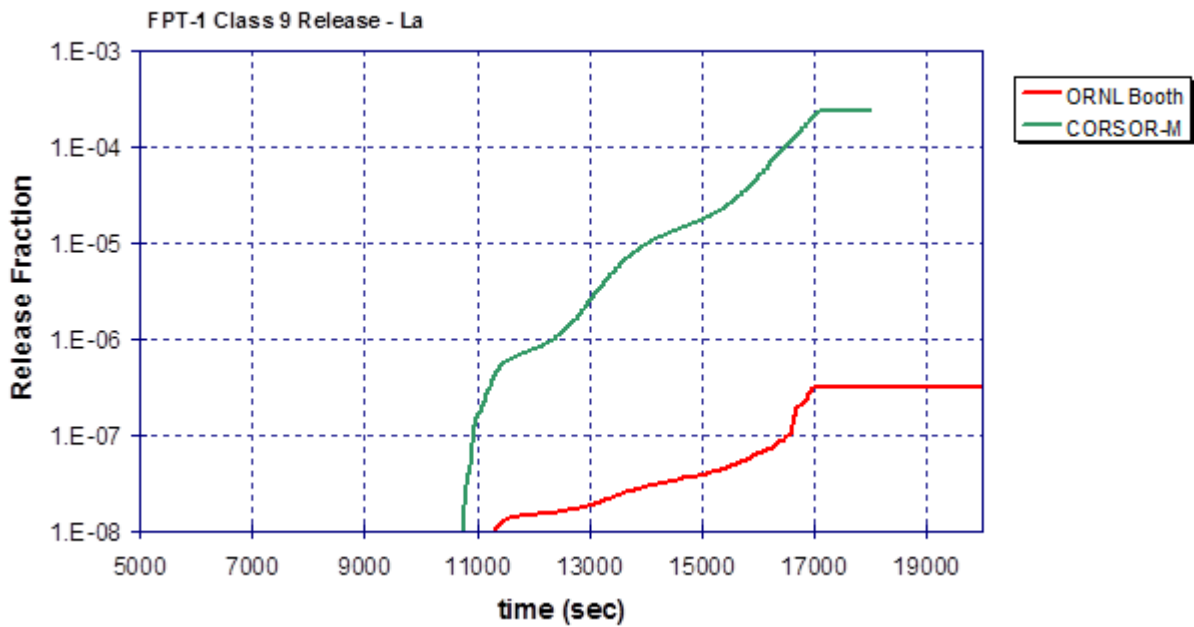
Figure 3-18   Comparison of ORNL-Booth versus CORSOR-M for La release (Class 9)
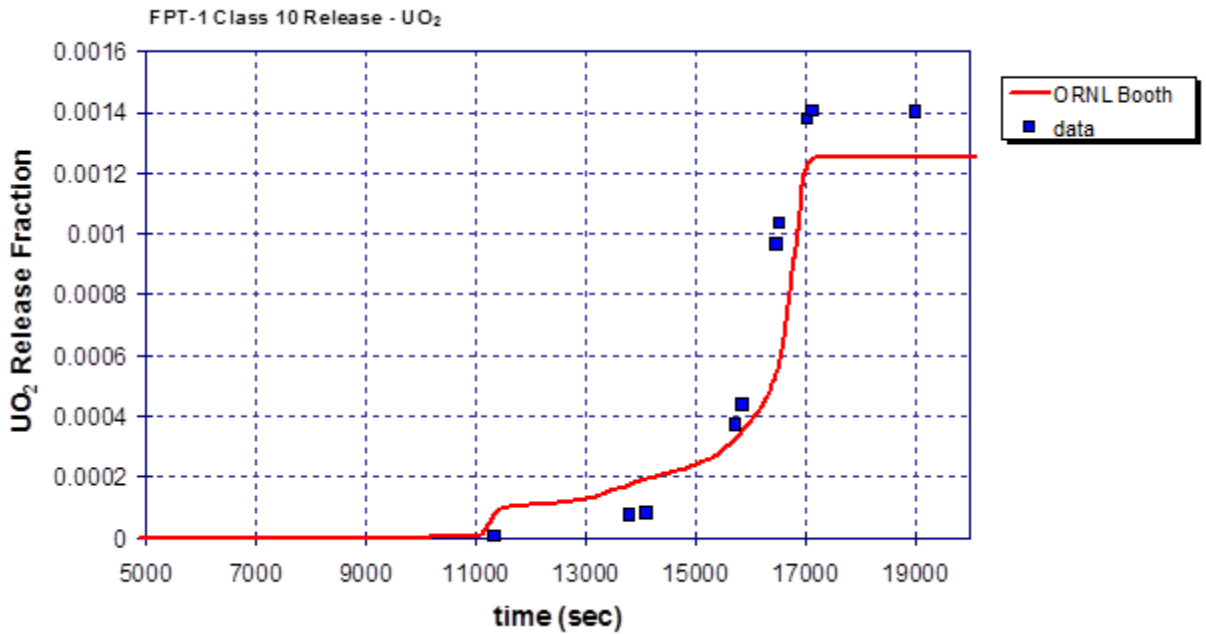
Figure 3-19 Comparison of ORNL-Booth versus CORSOR-M for UO₂ release (Class 10)
[Note: The UO₂ scaling factor was adjusted to match observed releases. La and Ce releases are not expected to be greater than UO₂ release, but may be less, owing to lower volatility.]
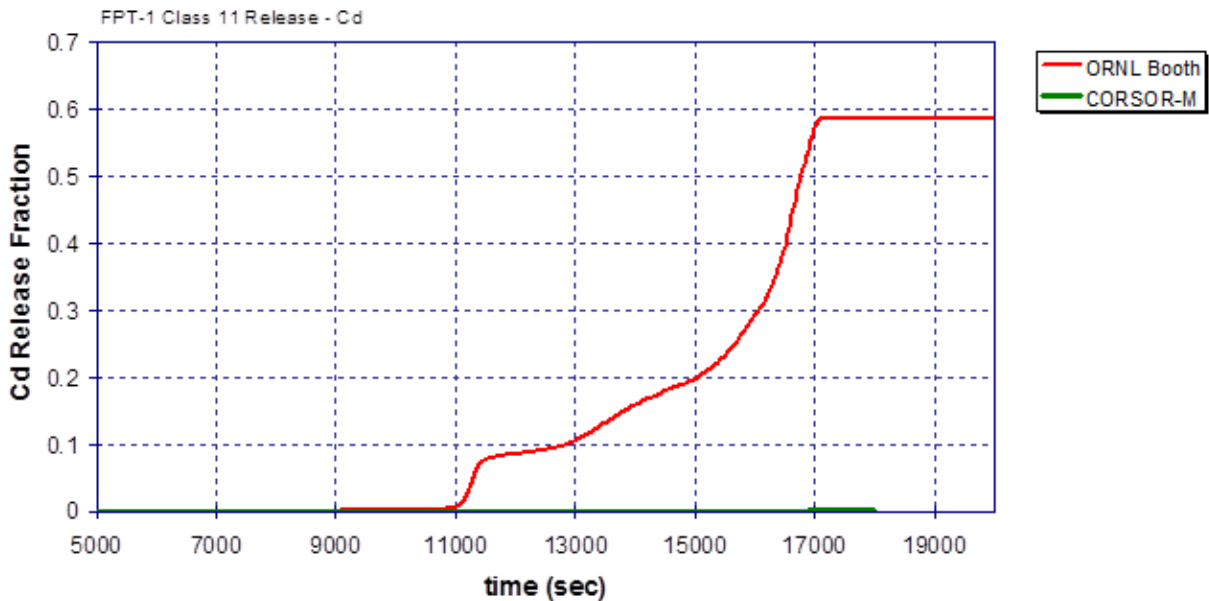
Figure 3-20 Comparison of ORNL-Booth versus CORSOR-M for Cd release (Class 11)

FPT-1 Class 12 Release (Sn)
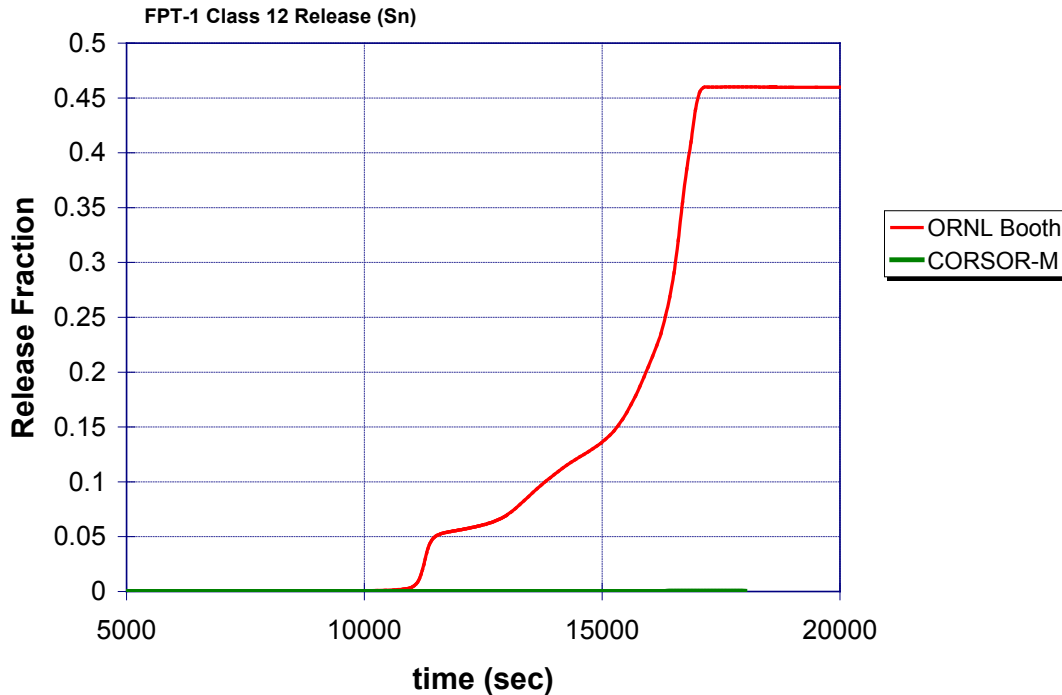
Figure 3-21   Comparison of ORNL-Booth versus CORSOR-M for Sn release (Class 12)

Comparison to ORNL VI Tests and VERCOR Tests [16]

After optimizing the ORNL-Booth fission product release parameters for the FPT-1 experiment, it was useful to compare the modified model to the original ORNL test data upon which the CORSOR-M model was developed. The following section explores the application of the modified ORNL-Booth release modeling to selected ORNL-VI test results and the VERCORS test data. The comparisons are made mainly to the Cs release observed in these experiments since all other releases are simply scaled to the Cs release in the Booth implementation in MELCOR, and these data were readily available. In the case of VERCORS 4, more data on release of other fission products were readily available and comparisons to these releases included. The MELCOR models were obtained from a Nuclear Safety Institute of the Russian Federation (IBRAE) MELCOR validation exercise [17] investigating the MELCOR default release models. The experimental data are taken from Reference [17]. These analyses were performed using a MELCOR model of these simple experiments. The present analyses make use of the modified ORNL coefficients and compare results with the MELCOR default CORSOR-M release model. A schematic of the VERCORS testing facility is shown in Figure 3-22; the general layout is similar in the ORNL VI tests. The tests examined are summarized in Table 3-4. The tests involved both oxidizing and reducing conditions.
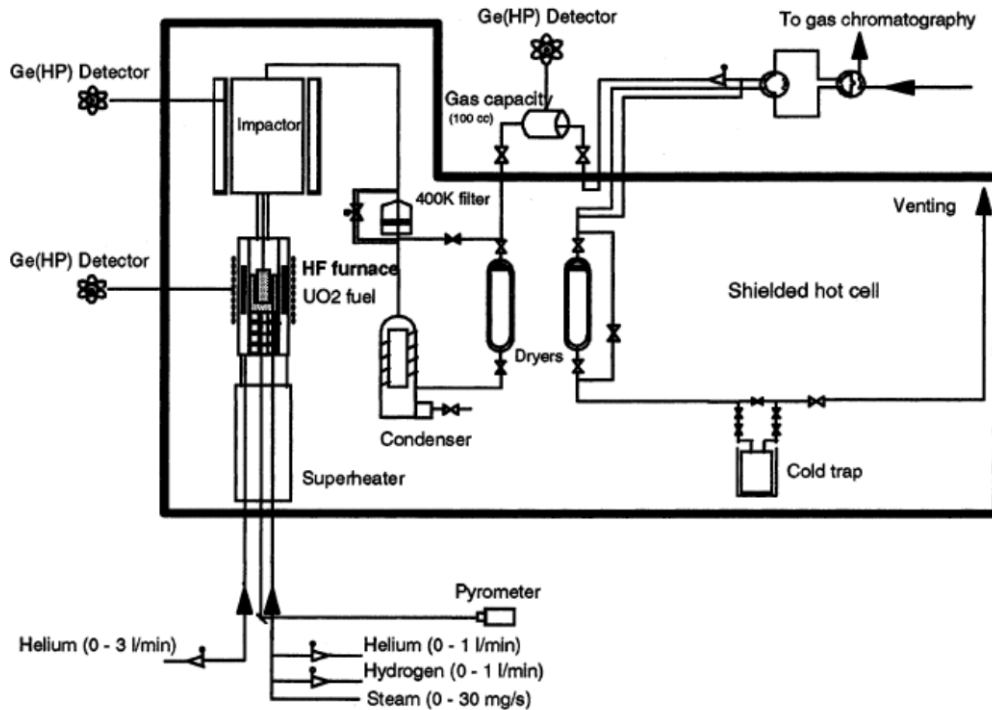
Figure 3-22   Schematic of VERCORS Test Facility for measuring fission product release from small fuel samples

Table 3-4   Test conditions for selected ORNL VI tests and VERCORS tests.

Test	Hydrogen	Steam	Max Temperature
ORNL VI-2	0	1.8 liter/min	2300 K
ORNL VI-3	0	1.6 liter/min	2700 K
ORNL VI-5	0.4 liter/min	0	2740 K
VERCORS 2	0.027 gm/min	1.5 gm/min	2150 K
VERCORS 4	0.012 gm/min	1.5 – 0 gm/min	2573 K

In almost all cases, the modified ORNL-Booth model produces improved signatures, as shown in Figure 3-23 through Figure 3-25 for the VI tests and in Figure 3-26 through Figure 3-32 for the VERCORS tests.

In test VI-2 run under steam conditions, the peak temperature attained was ~2300 K. Both models over predicted the Cs release for this test, with the modified ORNL-Booth treatment performing slightly better (Figure 3-23). Test VI-3 was similar to VI-2 except that higher temperatures were attained. In this test, both models were closer to the data, and again the modified ORNL-Booth model performed somewhat better (Figure 3-24). From these two tests, it would seem that the release rate in the 2300 K range is still slightly over predicted for oxidizing conditions. Test VI-5 conducted under reducing conditions was well predicted by both models, as shown in Figure 3-25. Table 3-5 through Table 3-7 provides total releases predicted by CORSOR-M and ORNL-Booth compared with totals reported for the ORNL VI tests 2, 3 and 5.

Both VERCORS 2 and 5 were run in mixed conditions with both steam and hydrogen. In VERCORS 5, the steam flow was reduced to zero (reducing conditions) for the high temperature plateau. Test VERCORS 2, like ORNL VI–2 was performed at a lower temperature and produced a comparatively lower Cs release (Figure 3-26). The modified ORNL-Booth model captured this lower release where the CORSOR-M model did not. Test VERCORS 4 was performed under completely reducing conditions during the release phase. In this case CORSOR-M under predicted the release, whereas the modified ORNL-Booth model captured the release behavior reasonably well.
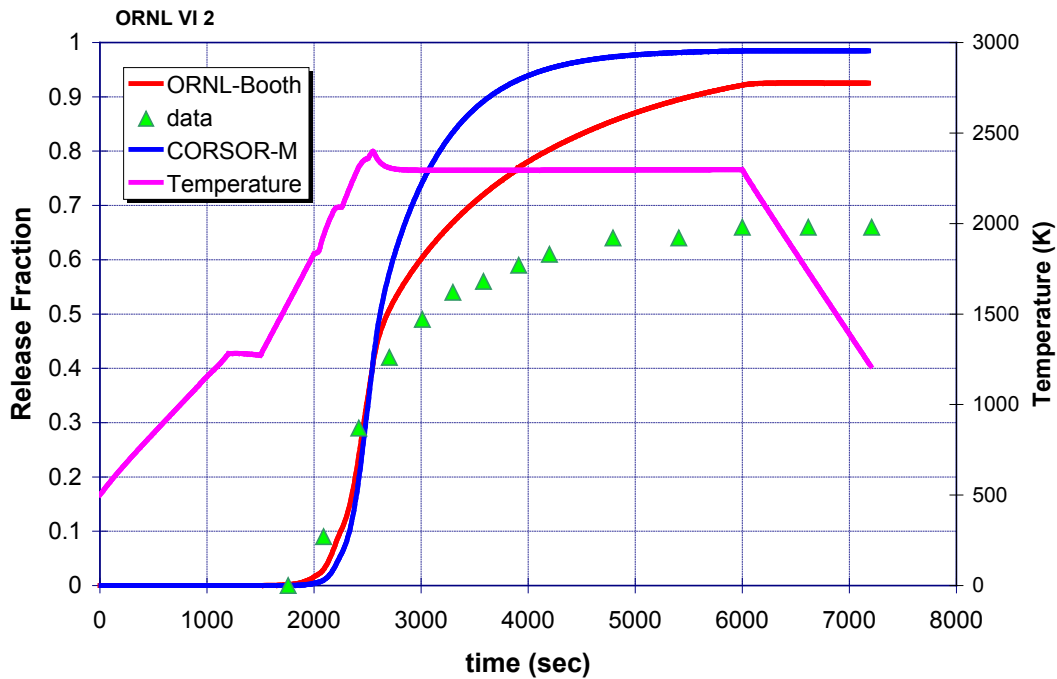
Figure 3-23   Comparison of Cs release for modified ORNL-Booth with CORSOR-M for VI-2 run under steam oxidizing conditions
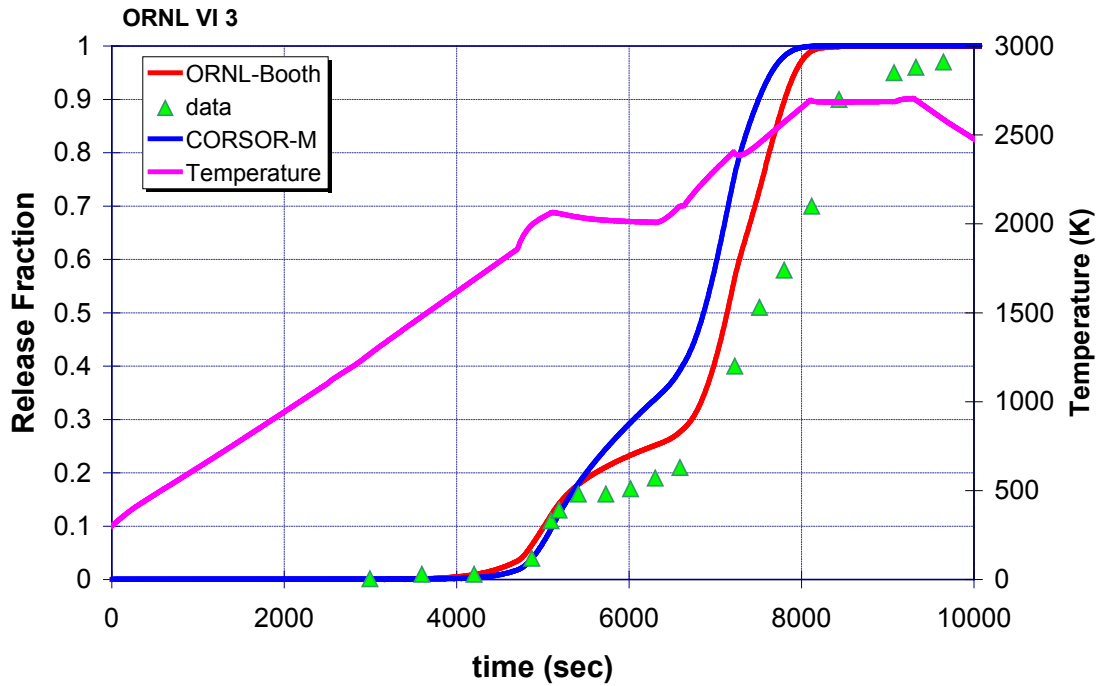
Figure 3-24   Comparison of Cs release for modified ORNL-Booth with CORSOR-M for VI-3 performed under steam oxidizing conditions
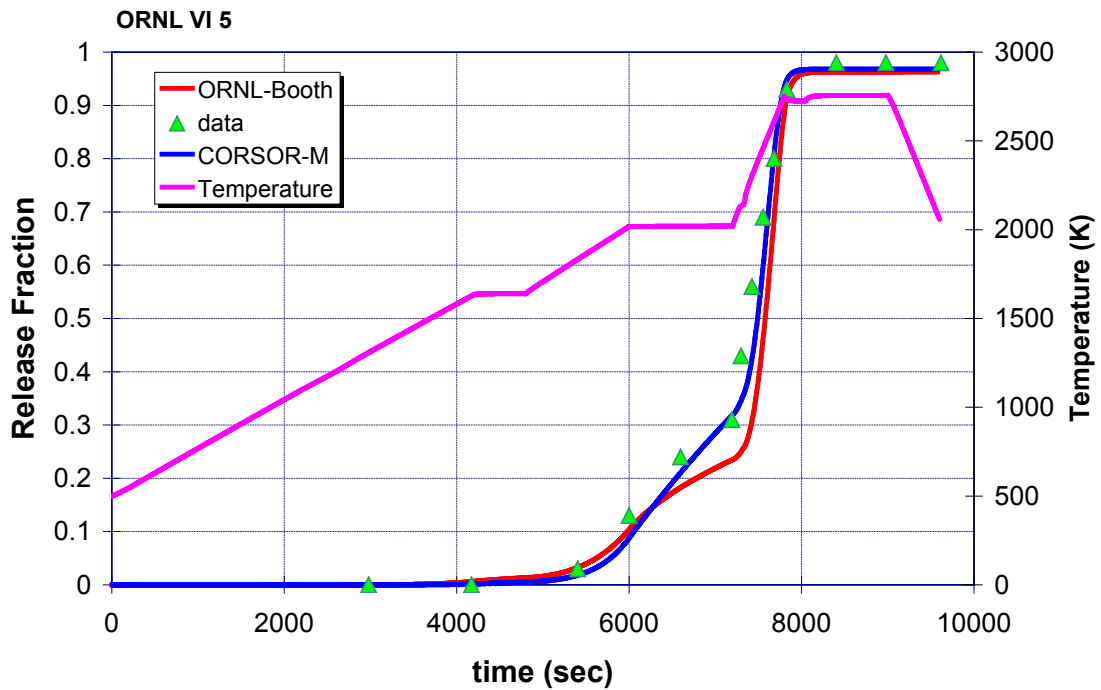
Figure 3-25   Comparison of Cs release for modified ORNL-Booth with CORSOR-M for VI-5 performed under steam reducing conditions

Table 3-5   Release fraction from ORNL VI-2.[7]

	Experiment	CORSOR-M	ORNL-Booth
Kr	-	0.98	0.92
Cs	0.67	0.98	0.92
Ba	0.18	0.003	0.002
Sr	-	0.003	0.002
I	0.4	0.98	0.81
Te	-	0.97	0.81
Ru	-	1×10^{-7}	0.006
Mo	0.86	0.06	0.42
Ce	-	1×10^{-8}	1.1×10^{-7}
Eu	-	1×10^{-5}	1.1×10^{-7}
U	0.003	1×10^{-5}	0.001
Sb	0.68	0.04	0.93

Table 3-6   Release fraction from ORNL VI-3.

	Experiment	CORSOR-M	ORNL-Booth
Kr	1	1	1
Cs	1	1	1
Ba	0.3	0.04	0.004
Sr	0.03	0.04	0.004
I	0.8	1	1
Te	0.99	1	0.99
Ru	0.05	10^{-5}	0.03
Mo	0.77	0.15	0.88
Ce	0	2×10^{-6}	4×10^{-7}
Eu	0	0.0005	4×10^{-7}
U	0	0.0005	0.003
Sb	0.99	0.2	0.93

Table 3-7   Release fraction from ORNL VI-5.

	Experiment	CORSOR-M	ORNL-Booth
Kr	1	0.97	0.96
Cs	1	0.97	0.96
Ba	0.76	0.04	0.005
Sr	0.34	0.04	0.005
I	0.7	0.97	0.96
Te	0.82	0.95	0.96
Ru	0	10^{-5}	0.03
Mo	0.02	0.11	0.85
Ce	0.02	3×10^{-6}	4×10^{-7}
Eu	0.57	0.0008	4×10^{-7}
U	0	0.0008	0.003
Sb	0.18	0.19	0.89

[7] NUREG/CR-6261 provides a summary of the ORNL VI and HI test series; however, unreported release fractions are present for some elements. The missing data are represented with a '-' in Table 3-5.
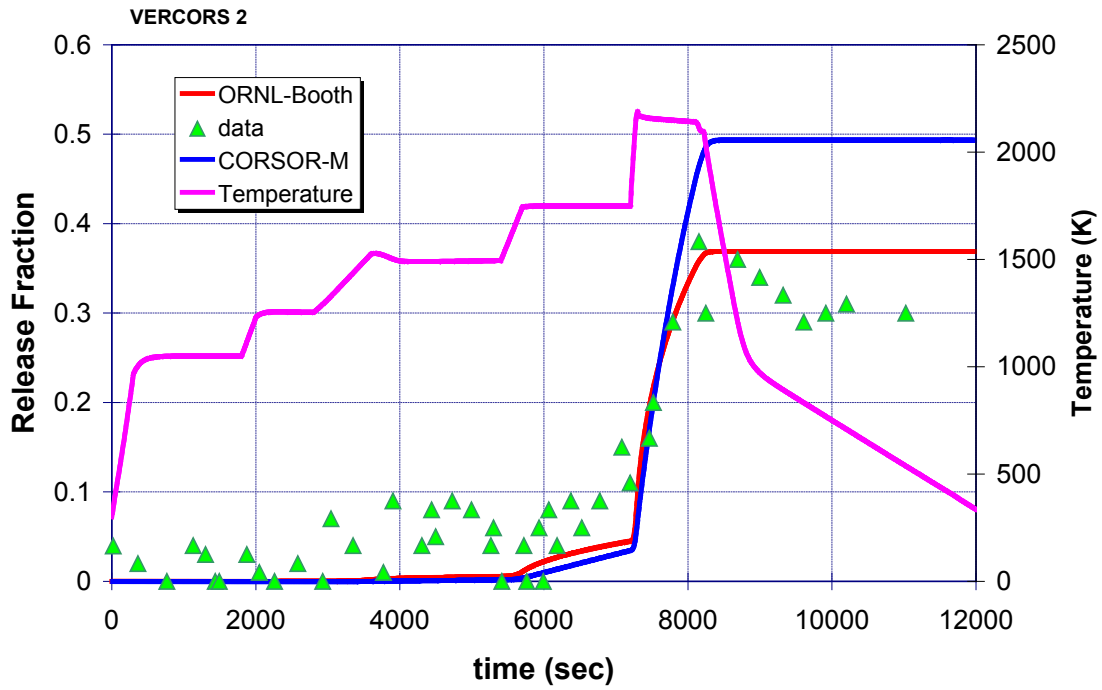
Figure 3-26   Comparison of Cs release for modified ORNL-Booth with CORSOR-M for VERCORS-2
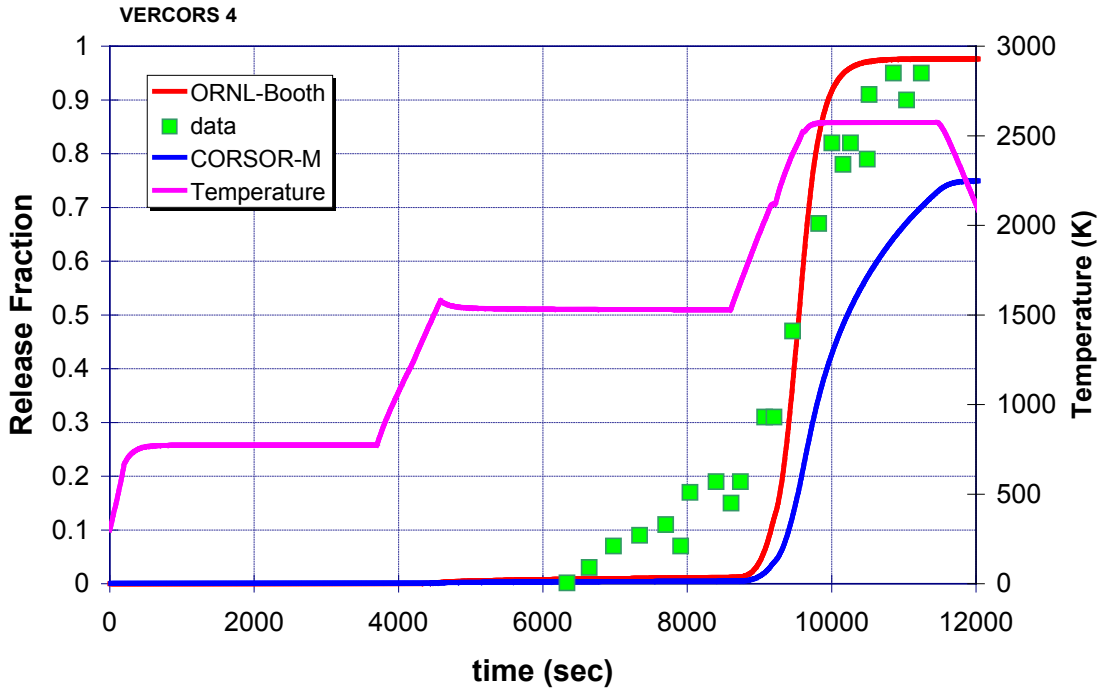
Figure 3-27 Comparison of Cs release for modified ORNL-Booth with CORSOR-M for VERCORS-4
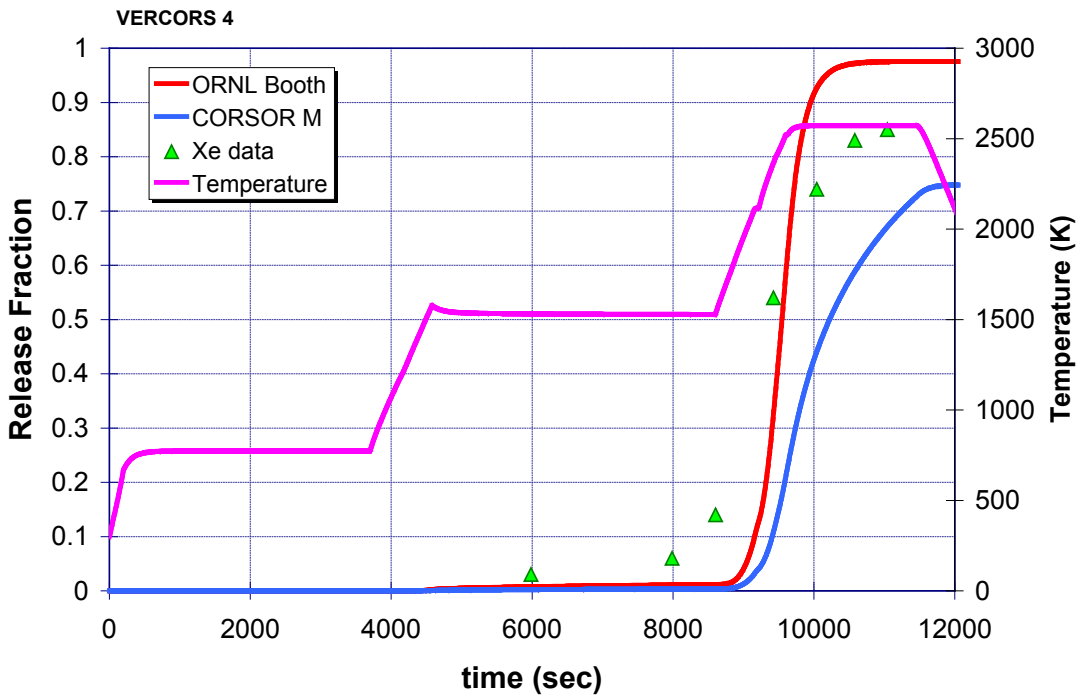
Figure 3-28 Comparison of Xe release for modified ORNL-Booth with CORSOR-M for VERCORS-4
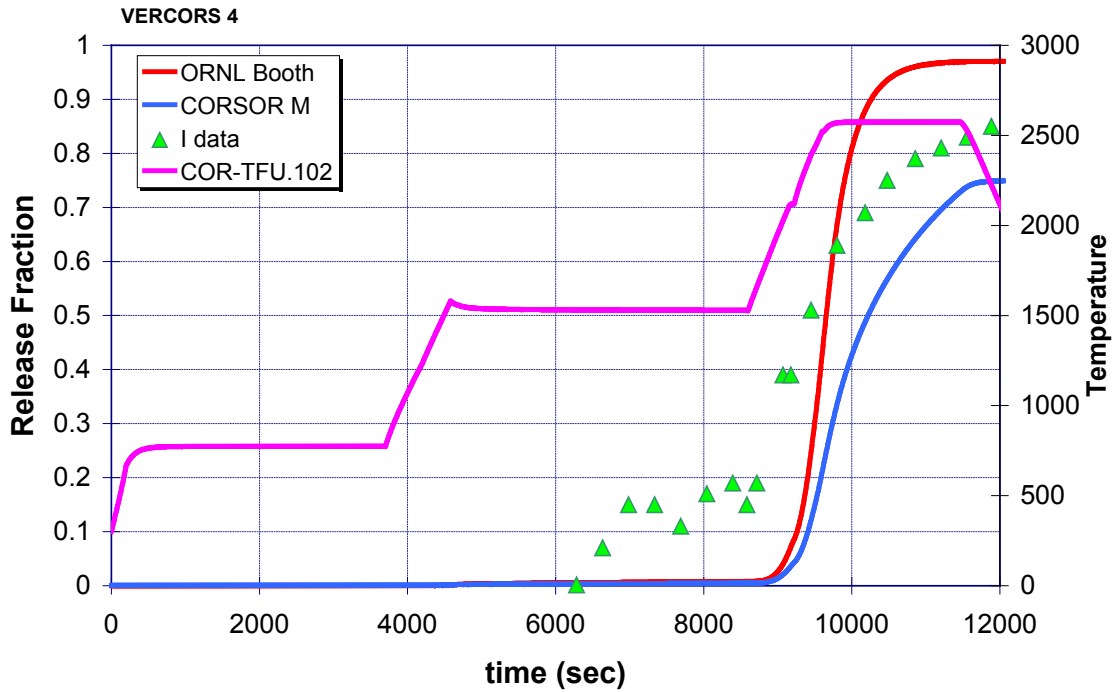
Figure 3-29   Comparison of Iodine release for modified ORNL-Booth with CORSOR-M for VERCORS-4
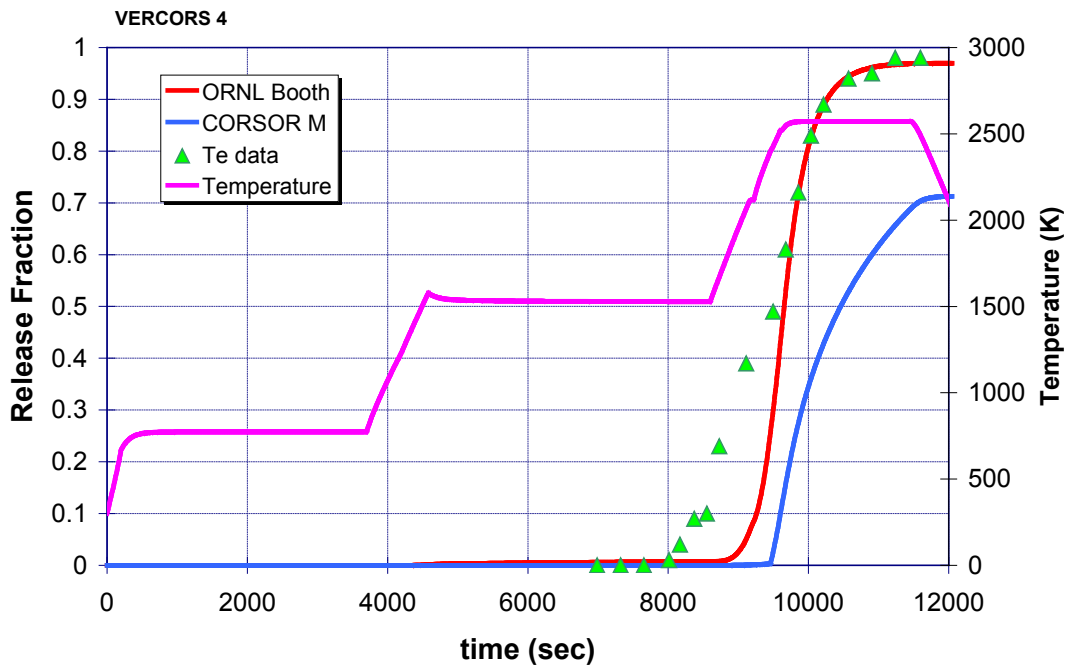
Figure 3-30   Comparison of Te release for modified ORNL-Booth with CORSOR-M for VERCORS-4
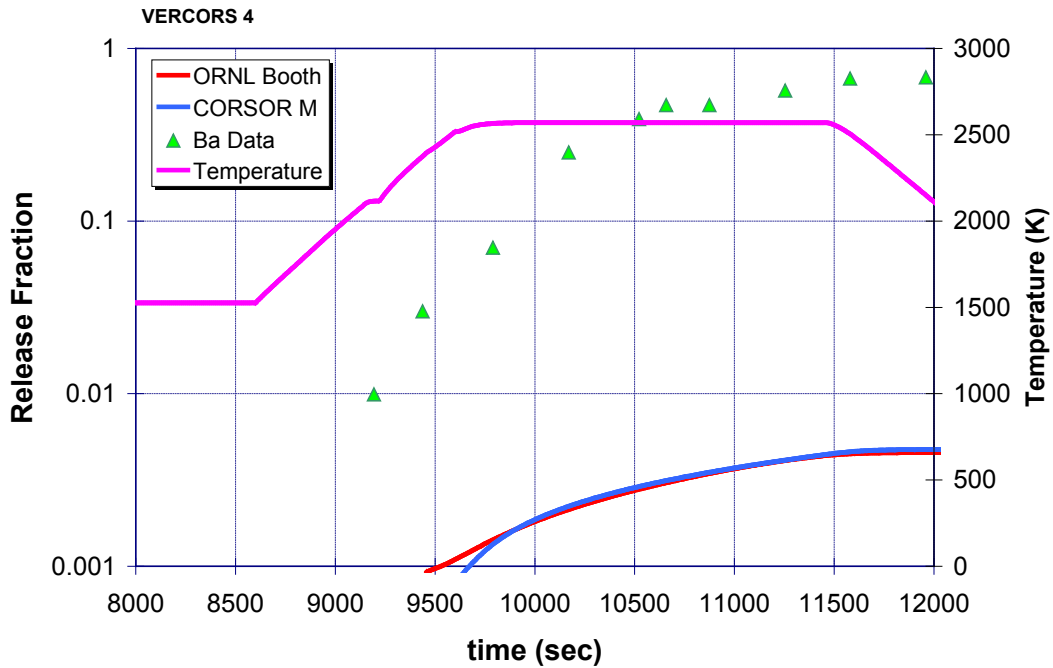
Figure 3-31   Comparison of Ba release for modified ORNL-Booth with CORSOR-M for VERCORS-4
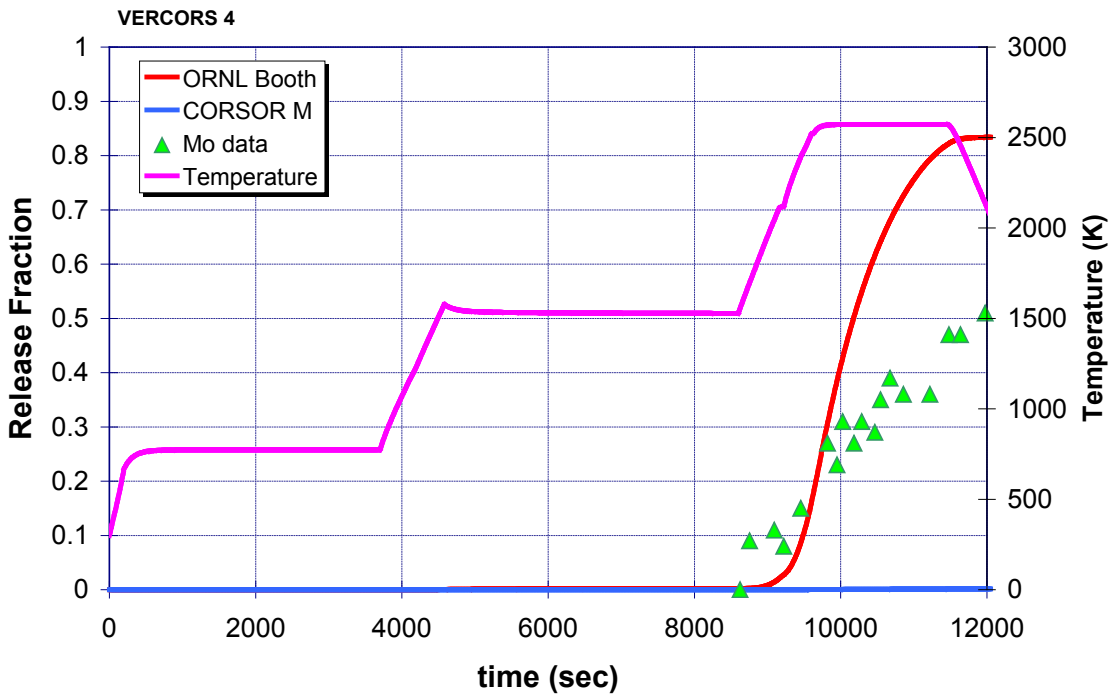
Figure 3-32   Comparison of Mo release for modified ORNL-Booth with CORSOR-M for VERCORS-4

The use of the modified ORNL-Booth model produces significantly improved predictions for both the in-pile Phebus FPT-1 test as well as for the original small scale ORNL VI and French VERCORS tests upon which the original CORSOR and Booth models were developed. Barium behavior however remains somewhat problematic in that the small-scale tests generally predict Ba release greater than is ever observed in the in-piles tests. It is believed this is due to the fact that in the small-scale tests, the cladding is almost completely oxidized, whereas considerably less coherent conditions are encountered in the in-pile integral tests. It is conjectured that the Ba speciation in the small-scale tests is more volatile than that produced in the in-pile tests where unoxidized Zr is plentiful.

Given the overall improvement realized in application of the modified ORNL-Booth model, user selection of the modified ORNL-Booth model is accepted as the best practice.

3.1.1.5   Evaluation of Fission Product Deposition Modeling and Speciation

Deposition in FPT-1 Circuit (RCS Deposition)
The modified ORNL-Booth release models have been shown to produce favorable release signatures when examining the Phebus FPT-1 test and produce good comparisons with the ORNL VI and French VERCORS tests. The modifications to the vapor pressures for Cs and Mo, which produced favorable release behavior in FPT-1, will have an effect on the subsequent deposition of these species in the RCS piping. The effect is illustrated in the following two figures showing deposition patterns in the Phebus FPT-1 test circuit and model containment.

Figure 3-33 shows the predicted deposition distribution in the FPT-1 experiment when the default CORSOR-M release model was used. While the total Cs release compares reasonably well with the measured value, and the total Cs transported to the containment is about right, the distribution of Cs deposits in the heated test section above the fuel (upper plenum) and in the steam generator tube do not compare well with the experiment. Deposits in the steam generator are over predicted and deposits in the heated plenum above the fueled region are under predicted. In fact, deposits of Cs in the plenum were never greater than 0.1% and were predicted to be completely revaporized before the end of the test. Under predicting deposition in the hot plenum region is a big factor in the over predicting of the steam generator tube deposits.

Figure 3-34 shows the Cs distribution predicted for FPT-1 when the modified ORNL-Booth model is used. The lower vapor pressure of the presumed Cs_2MoO_4 results in Cs predicted to be in aerosol form in the hot upper plenum region and as a result, Cs deposited in the upper plenum remains for the duration of the test. This together with a slightly lower total Cs release results in half as much predicted to be deposited in the steam generator tubes, considerably closer to the observed tube deposition. The amount reaching the containment remains about the same, which from a "release to the environment" point of view, one can observe that either model retains about the right amount of fission products within the simulated RCS. The changes in Cs deposition within the RCS could alter the decay heat distributions throughout the RCS, which in turn could affect revolatilization of other more volatile deposited species, such as CsI, which is transported in addition to the presumed dominant Cs_2MoO_4.
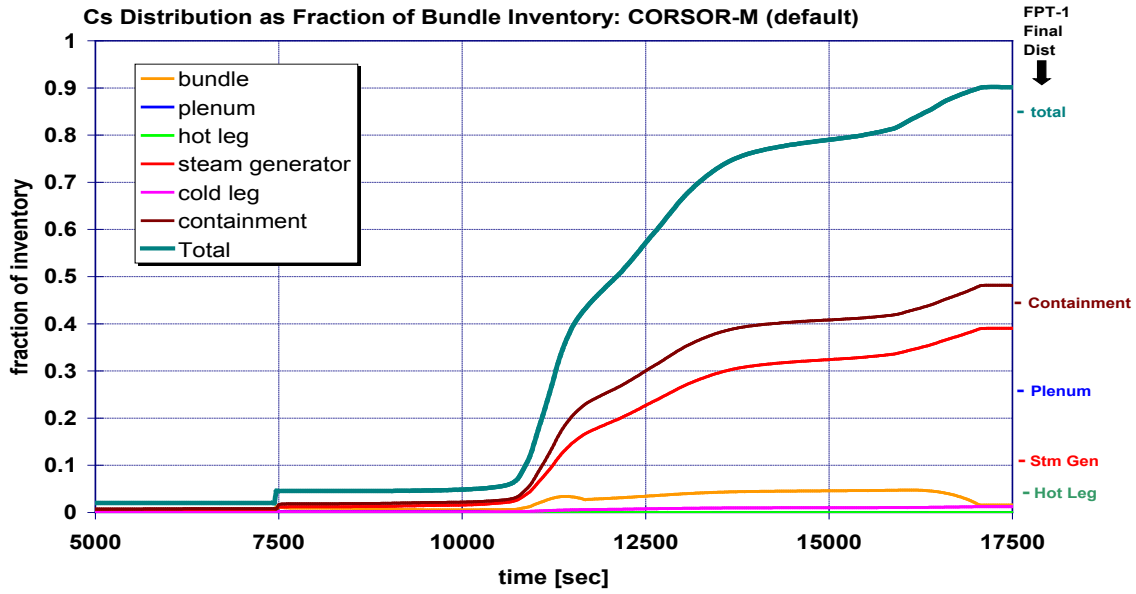
Figure 3-33   MELCOR-predicted fission product deposition in FPT-1 circuit using default CORSOR-M release modeling
[Note: Predicted plenum deposits for this case were less than 0.1 percent, not visible on this scale, and were subsequently revaporized.]
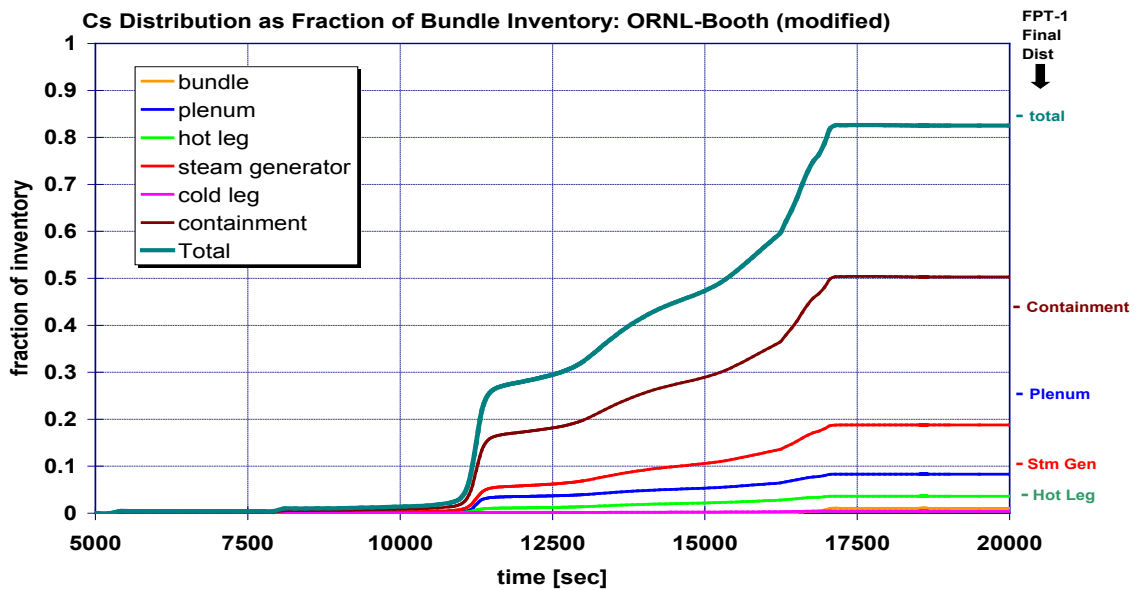
Figure 3-34   MELCOR-predicted fission product deposition in FPT-1 circuit using default ORNL-Booth release modeling

Deposition within the Phebus Containment
For completeness, the deposition behavior calculated for the FPT-1 containment model is
shown in the following figures. Shown is the total airborne aerosol mass predicted using the
sources resulting from the ORNL-Booth release modeling. The suspended mass is normalized
to the peak value in order to make comparison to the measured data; this normalization was
made necessary because of differences between the magnitude of mass predicted to be
transported to the containment and the measured value. MELCOR predicted only about half of
the suspended total mass that was measured. The discrepancy is due to not activating the Ag
release model for the Ag/In/Cd control rods and the rhenium (Re) in the experiment
thermocouples.

The overall depletion signature prior to the peak airborne value compares quite well. After
reaching the maximum value however, the MELCOR predicted suspended mass depletes less
rapidly than was actually observed. This is apparently due to MELCOR under predicting the
particle size as shown in Figure 3-36, and consequently under predicting the gravitational
settling component of containment deposition. Certainly the under prediction of the suspended
mass by a factor of two also resulted in lower aerosol number concentration, perhaps
significantly so if the mass is missing from the smaller particle size range, and this may in turn
have resulted in slower particle agglomeration rate and therefore smaller agglomerated particle
sizes. If so, this could explain the lower aerosol depletion rate by gravitational settling.

Diffusiophoresis is the other dominant form of aerosol deposition in the FPT-1 containment, and
may also be under predicted; however, test data do not provide resolution in this respect.
Under prediction of the containment depletion rate errs on the conservative side since more
fission products remain suspended in this analysis that might be available for release to the
environment.
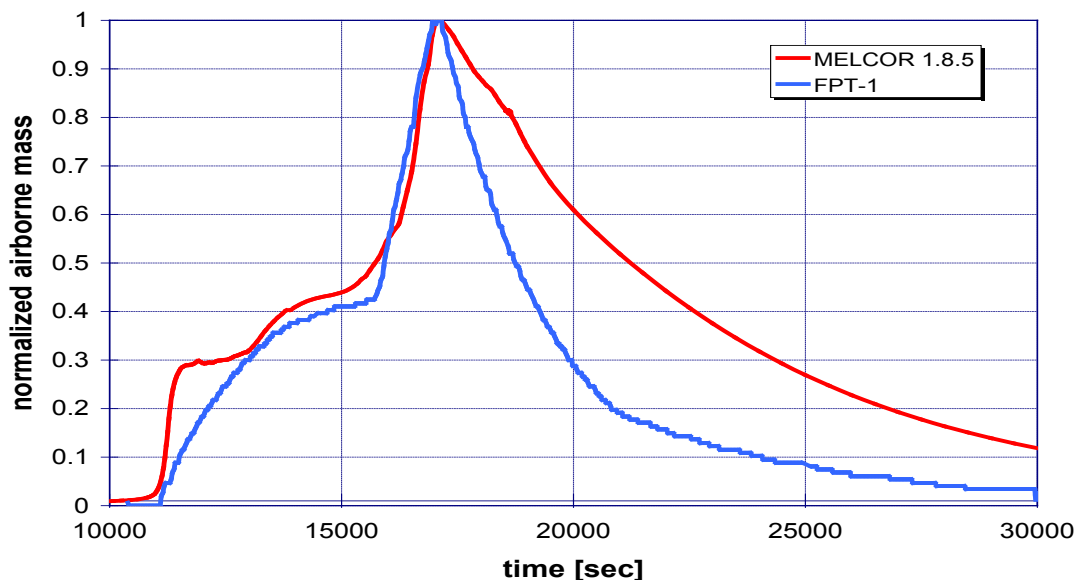
Figure 3-35   Normalized aerosol depletion rate of airborne aerosol in FPT-1 containment
*[Note: The under prediction of gravitational settling may be the reason for the low
prediction of the depletion rate.]*
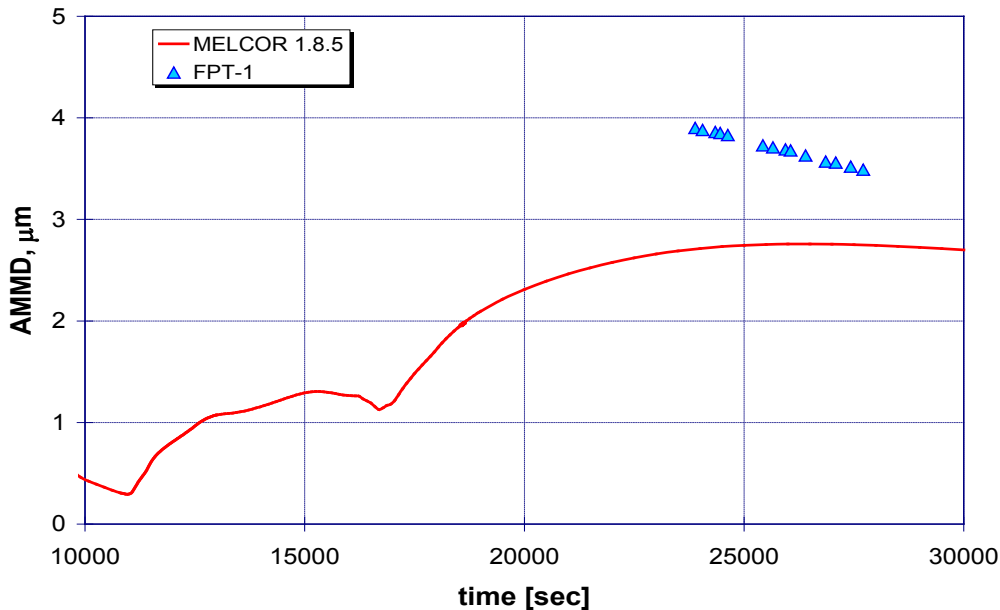
Figure 3-36 **Predicted and measured aerodynamic mass mean aerosol diameter in FPT-1 containment**

[Note: Under prediction of the agglomeration rate from too low of an airborne total mass may be responsible for the under prediction of the mean particle size.]

New Speciation Modeling[8]

Based on the chemical analysis of fission products deposited throughout the simulated reactor coolant circuit and containment of the Phebus facility, significant amounts of molybdenum were transported. This was unexpected because molybdenum has a low vapor pressure and was not expected to be released in large quantities. However, the molybdenum combined with the cesium and formed cesium molybdate. The vapor pressure of cesium molybdate is much higher than molybdenum (see Figure 3-5). In light of the Phebus findings, the chemical speciation of cesium was updated for the SOARCA project.

Prior to the Phebus experiments, the common cesium speciation practice was to combine all available iodine with the required amount of cesium to form Class 16 (cesium iodide) and place the remaining cesium in Class 2 (cesium hydroxide). To incorporate the Phebus findings, Class 17 has been created to accommodate cesium molybdate. The new speciation of cesium still combines all available iodine with cesium as cesium iodide but the remaining cesium is combined with molybdenum to form cesium molybdate with the exception of a small portion of cesium allocated to Class 2 (cesium hydroxide).

In summary, the best practice speciation manually reconfigures (i.e., through user input specifications) the radionuclide and decay heat classes that contain cesium, iodine, and/or molybdenum as follows:

---

[8] Whereas, the recent modifications to Version 1.8.6 (Version YR) for the SOARCA project implemented the new ORNL-Booth fission product release model as the new default model (see Section 3.1.1.4), the associated reconfiguration of the radionuclide masses must be done through user input specification as summarized in this section.

- Class 2 – Characteristic released compound is CsOH with the default inventory representative of the cesium in the fuel–cladding gap (5% of the initial core inventory of cesium)

- Class 7 – Characteristic released compound is Mo with the default inventory reduced by the amount allocated to Class 17

- Class 16 – Characteristic released compound is CsI with the default inventory representing all iodine and the necessary cesium to combine with the iodine to form CsI

- Class 17 – Characteristic released compound is Cs_2MoO_4 with the cesium not in the gap (included in Class 2) and not combined with iodine in Class 16, combined with the necessary molybdenum to form this class

The prescribed user defined definition of the fuel–cladding gap inventory is specified as follows [18]:

- Class 1 – 5% of the noble gases

- Class 2 – 100% of this class equating to the amount of cesium needed additional to the cesium allocated to the gap as CsI (in Class 16) to raise the total cesium in the gap to 5% of the total core inventory

- Class 3 – 1% of the barium inventory

- Class 5 – 5% of the tellurium inventory

- Class 16 – 5% of the CsI inventory

3.1.1.6 Release of Structural Aerosols

Experimental measurements of aerosol release and transport during fuel assembly melting consistently show significant releases of non-radioactive species such as tin and (in PWR assembly experiments) Ag-In-Cd. The former is released primarily from fuel cladding (tin is an alloy constituent of Zircaloy); the latter is released from (PWR) control rods. MELCOR includes specialized models to vaporize Ag-In-Cd control materials from PWR control rods. The control material is subsequently tracked in the RN like other radionuclides. The control rod radionuclide model was used in the SOARCA project and is recommended for PWRs. However, MELCOR does not include a release model for tin from the Zircaloy.

The release of tin from the Zircaloy was included using the in-vessel radionuclide release model of "non-fuel" materials in the Core (COR) Package, which is enabled through user input. However, the in-vessel structural release model is not a mechanistic treatment of diffusion and release of volatile constituents from core structures. Rather, the model provides a simple framework for extending the CORSOR models for radionuclide release to examine the effects of the additional mass associated with aerosols generated during the oxidation and melting of cladding and control rod guide tubes. The tin structural release model was tuned to match observations from experiments.

First, the structural aerosol release model requires specification of non-fuel materials recognized by the COR Package to an RN class. The structural aerosols are specified from the

list of materials tracked in the COR Package. The structural materials available for conversion include the following:

- Unoxidized zirconium
- Zirconium oxide
- Unoxidized steel associated with control rods (blades)
- Oxidized steel associated with control rods (blades)
- Control rod poison

The fraction of the total mass of each of these materials that is available as a potential aerosol source is defined. In principle, this fraction should represent the mass <u>fraction</u> of volatile constituents in the material. This information is specified on input records for card RNCRCLxx.

The release rate associated with core structure materials is estimated using the active RN fission product release model (i.e., the user-selected version of CORSOR.) Scalar multipliers are applied to CORSOR to represent differences in the release rates associated with migration through a UO_2 matrix versus Zircaloy, steel, or other core structural materials. The CORSOR release rate multipliers are specified via sensitivity coefficient 7100. The temperature used to calculate the release rate of a particular material is tied to the corresponding structure temperature in the COR Package (i.e., zirconium to fuel cladding, and steel plus control poison to non-supporting structure.)

Modeling the evaporation and release of control poison in BWRs is not a concern because the vapor pressure of boron carbide is very high (sublimation occurs at temperatures above 2500°C). However, release of non-radioactive vapor and aerosols due to chemical reactions between B_4C and steam is modeled by the B_4C oxidation model in the COR Package. The mass of vapor species generated by these reactions is transferred to the CVH Package for transport; the mass of condensed aerosols (primarily B_2O_3) is transferred to the RN Package for transport.

A significant limitation of the non-fuel release modeling framework in MELCOR is that the mass of materials represented in the COR Package is not decremented to reflect the amount sourced to the RN Package. Further, there is no numerical limit to the amount of structural aerosol that can be generated for a given core material. Therefore, material fractions and CORSOR release rate multipliers must be defined carefully to prevent non-physical results.

No direct experimental information on release rates of core structural materials is available to aid in selecting appropriate multipliers for the non-fuel release option in MELCOR. Realistic values for the volatile mass fraction of tin in Zircaloy were used, namely 1.45 wt/%. Based on the observations made by R. Gauntt [60], the release rate of tin from unoxidized Zr was assumed to be a factor of ten smaller than the rate from ZrO_2 (i.e., SC7100 = 0.1 for Zr and 1.0 for ZrO_2).

The non-fuel release model is tied to the particular model for fission product release selected for a calculation. Reasonable values of the integral release were achieved using unmodified CORSOR release coefficients (i.e., the same as fission product release from fuel). Depending on the particular release expression used, the total quantity of structural tin released ranges from 18 to 47 percent of the total available as an alloy agent in Zircaloy fuel cladding. It is recommended to assign the released structural tin aerosols a separate RN class dedicated for structural aerosols.

3.1.1.7   Vessel Lower Head Failure and Debris Ejection

The base case approach for modeling lower head failure (LHF) of the vessel and debris ejection includes some special non-default modeling options in MELCOR. A schematic of MELCOR's lower head heat transfer model is shown in Figure 3-37. The solid debris convects to the lower head wall. Solid debris in the lower plenum is assumed to be wettable by lower plenum water, if present. Earlier versions of MELCOR included a one-dimensional model for the CCFL on water access to the debris. The one-dimensional CCFL greatly restricted the debris heat transfer and was highly susceptible to the lower plenum core cell nodalization (see core plate failure discussion). The new heat transfer model recognizes the potential for multi-dimensional flow patterns in the lower plenum without a one-dimensional CCFL restriction. Hence, the film and nucleate boiling debris bed-to-water heat transfer correlations are applicable for debris submerged under water.

Any molten debris will convect to the lower head using the molten debris bed heat transfer correlations. A separate lower temperature metallic molten pool (MP1) can exist as well as a higher melting temperature mixed oxide molten pool (MP2). There is two-dimensional radial and azimuthal conduction through the vessel wall. On the outer surface of the vessel, there is heat transfer to the flooded cavity using inverted cylindrical nucleate boiling correlations.

The other key modeling options include the method for modeling LHF and assumptions regarding the resultant discharge of debris. Penetration failure is not modeled as a mechanism for vessel failure. Rather, only gross creep rupture of the lower head is modeled. In the SNL LHF tests [19], gross creep rupture of the lower head was measured to be the most likely mechanism for vessel failure. In addition, past observations using MELCOR's penetration model suggest that it lacks sufficient spatial resolution to adequately model the multi-dimensional heat transfer effects (i.e., it is a relatively simple lumped capacitance model). The lower head creep rupture model uses the code's default settings. A Larson-Miller parameter is calculated using a one-dimensional temperature profile through the lower head. A cumulative strain is calculated using a lifetime rule and failure occurs with an 18% strain. Upon vessel failure, molten and solid debris are assumed to discharge simultaneously.
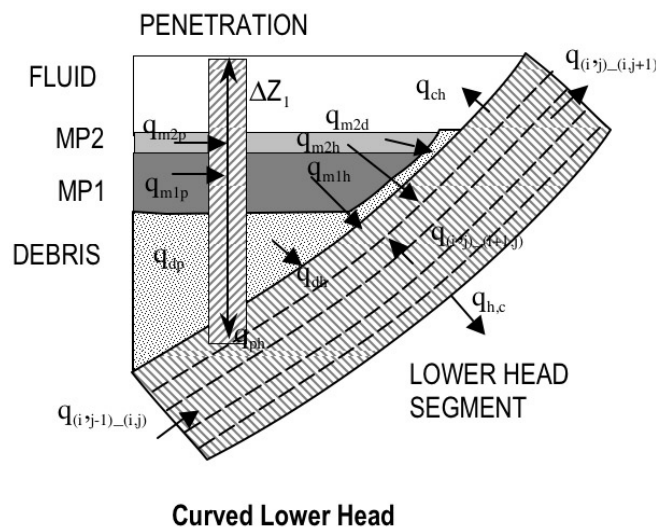
Figure 3-37   MELCOR lower head nodalization

3.1.1.8   Ex-vessel Phenomena - CCI and Hydrogen Combustion

Following vessel failure, molten core-concrete interactions (MCCI) will take place in the reactor cavity of the containment. If there is a pool of water in the reactor cavity, then there is simultaneous debris heat transfer to the overlying pool of water and into the concrete. If there is inadequate heat transfer to cool the debris, the debris will ablate the concrete and release combustible gases. However, if the debris is cooled below the concrete ablation temperature, then there is no combustible gas production and, therefore, no accompanying pressure loading and combustion potential.

The simplified one-dimensional geometric configuration of the debris underestimates heat fluxes observed in the Melt Attack and Coolability Experiments (MACE) program [20] when default MELCOR values are used. In particular, the MACE tests showed cracking of the crust with water ingression and multi-dimensional effects that greatly enhanced the amount of cooling when water was present, which was not considered within the MELCOR MCCI framework. As shown in Figure 3-38, the nominal heat flux calculated by MELCOR, represented by the 1*K curve, fails to agree with the MACE heat flux data, ranging between 1000-5000 kW/m^2. By enhancing conductivity by 10 to 100 times the original MELCOR calculated conductivity (K), improvement in agreement with the MACE data was observed. Modifications to the MELCOR code were performed giving users the ability to enhance the default MELCOR heat transfer calculations by specifying constant multipliers to the debris conductivity and surface heat flux (i.e., a method to reflect cracks and multi-dimensional effects). A 10x surface heat flux multiplier and 5x debris conductivity multiplier for oxide and metallic debris were used to enhance the ex-vessel debris-to-water heat transfer model and are the recommended best practice. The enhanced heat transfer increased the ex-vessel debris cooling while water was present which reduces the rate of concrete ablation. The concrete ablation rate was unchanged in cases where water was not present.

The default MELCOR combustion model was used by enabling the BUR Package, which is performed through user input. Special attention was made within the user input to include horizontal and vertical propagation of burns and the time delay for the flame front to span the width of the control volume. MELCOR does not include models for detonation. Hence, all burns are subsonic deflagrations with appropriate models for steam dilution, hydrogen and oxygen concentrations, and propagation to adjacent locations. Finally, in cases without an obvious ignition source, sensitivity calculations could be performed that delay combustion to simulate the occurrence of a spontaneous ignition source in the containment (e.g., debris ejection at vessel failure, reenergizing equipment, etc.). Delaying the ignition event would allow hydrogen and other combustion products to accumulate leading to more energetic burns. A user can model delayed ignition by adjusting the concentrations capable of supporting a deflagration event.

The associated structural damage from a hydrogen burn is simulated through user-specified failure paths. In SOARCA, plant walk-downs and separate structural assessments were performed for locations where hydrogen burns were considered possible. For the Surry calculations, this included the primary containment and the surrounding buildings for the interfacing systems loss of coolant accident (ISLOCA) scenario (i.e., the Safeguards Area, Containment Spray Pump Area, and Main Steam Valve House).   Hydrogen combustion was not observed in the Surry analyses. However, the BWR reactor building experienced a combustion failure. Leakage and failure flow paths are specified that model failure of blowout panels, walls, ceilings, doors, and other vulnerable locations. For example, the resulting damage to the reactor building in the Peach Bottom SOARCA station blackout calculations due to a hydrogen burn was comparable to what was observed in the Fukushima accident.
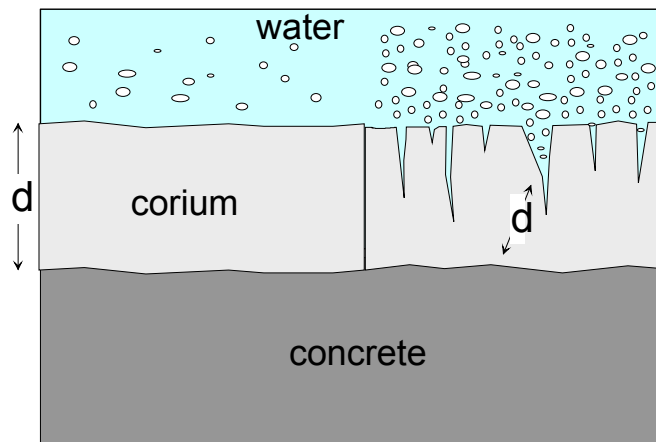
Corium Crust to Water Heat Flux
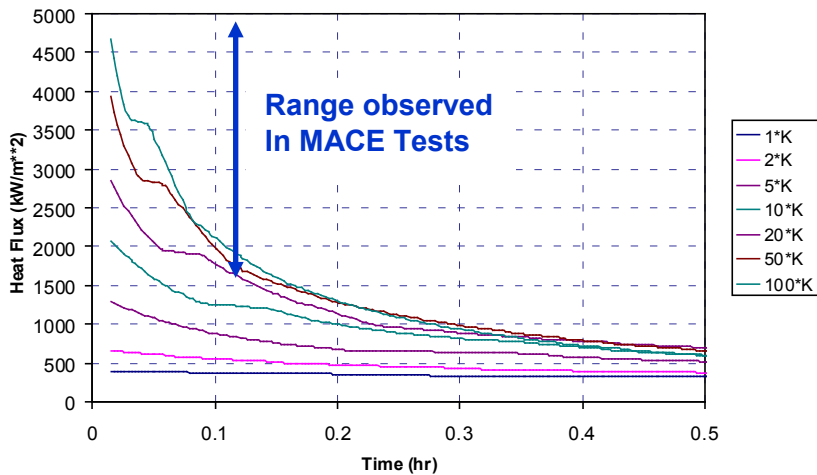
Figure 3-38 Heat transfer from an overlying water pool to an ex-vessel debris bed.

3.1.2 Pressurized Water Reactor Best Practices

Modeling practices discussed in this section are typically applicable to PWR MELCOR models and were applied to the SOARCA Surry model. The provided best practices are generally related to unique hardware found in PWRs but not BWRs.

3.1.2.1 Pump Seal Leakage and Blowout

Based on insights from the Surry Individual Plant Examination, which used the Rhodes probabilistic model for seal leakage, a simple model has been incorporated into MELCOR analyses using user input. The key attributes of the model are implemented as follows. Upon a loss of seal cooling in a station blackout sequence, the seals will leak at 21 gpm. In an unmitigated station blackout scenario, the fluid exiting the loop seal will approach saturation conditions at approximately 2 hours and the seal leakage flow will increase to 182 gpm per reactor coolant pump. The seal leakage values are based on normal operating conditions. The flow rate will change appreciably as a function of pressure, subcooling, and steam quality.

3.1.2.2   Loop Seal Clearing and Effects on Progression

The NRC has a separate research program examining thermally induced steam generator tube rupture (TISGTR) [65]. Detailed computational analyses are being performed to investigate the timing and sensitivity of high temperature natural circulation tube failure versus failures of other components in the RCS during severe accident natural circulation conditions. The clearing of the loop seal was identified as a key event that could increase the likelihood of tube failure under certain circumstances. Furthermore, NUREG-1570 (i.e. "Risk Assessment of Severe Accident-Induced Steam Generator Tube Rupture") previously assessed the potential for tube failure in high-pressure station blackout conditions.

MELCOR includes basic thermal-hydraulic models for loop seal clearing and the prediction of thermal failure of steam generator tubes. However, the thermal gradients and flow behavior is extremely complex in the RCS during natural circulation conditions. The base case response utilizes the MELCOR models for natural circulation (i.e., discussed further below), loop seal clearing, and user specified RCS component thermally induced failure models. Sensitivity calculations were also performed that assume steam generator tube failure before hot leg nozzle failure (i.e., the first creep rupture location calculated in the Surry station blackout calculations).

3.1.2.3   RCS Natural Circulation Treatment

Natural circulation is important in severe accident sequences because circulating steam from the core to upper reactor internals, the hot leg, and the steam generators (SGs) (1) transfers heat away from the core, (2) changes the core melt progression, and (3) changes in-vessel fission product distribution. More importantly, the resultant heating of the piping connected to the vessel could progress to a thermal stress (i.e., creep rupture) failure of the primary pressure boundary and a subsequent depressurization. As shown in Figure 3-39 [21], three natural circulation flow patterns can be expected during a severe accident for a Westinghouse PWR: (1) in-vessel circulation, (2) countercurrent hot leg flow, and (3) loop natural circulation. For high pressure accidents that do not include RCS pipe breaks (e.g., a station blackout), whole loop, single-phase natural circulation flow (i.e., the left hand side of Figure 3-39) is not expected during the core degradation phase of the accident. Consequently, the prediction of the first two natural circulation flow patterns is critical for predicting severe accident progression. The first two natural circulation flow patterns have been studied (a) experimentally in the 1/7th-scale natural circulation test program by Westinghouse Corporation for the Electric Power Research Institute (EPRI) [22], [23], (b) computationally using the FLUENT computational fluid dynamics (CFD) computer program [24], [25], and (c) analytically using SCDAP/RELAP5 [54]. Subsequently, MELCOR was used to model the 1/7th-scale natural circulation tests [26].

More recently, the NRC has continued improving natural circulation modeling as part of its steam generator tube integrity program [27], [28]. The natural circulation modeling techniques used in MELCOR plant models were based on work performed as part of the code assessment of the 1/7th-scale tests [26], which closely followed the previous work performed by Bayless [21]. The natural MELCOR modeling approach in the Surry model has been recently updated to incorporate some of the modeling advances used by Fletcher using SCDAP/RELAP5 [27]. The key features of the MELCOR natural circulation models, which were adapted from the recent SCDAP/RELAP5 work, are the following:

- 5 radial rings in the vessel and upper plenum for natural circulation

    o   Separate axial and radial flow paths throughout the core and upper plenum
    o   Radial and axial blockage models in the core during degradation

- Explicit modeling of all internal vessel structures for heat transfer

    o   Convective heat transfer
    o   Gas-structure radiation in the upper plenum
    o   Structure-to-structure thermal radiation within the core
    o   Variable Zircaloy emissivity as a function of oxide layer thickness
    o   Variable steel emissivities in the core as a function of temperature

The hot leg is divided in half to represent the counter-current natural circulation flow. The flow rate is matched to a Froude Number correlation from the FLUENT CFD analysis [27] for the Westinghouse SG,

$$Q = C_D [g (\Delta\rho / \rho) D^5]^{1/2} \hspace{4cm} \text{Equation 12}$$

where,
  Q is the volumetric flow rate in the hot leg,
  C_D = 0.12 (from FLUENT CFD calculations),
  g is the acceleration due to gravity,
  ρ is the average fluid density,
  $\Delta\rho$ is the density difference between the hot and cold fluid streams, and
  D is the pipe diameter

- Steam generator tube-to-hot leg flow ratio tuned results from the FLUENT CFD analysis [27]

    o   Tube mass flow rate/hot leg mass flow rate (M-ratio) = 2

- Explicit modeling of all key heat transfer processes in the hot leg and the steam generator

    o   Augmented convective heat transfer in hot leg based on FLUENT turbulence evaluations

    o   Gas-to-structure radiative exchange in the hot leg and steam generator

    o   Ambient heat loss through the piping and insulation

- Steam generator mixing fractions based on FLUENT CFD analysis [27]

- o Inlet plenum subdivided into 3 regions for hot, mixed, and cold regions
- o Flow ratio into hot tubes tuned to a 0.85/0.15 split
- o Flow ratio into cold leg piping tuned to a 0.85/0.15 split
- o Flow divided in the SG tubes in a 0.41/0.59 tube split[9]

- Individual modeling of relief valves

  - o When the valves are lumped, it creates a very large flow that non-physically disrupts natural circulation flow patterns and the timing of the valve openings

- Creep rupture modeling

  - o Hot leg nozzle carbon safe zone region
  - o Hot leg piping
  - o Surge line
  - o Steam generator inlet tubes

The MELCOR hot leg and SG nodalization for Loop A is shown in Figure 3-40. Control volume reactor system codes like MELCOR or SCDAP/RELAP5 have limitations in modeling buoyancy plumes associated with natural circulation flow. Hence, the MELCOR system model analyses are performed by incorporating flow buoyancy or drag adjustments to the hot leg circulation rate to achieve the target value for hot leg discharge coefficient. The drag coefficient was formulated based on an experimental correlation for flow through horizontal ducts connecting two tanks containing fluids of different densities. The special natural circulation flow paths described above are shown in red in the figure. The natural circulation control logic identifies single potential single-phase natural circulation conditions and activates the special flow paths to achieve the conditions described above.

Finally, it should be noted that the recent work of Fletcher [27] for the NRC steam generator tube integrity program revealed a sensitivity of tube failures to the hot and cold tube split, the tubes receiving the peak plume temperatures, and the highly refined axial nodalization through the tube sheet and into the steam generator. These specific aspects of the modeling specifically addressed the potential for a TISGTR, which were not incorporated in the MELCOR models.[10] To evaluate this potential consequence while acknowledging the potential limitations in the MELCOR model and/or vulnerabilities or defects in the plant tubes, the SOARCA project will perform sequences where TISGTRs were specified to occur prior to other RCS natural circulation failures in follow-up SOARCA uncertainty analysis studies.

---

[9] It was not practical to represent the 41%/59% hot/cold split of the SG tube regions in the MELCOR model due to the complications of a single model nodalization for all conditions. A 50%/50% tube split was used.

[10] Unlike SCDAP/RELAP5, MELCOR cannot be renodalized at the start of the natural circulation phase with a more detailed model due to the control volume and flow path being fixed upon initiation of the simulation. Consequently, the MELCOR model must calculate the early two-phase thermal-hydraulic transient, the natural circulation phase, the post creep rupture blowdown, the accumulator reflood of the degraded core, and the final boil-off and core degradation to vessel failure. It was not practical to use a highly detailed steam generator nodalization for the scope of a MELCOR source term calculation.
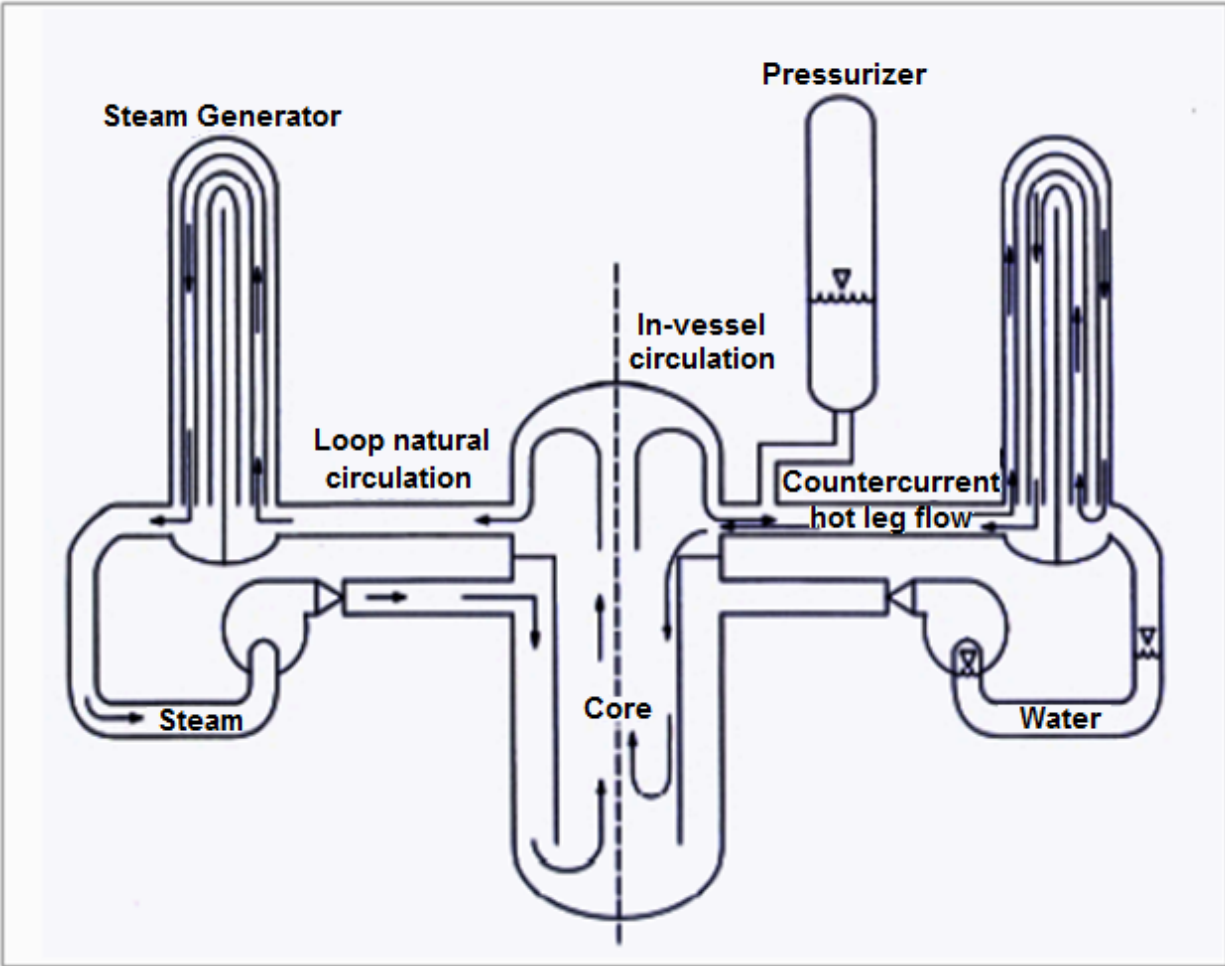
Figure 3-39   In-vessel, full-loop, and hot leg natural circulation flow patterns in a PWR severe accident
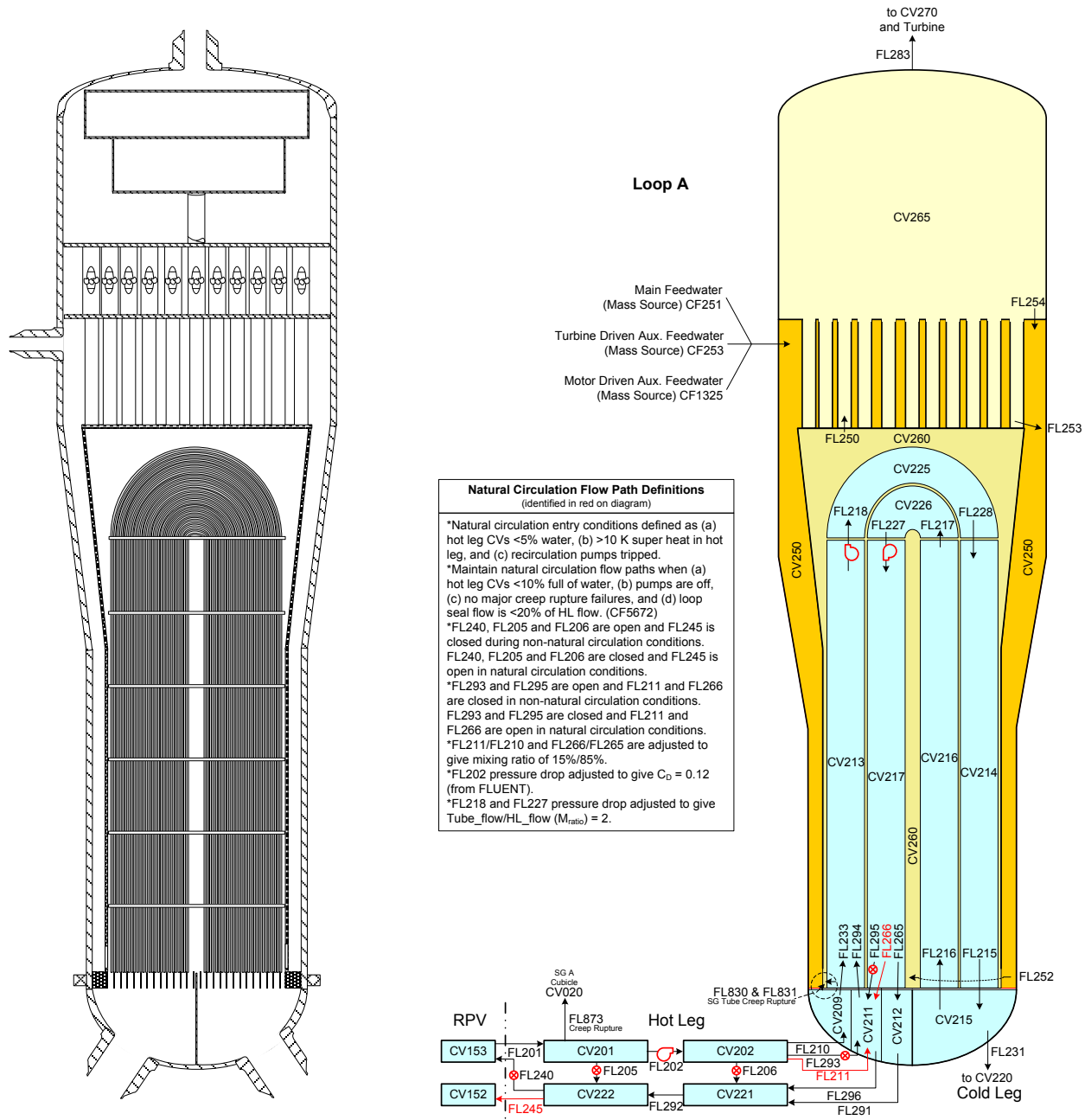
Figure 3-40   MELCOR hot leg and steam generator nodalization including the special natural circulation flow paths

3.1.2.4   Core Plate Failure

The timing of core plate failure affects the relocation of the degraded core materials from the core region into the lower plenum. As discussed above, the hot relocated core materials will boil away the water in the lower plenum, which will lead to vessel LHF. The MELCOR representation of the Westinghouse core plate assembly includes a separate representation of the various supporting structures. At the lowest level is the bottom support casting. The bottom support casting is part of the integrated core barrel structure. The mass of the core is

transmitted from the core plate via support columns that span the gap to the core support forging. Within the gap is a flow mixer plate (see Figure 3-41).

The MELCOR lower head support nodalization is shown in the left side of Figure 3-42. The weight of the core material mass is transmitted through the columns to the bottom support casting. The local thermal-mechanical failure of the lower core plate, the flow mixer plate, and the lower support forging are calculated internally by MELCOR using Roark's engineering stress formulas [64]. The failure is based on exceeding the yield stress at the local material temperature conditions. After the core plate fails, it is assumed that the debris falls past the columns but is temporarily supported by the flow mixer plate. However, since the flow mixer plate is relatively thin, the hot debris will quickly fail the plate (i.e., again according to the Roark stress formulas). The debris subsequently falls to the lower support forging, which is very thick but eventually fails. The sequential failure of the supporting structures is affected by vessel water level, which is also exposed to the sequentially relocating debris. Once the lower support forging fails, the debris falls onto the lower head.

Fully molten materials will relocate through the structures until freezing on supporting structures or reaching the lower head. Due to the high melting temperature of U-Zr-O eutectic core debris material (i.e., assumed to melt at 2800 K), most of the fuel and cladding debris will be frozen during the core support structure failures. However, some unoxidized Zr or control material may have enough superheat to relocate through the structures onto the lower head.
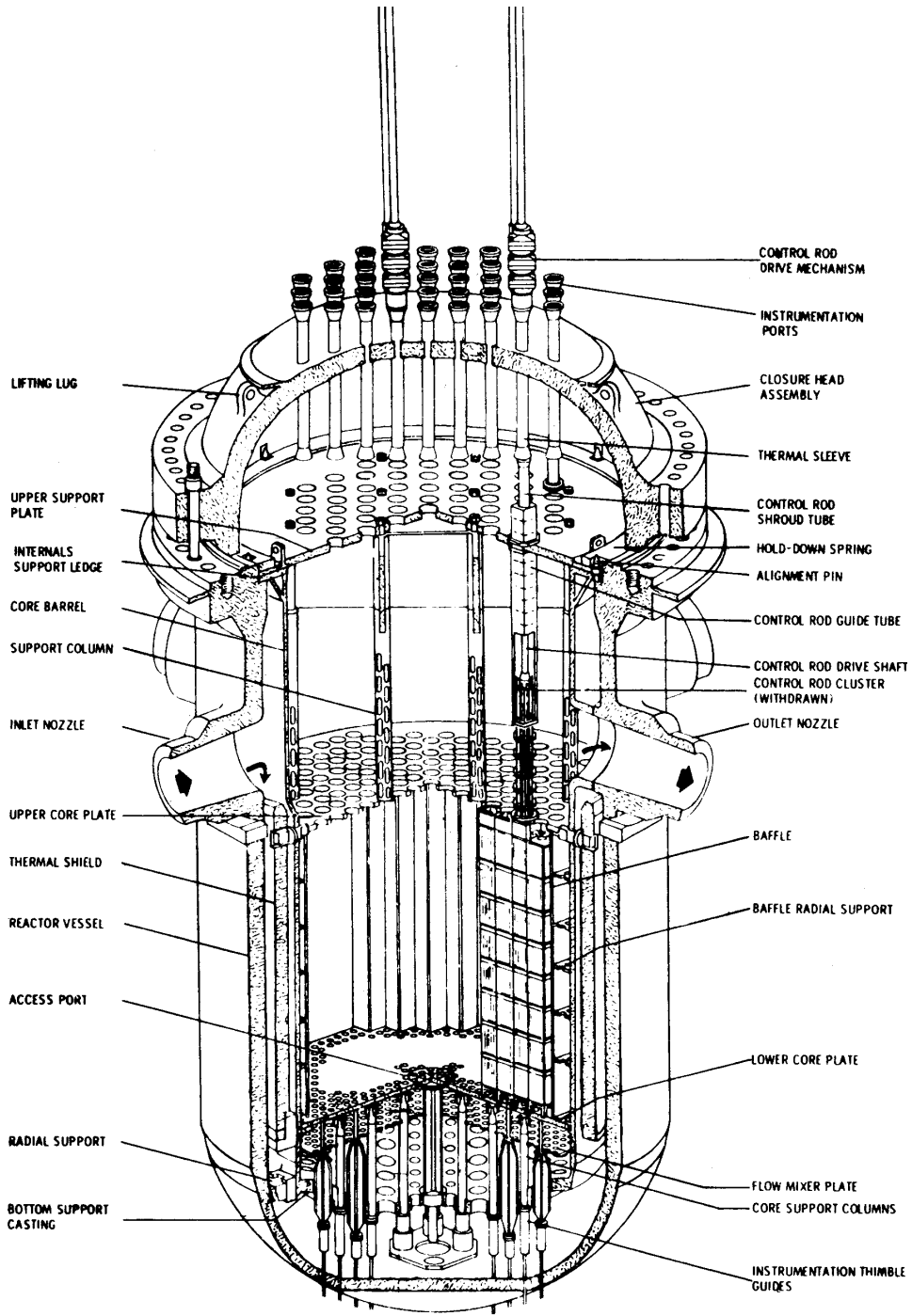
Figure 3-41 Westinghouse PWR reactor vessel internals

Labels (left side, top to bottom):
LIFTING LUG
UPPER SUPPORT PLATE
INTERNALS SUPPORT LEDGE
CORE BARREL
SUPPORT COLUMN
INLET NOZZLE
UPPER CORE PLATE
THERMAL SHIELD
REACTOR VESSEL
ACCESS PORT
RADIAL SUPPORT
BOTTOM SUPPORT CASTING

Labels (right side, top to bottom):
CONTROL ROD DRIVE MECHANISM
INSTRUMENTATION PORTS
CLOSURE HEAD ASSEMBLY
THERMAL SLEEVE
CONTROL ROD SHROUD TUBE
HOLD-DOWN SPRING
ALIGNMENT PIN
CONTROL ROD GUIDE TUBE
CONTROL ROD DRIVE SHAFT
CONTROL ROD CLUSTER (WITHDRAWN)
OUTLET NOZZLE
BAFFLE
BAFFLE RADIAL SUPPORT
LOWER CORE PLATE
FLOW MIXER PLATE
CORE SUPPORT COLUMNS
INSTRUMENTATION THIMBLE GUIDES

Figure 3-42   MELCOR Westinghouse lower vessel nodalization

3.1.2.5   Interfacing Systems Loss of Coolant Accident

The ISLOCA scenario analyzed in the SOARCA project identified several modeling and phenomenological aspects that were important to the timing and magnitude of radionuclide releases to the environment. While some of the aspects are probably specific to only the Surry units, some may be applicable to modeling an ISLOCA at any plant.

The ISLOCA scenario (in a PWR) involves the pressurizing of low head safety injection (LHSI) piping outside of containment to normal reactor operating pressure. The pressurizing results from the failure of two serial check valves. The piping outside of containment is not rated to normal reactor pressure and so is assumed to rupture causing a loss-of-coolant accident. The rupture is not initially isolable due to the inability of isolation valve(s) to close against the blowdown. The rupture is not isolable later due to the motors on the isolation valves being flooded. The refueling water storage tank (RWST) is eventually exhausted with its contents having been pumped into auxiliary buildings outside of containment where the pipe rupture occurred. A key assumption specific to the scope of this analysis in SOARCA was that no makeup water was provided to the RWST. The reactor boils dry and the core melts releasing radionuclides through the failed injection piping to the auxiliary buildings. Hydrogen from core oxidation propagates through the piping to the auxiliary buildings and deflagrates failing the building boundaries. Radionuclides release through the failed buildings to the environment bypassing containment.

Several aspects of the LHSI piping are important to represent in a computer model (e.g., a MELCOR model) used to simulate an ISLOCA, including:

- The size of the flow limiting venturi in the piping (and the choked flow through the venturi)

- The length, size, and schedule of the piping

- The fittings (elbows, tees, etc.) in the piping

- The extent to which the piping is insulated

- The section(s) of the piping susceptible to overpressure rupture, i.e., the sections of piping outside of containment that are not rated to normal reactor operating pressure

- The orientation of the piping where it connects to a cold leg of the reactor (possibly important with respect to eventually ending leakage through the piping, for example, by operating the residual heat removal system residual heat removal system (RHR) at mid-loop water level)

The interconnected buildings into which the RCS would depressurize given an ISLOCA are important to include in a simulation. At Surry these buildings are the Safeguards Area, Containment Spray Pump Area, and Main Steam Valve House. In the ISLOCA scenario postulated for Surry, the RCS depressurizes into the Safeguards Area and fission products are released to the environment through all three buildings.

As the buildings into which the RCS would depressurize in an ISLOCA have recognized contamination potential, they are exhausted by a filtered safety-related ventilation system given a loss of coolant accident (LOCA). On a safety injection signal, the system is automatically

started. The system has particulate and iodine filtration and dual parallel redundant fans. The fans exhaust to a stack. This ventilation system is important to model in an ISLOCA simulation as evidenced in the SOARCA simulation where substantial amounts of radionuclide aerosols were captured in the exhaust ventilation filters.

Several phenomena showed to be important in the SOARCA Surry ISLOCA modeling and the best practice suggestion is that they all be addressed in any ISLOCA analysis. The phenomena and their impact are discussed below.

Turbulent deposition and impaction
The deposition of aerosolized radionuclides in the LHSI piping by means of turbulent deposition and inertial impaction showed to be very meaningful in the SOARCA Surry ISLOCA analysis. Turbulent deposition results when velocity fluctuations normal to the generalized direction of a turbulent flow push particles carried by the flow to the wall. Inertial impaction results at geometrical irregularities, an elbow for example, where the inertia of a particle causes it to stray from flow streamlines and collide with the wall. Turbulent deposition and impaction modeling was added to the MELCOR code to address these phenomena in the SOARCA Surry ISLOCA analysis. The modeling was benchmarked against the Light Water Reactor Aerosol Containment Experiment (LACE) series of tests [58].

Resuspension
As aerosol deposition in LHSI piping progressed, the deposits formed might be susceptible to breaking loose from the pipe wall given the high velocities that would exist in the piping. Consideration needs to be given in an ISLOCA analysis to the associated resuspension potential here. In the SOARCA analysis the assumption was made that aerosols, once deposited, were no longer in a form that could be readily aerosolized, i.e., the deposits might break loose and carry into the auxiliary buildings but would not become aerosolized and so would not disperse to the environment.

Revaporization
The radionuclide deposits that built up in the LHSI piping in the SOARCA simulation generated significant heat from fission product decay. The heat generation was significant enough to raise the temperature of the deposits to the point where the more volatile radionuclide classes, CsI for example, revaporized. Upon revaporization, the radionuclides once again transported in the piping and escaped through the pipe rupture into the auxiliary buildings.

Gamma heating
The thickness of the LHSI piping walls at Surry are such that as little as 33% of the gamma radiation emitted by radionuclide deposits in the piping would be absorbed in the steel walls. This proved important with respect to the revaporization of deposits in the SOARCA analysis.

Pool scrubbing and cooling
The pipe rupture in the SOARCA Surry ISLOCA scenario was determined to be submerged during core degradation as was a significant length of the LHSI piping. Meaningful scrubbing of aerosols results as the carrier gas bubbles up through the submerging pool. The submerged piping was kept cool by the pool which suppressed the revaporization of substantial radionuclide deposits that formed in the piping.

Hydrogen deflagration
The hydrogen produced and released to the auxiliary buildings in an ISLOCA would have the potential to destroy the buildings if it were to burn suddenly. This was judged to happen in the SOARCA simulation in the form of grossly opening the roof of a mostly subterranean building.

A few actions that the operators would perform by existing emergency procedure would be critical to delaying the onset of core damage in an ISLOCA. At Surry the actions would be the following:

- Stopping LHSI Pump A (estimated at 6 min and 17 sec)

- Stopping LHSI Pump B (estimated at 15 min and 44 sec)

- Isolating the LHSI pump suctions from the refueling water storage tank (estimated at 16 min and 18 sec)

- Stopping and or throttling high head safety injection (HHSI) pumps to conserve RWST inventory

With these actions scripted in the analysis, MELCOR predicts the onset of core damage at 12 hr and 49 min. Without these actions accomplished, MELCOR predicts the onset of core damage dramatically earlier. It is imperative to represent operator actions in ISLOCA modeling.

There are several occurrences to watch for in an ISLOCA simulation as identified in the SOARCA Surry ISLOCA analysis, including:

- Equipment flooding, e.g., isolation valve, LHSI pump, and HHSI pump flooding

- Hydrogen deflagrations energetic enough to fail building boundaries

- Excessive particulate loading on ventilation filters considering aerosols originating from;

    o Core degradation, e.g., radionuclides released from the fuel and tin released from cladding

    o Core-concrete interactions (concrete dust)

    o Fires in the auxiliary buildings (smoke and particulate)

- Exhaust ventilation fan automatic shutdown because of excessive pressure drop across particulate-loaded filters

- Exhaust ventilation filter over-temperature failure

- Problematic heat generation from fission product decay in radionuclide-loaded exhaust ventilation filters

- Excessive localized aerosol deposition in the LHSI piping from turbulent deposition and inertial impaction such that the piping actually indicates to be blocked by the deposits

The ultimate operator action anticipated to end an ISLOCA at Surry is entering RHR with reactor water level stabilized at the level consistent with mid-loop operation, i.e., aligning and operating RHR in recirculation mode. The mid-loop level is attainable because the LHSI piping connects to the top of the cold legs. With the RCS subcooled at atmospheric pressure, leakage through the broken LHSI piping would stop with level below the top of the cold legs. This condition

should be attainable with managed HHSI and successful RHR entry. It is important to realize that the availability of this strategy is somewhat unique to Surry given that the RHR systems are entirely separate from the LHSI systems in the Surry units. This is not especially typical of US PWRs. It is also important to realize that RHR entry at Surry before exhaustion of the RWST would be tenuous and that the net positive suction head margin at the inlets to the RHR pumps might be only minimally satisfactory. The feasibility of ending an ISLOCA through the use of RHR needs to be investigated in detail in any ISLOCA analysis.

3.1.3   Boiling Water Reactor Best Practices

Modeling practices discussed in this section are typically applicable to boiling water reactor MELCOR models and were applied the SOARCA Peach Bottom model. The provided best practices are generally related to unique hardware found in BWRs but not PWRs.

3.1.3.1   Debris Spreading on the Drywell Floor of a BWR Mark I Containment

The floor of a Mark I containment is divided into three distinct regions for the purposes of modeling molten-core/concrete interactions, as illustrated in Figure 3-43. The first region (which receives core debris exiting the reactor vessel) corresponds to the reactor pedestal and sump floor areas (CAV 0). Debris that accumulates in the pedestal can flow out into the second region (through an open doorway in the pedestal wall), corresponding to a 90° sector of the annular portion of the drywell floor (CAV 1). If sufficient debris accumulates in this region, it can spread further into the third region, which represents the remaining portion of the drywell floor (CAV 2). Debris within each region is assumed to be fully-mixed, but has a distinct temperature and composition from neighboring regions.

Two features of debris relocation among the three regions are modeled by user-defined controls. The first models debris overflow from one region to another. The second manages debris spreading across the effective radius of the regions outside the reactor pedestal (CAV 1 and 2). User specified control functions monitor debris elevation and temperature within each region, both of which must satisfy user-defined threshold values for debris to move from one region to its neighbor. More specifically, when debris in a cavity is at or above the liquidus temperature of concrete, all material that exceeds a predefined elevation above the floor/debris surface in the adjoining cavity is relocated (6 inches for CAV 0 to CAV 1, and 4 inches for CAV 1 to CAV 2). When debris in a cavity is at or below the solidus temperature of concrete, no flow is permitted. Between these two debris temperatures, restricted debris flow is permitted by increasing the required elevation difference in debris between the two cavities (more debris 'head' required to flow).

Debris entering CAV 1 and CAV 2 is not immediately permitted to cover the entire surface area of the cavity floor. The maximum allowable debris spreading radius is defined as a function of time using control function logic. If the cavity debris temperature is at or above the liquidus temperature, a maximum transit velocity (corresponding to the shortest transit time) is applied to determine the remaining distance between the debris front and the containment liner. Traveling at the maximum velocity, the transit times to contact the containment liner are specified as 10 minutes for CAV 1 and 30 minutes for CAV 2. When the debris temperature is at or below the concrete solidus, the debris front is assumed to be frozen. A linear interpolation is performed to determine the debris front velocity at temperatures between these two values[11]. The specified transit times coincide with the consensus that molten core migrates to the liner if

---

[11] The debris spreading model compares debris temperatures to the liquidus and solidus temperatures of concrete because MELCOR does not currently allow user access to the debris liquidus and solidus temperatures.

the bulk temperature permits relocation. This assumption was made concerning a dry cavity and may not be appropriate for a flooded cavity where energy extraction from the debris leading edge and surface become more relevant.
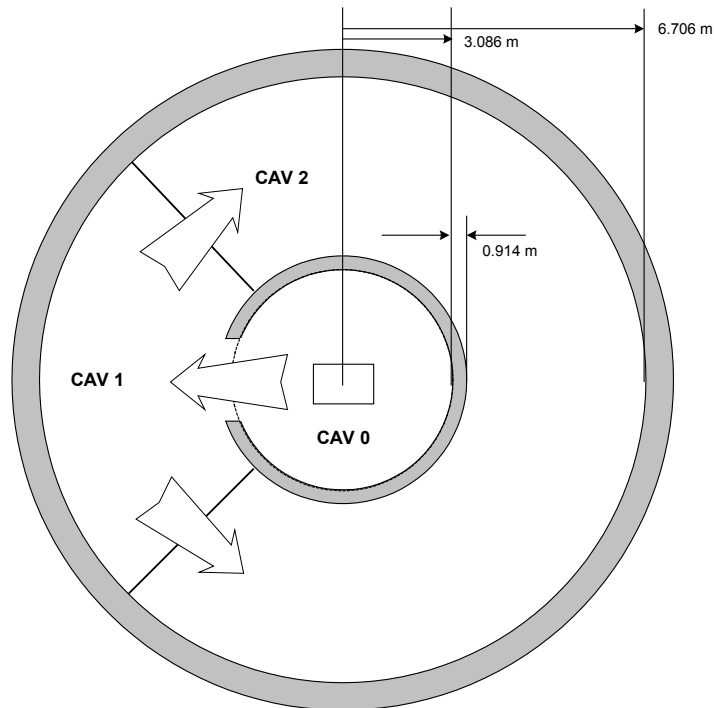
Figure 3-43   Discrete regions of the drywell floor to represent debris spreading

3.1.3.2   Traversing In-core Probe Guide Tube Leakage

The traversing in-core probe (TIP) system performs in-core instrumentation calibration of the local power range monitors (LPRMs). Three fissile material probes are normally stored in a shield chamber located outside the containment pressure boundary. When operating, each of the probes is driven by a steel cable from the shield chamber through a guide tube to an indexing unit. The indexing units serve to direct the TIP probe into various exit tubes connected to the LPRMs in the core to perform calibrations. Calibration exercises take approximately 1 hour and are performed once every four months. The conditional probability of a containment bypass due to a station blackout (SBO) coinciding with TIP calibration was precluded by the truncation limit for event selection.

A sensitivity calculation was performed to evaluate the effect of unisolated TIP guide tubes on accident progression and radionuclide source term for the long term station blackout accident sequence. The guide tubes were modeled as a single-lumped control volume to model the hydrodynamic volume while flow losses were captured by flow paths, a combined length of approx. 150 feet, connected at each end. Heat transfer between flowing gas and the guide tube(s) was accounted for; and the tube internal wall was modeled to represent an aerosol deposition surface [62]. The diameter of a TIP probe is approximately 0.211 inches. The internal diameter of the TIP guide tube is 0.280 inches and the diameter of the drive cable is 0.258 inches. Therefore, the available cross-sectional area for flow through an operating guide is small (0.009 in^2 per tube if the probe is inserted and 0.06 in^2 if the probe is withdrawn into its

shield chamber). When the probes are withdrawn, an alternating current actuated ball valve, located on the guide tube, isolates the system. The globe valve functions only when the TIP probe is fully withdrawn because the drive cable for the in-core probe runs through the valve body. If the probe cannot be retracted, operators can explosively close a direct current actuated squib shear valve to shear the drive cable and seal the guide tube.

3.2 MELCOR Code Enhancements for the SOARCA Project

At the start of the SOARCA project, three code development activities were identified to enhance MELCOR. Each of these activities had previously been included manually in the best practices approach for analysis, through (a) changes to default setting, (b) user-specified control logic, or (c) the addition of user-specified filter models, respectively. The incorporation of these items as defaults or code models simplified their implementation. Section 3.2.1 summarizes the new defaults that had been previously specified as best practice settings in Appendix A. The fuel collapse model described in Section 3.1.1.1 was added as a new modeling option. Previously, the user specification of control functions for the model required thousands of lines of input. Finally, a vapor scrubbing model was added, which is described in Section 3.2.3. Previously, user-specified vapor filters were used to scrub fission product vapors exiting BWR spargers.

3.2.1 Updated MELCOR Defaults to Reflect Current Best-estimate Modeling Practices

In support of SOARCA MELCOR calculations using Version 1.8.6 and as the new standard for Version 2.1, some default values were updated based on best-estimate modeling practices. The values are summarized in Appendix B. The new defaults reflect long term practices to better model severe accident phenomena, improve numerical robustness, or activate newer models. In addition, the standard modeling practices include modeling cesium molybdate using RN package Class 17. Previously, Class 17 did not have physical parameters representative of any specific substance. Consequently, all physical properties were added as defaults to facilitate modeling cesium molybdate without additional user input. The updated ORNL-Booth fission product release model and updated modeling parameters are described in Section 3.1.1.4. Other updates to the default MELCOR settings are summarized in Appendix B. A new "default" record permits the user to specify whether the default parameters correspond to prior SOARCA or post SOARCA updated parameters by specifying either "1.8.6" or "2.1", respectively.

3.2.2 Add a Simplified Thermo-mechanical Fuel Collapse Model

As described in Section 3.1.1.1 under the description of the fuel degradation and relocation treatment, a simple parametric model was developed to simulate thermal-mechanical collapse of fuel rods only supported by highly oxidized Zircaloy shells at high temperatures. Previously, the implementation of the control system logic to perform these calculations required several thousands of lines of input. The new model was coded into the MELCOR code to eliminate the burden of creating a file of user-specified control logic. The model is activated through a simple user directive that identifies the appropriate lifetime failure function table. The lifetime failure function table specifies the time remaining to collapse versus the local oxidized cladding temperature. The logic is only implemented once the unoxidized cladding thickness drops below 0.1 mm, by default, or a user specified thickness.

3.2.3   Fission Product Vapor Scrubbing with Aerosol Scrubbing

In previous calculations, it was observed that the Suppression Pool Aerosol Removal Code (SPARC) fission product scrubbing model in MELCOR would not recognize fission product vapors except elemental iodine. The SPARC model automatically scrubbed all aerosols but elemental iodine vapor, and all fission product vapors except elemental iodine would flow through the pool without any retention. However, the temperature of the carrier gas and fission products flowing to pool spargers could have a significant vapor pressure and a mixture of vapors and aerosols should be considered for retention. This lack of retention was particularly significant for cesium iodide vapor, which can have a relatively high vapor pressure when discharged into a BWR sparger deep within the wetwell pool. The model applied in SOARCA was updated to calculate scrubbing based on the same parameters used for elemental iodine, and now accounts for the non-condensable fraction, bubble size, discharge gas temperature, pool subcooling, and pool depth.

4. MELCOR CODE DEVELOPMENT AND VALIDATION BASIS

MELCOR has been under continuous development by the NRC and SNL where software quality assurance (SQA) is an integral part of the development process. The MELCOR SQA program is adapted from two internationally recognized standards, CMMI and ISO 9001. These standards provide elements of traceability, repeatability, visibility, accountability, roles and responsibilities, and objective evaluation. The MELCOR SQA program focuses on reducing code error, improving documentation of all processes, and continuous integration of procedures into daily work processes. An essential part of SQA is proper validation of physical models encoded into analytical tools to provide developers the necessary guidance in developing and improving algorithms and numerical methods for describing physical processes. Moreover, validation results are essential for code users in order to gain confidence in applying the code to real-world applications. It is important that such validation exercises be performed objectively by developers, who may better understand the nuances of particular models, as well as users, who may have a more distant knowledge of the internal models but may have a greater knowledge of real-world applications.

The MELCOR code has been validated against numerous separate effects tests, integral tests such as Phebus, and actual accident studies such as Three Mile Island Unit 2 (see references [1], [31] - [43], and [61]). When MELCOR 1.8.6 was released, validation calculations were performed on many of the same validation test cases used for MELCOR 1.8.5 and results were compared between the two code versions and found to be agreeable. Furthermore, when existing plant decks were converted from MELCOR 1.8.5 to MELCOR 1.8.6 they were scrutinized for deviations in results. Some assessments, performed by SNL or other code users have been documented in the MELCOR Code Assessment Program (MCAP) meetings and the European MELCOR User Group (EMUG). However, even though internal validations were performed for MELCOR 1.8.6, an assessment report was not published because of similarities in the physics models between MELCOR 1.8.6 and MELCOR 2.1 which was released very shortly after MELCOR 1.8.6. Currently, a validation report is in preparation for MELCOR 2.1, covering an expanded set of validation test cases which will include results for Version 1.8.6 for comparison.

The purpose of this section is not to provide a complete MELCOR validation test report, but rather to provide an overview of the validation program. Code validation supports the application of MELCOR for state-of-the-art analyses.

4.1 Selection of Validation Test Cases

An objective of the MELCOR development team is to assess new code models against available test data, where that data exists. Both separate effects tests as well as integral tests are used for code assessment. Separate effects tests are designed to focus on an individual physical process, to eliminate the combined effects of multiple physical models which may obscure the validation of a particular model. However, it may be impossible to design a single test that isolates a single process and separate effects tests often ignore the important coupling between processes that are inherent in real world applications. Integral tests are valuable for examining the relationship between such coupled processes. Tests should be selected that are applicable to the calculation domain of the code and this domain should be clear to code users. Often, this requires significant analytical experience in applying the code to real-world problems to understand the calculation domain.

MELCOR has been assessed against numerous severe accidents performed by the NRC, EPRI, DOE, as well as many international research programs. Often, international standard problems (ISPs) are used as reference validation cases because they are "standard" problems that are assessed against other codes which may have alternate modeling capabilities. These ISPs are generally well documented, and may provide code-to-code comparisons to compare modeling approaches.

An important aspect of validation is that of coverage. Ideally, it is desirable to target each physics model available in the code with one or more validation test cases that can expose the capabilities of the model in simulating test conditions and responses. However, limited resources require some prioritization of effort in determining those processes that are most uncertain and contribute most to the sensitivity of results. There is a significant amount of effort involved in developing an input model, and understanding the results in light of the uncertainties inherent in the experiment design. This effort involves comparison of important measurements to calculated results, interpretation of discrepancies, and variation of model parameters and nodalization to best describe the particular case. Often analysts can be tempted to manipulate input variables to get the 'best' results compared to data. However, it is more desirable to focus on what can be learned from the analysis in terms of exposing specific modeling adequacies or deficiencies. Furthermore, it is desirable to understand the numerical convergence of such calculations by examining both spatial and temporal nodalization of the model.

More than 50 such validation tests have been proposed for the MELCOR 2.1 assessment document.   Table 4-1 shows a summary of such tests categorized by physics examined by the test, i.e., RN transport, core heat-up and degradation, containment, ex-vessel corium, and integral tests. Important physics assessed in this study includes, but is not limited to, heat-up/heat transfer, oxidation of materials, reflood cooling, core degradation, molten pool modeling, fission product release, vessel failure, critical flow, MCCI, direct containment heating (DCH), condensation, containment stratification, hydrogen burn, hygroscopic effects, aerosol deposition, radionuclide transport, iodine pool chemistry, suppression pool scrubbing, vent cleaning, engineering safety features such as sprays (washing of radionuclides and cooling of atmosphere) and ice condensers. These validation tests exercise all the MELCOR physics packages to at least some degree, with the exception of the Condenser, Fan Cooler, and Passive Autocatalytic Recombiner Packages. Furthermore, specific models such as the point kinetics model, high temperature gas reactor models, spent fuel pool models, lower head penetration models, mechanical failure models, the integral heat exchanger model, flashing models, and the counter-current stratified flow model are not assessed in the current set of validation tests.

Table 4-1 MELCOR validation tests.

Integral Tests/ Accidents	Core	RN Transport	Containment	Ex-Vessel
Bethsy	LOFT-FP2	FALCON 1 & 2	NUPEC M-8-1, M-8-2	OECD-MCCI
Flecht-Seaset	PBF-SFD	VANAM-M3	IET 1 - IET7 and IET 9 - IET 11	SURC
GE Level Swell	CORA-13	LACE-LA4	PNL Ice condenser tests	IET-DCH
RAS MEI	DF-4, MP1, MP2	LACE-LA1 & LA3	Wisconsin flat plate	
NEPTUN	FPT1, FPT3	STORM	DEHBI	
TMI-2	LHF/OLHF	AHMED	CVTR	
	VERCORS	ABCOVE	HDR V44	
	ORNL VI	CSE-A9	HDR E-11	
	Quench 11	DEMONA	NTS-Hydrogen Burn	
		RTF ISP-41	GE Mark-III Suppression Pool	
		VERCORS	Marviken Blowdown Tests	
		ORNL VI	CSTF Ice Condenser test	
		Marviken ATT-4	LOFT-FP2	

4.2 Discussion of MELCOR Validation Tests

Assessment analyses have been performed historically as part of the MELCOR code development process. Table 4-2 summarizes the status of code validation tests, including aerosol tests, for various versions of MELCOR and the plans for future documentation. It is desirable to perform an assessment analysis with each new model added to the code. For example, aerosol mechanics for nonhygroscopic aerosols are modeled using the Multi-Component Aerosol Module for CONTAIN (MAEROS) code where good verification of aerosol agglomeration physics and gravitational depletion was demonstrated in early versions of MELCOR based on Marviken, Aerosol Behavior Code Validation and Evaluation (ABCOVE), and the LACE testing. MELCOR Version 1.8.5 introduced extensions to treat hygroscopic aerosol effects where good validation against the Experiments on the Aerosol Behavior within a Multi-Compartment Containment (VANAM) M3 test (similar to the Demonstration of Nuclear Aerosol Behavior (DEMONA) test) as well as the Aerosol and Heat Transfer Measurement Device (AHMED) experiments was demonstrated. The Containment Systems Experiment (CSE) A9 test was used to validate the containment spray scrubbing modeling in MELCOR Version 1.8.5 in the CONTAIN-MELCOR parity assessment study. The CONTAIN-MELCOR parity study introduced numerous other containment behavior assessments including the Nuclear Power Engineering Corporation (NUPEC) mixing tests, the Nevada Test Site (NTS) hydrogen burn tests, and the Integral Effects Testing (IET) DCH experiments. Fission product release from fuel, including mixed oxide and high burnup were assessed against ORNL HI/VI tests and against more recent VERCORS experiments and documented in the Phebus Synthesis report using MELCOR Version 1.8.5. In Version 1.8.5 fission product release models were adjusted using sensitivity coefficient overrides to the Version 1.8.5 models. These were formalized as code options and defaults for code Version 1.8.6. MELCOR Version 1.8.6 also introduced expanded modeling detail for core melt progression processes, including molten pool convection treatments. These extensions provided improved prediction of the TMI-2 accident, some of which are still currently under assessment. The Phebus FPT-1 test stands as the most comprehensive integral assessment of core damage progression, hydrogen generation, fission product release and RCS deposition and containment natural depletion processes. This test provides good assessment of key deposition behavior in the reactor RCS and for containment depletion. Other code assessments for code Version 2.1 have been performed by IBRAE during the code Version 2.1 conversion process as indicated in Table 4-2. Detailed descriptions

as well as results and findings can be found in the most recent Volume III of the MELCOR manuals [61]; an ongoing effort to update the demonstration problems as well as include additional experiments is underway for MELCOR Version 2.1. A comparison of key phenomena modeled with various MELCOR code versions is provided in the following section to demonstrate good agreement is maintained as the development of the code progresses.

Table 4-2   Historical review of MELCOR assessment studies.

Assessment\Code Version	1.8.1 (1991)	1.8.2 (1992)	1.8.3 (1994)	1.8.4 (1995)	1.8.5 (1996)	1.8.6 (2005)	2.1 (2011-2012)	M 1.8.5 Volume 3	CONTAIN Parity	Phebus Synthesis	IBRAE Assessments	Separate[12] Assessments	M 2.1 Volume 3
ABCOVE Tests		x					x					x	x
ACRR DF-4		x										x	
ACRR MP-1/MP-2		x										x	
Ahmed Hydroscopic Tests					x	x	x		x				x
BETHSY (ISP-38)							x				x		x
BWR Mk-III Vent Clearing Tests				x	x		x		x				x
CORA 13	x				x				x				x
CSE Spray Experiments			x		x				x			x	x
CVTR						x	x		x			x	x
DEMONA		x										x	x
FALCON Tests							x				x		x
FLECHT-SEASET	x						x				x	x	x
GE Level Swell Tests			x				x		x			x	x
HDR E-11							x					x	x
HDR V44					x		x		x				x
HI/VI FP Tests					x		x			x			x
IET DCH Experiments					x		x		x				x
JAERI						x	x						x
LACE-LA1, LA3					x								x
LACE-LA4							x	x	x				x
LOFT-FP2	x				x		x				x	x	x
Marviken	x										x	x	
NEPTUN Experiment							x				x		
NTS H2 Burn Tests					x		x		x				x
NUPEC Mixing Tests					x		x	x	x				x
OECD MCCI													x
PBF-SFD1-4							x				x		x
Phebus B9+					x				x				x
Phebus FPT-1					x	x	x		x	x		x	x
PNL Ice Condenser Test	x				x				x			x	
Quench 6							x						x
RAS MEI Tests							x				x		x
RASPLAV Salt Tests							x				x		
RTF Iodine Tests (ISP41)					x				x				x
STORM				x			x					x	x
SURC MCCI							x				x		x
TMI-2					x	x	x	x				x	x
VANAM-M3 (ISP37)					x		x	x	x				x
VERCORS 1-6 & HT/RT FP Tests					x		x			x			x

---

[12] "Separate Assessments" means that there is a standalone report (SAND or NUREG report) that documents the work.

4.3   Comparisons of Code Versions

Many of the validation analyses referenced in this report, see Appendix C, were performed with earlier versions of the MELCOR code, since the MELCOR 1.8.6 validation report was not published. However, given the level of maturity in many of the existing MELCOR physics models, essential validation exercises for the most part are not strongly dependent on the code version. Even so, small modeling changes and coding errors can impact results. Therefore a discussion of code version and the impact on validation is presented here.

SNL is currently updating the validation report for MELCOR Version 2.1. MELCOR Version 2.1 is largely identical to Version 1.8.6 with respect to model pedigree; the main difference being conversion of the source code to FORTRAN 95. Changes made to 2.0 subsequent to its release have mainly affected new modeling for high temperature gas reactors. Significant code corrections made to 2.x were also made in the 1.8.6 version and made available to the SOARCA analysis team. The published MELCOR 2.1 validation report will also present validation results using MELCOR 1.8.6 for many of these analyses.

In order to better appreciate the significance of the historical validation analyses, an evolution of code development with code versions is required.

Appendix D provides a list of major code modifications that were made during the development cycle. Note that this list only considers those physics models that may be directly related to the assessments in Table 4-2 and the SOARCA project. It does not contain many usability features and physical models that were not used in the SOARCA project, such as the point kinetics or the intermediate heat exchanger models. It also does not catalog model corrections and other bugs that were addressed.

Finally, since many of the historical validation cases have already been updated with Version 2.1, the following sections provide comparisons of select computational results with the historic code assessment analysis. However, it is not the intention of this report to reproduce the details of the validation report here. Instead, the following discussions focus on some key physical models assessed.

4.3.1   Airborne Physics

MAEROS is a multisectional, multicomponent aerosol dynamics code that evaluates the size distribution of each type of aerosol mass, or component, as a function of time. MELCOR uses the MAEROS code for modeling aerosol agglomeration and deposition processes of nonhygroscopic aerosols. The MAEROS models have been in the code since MELCOR Version 1.8.0 with only error corrections and extension since. Hygroscopic models were added to the code in Version 1.8.4.

Agglomeration of non-hygroscopic aerosols from condensation of water vapor is assessed in the ABCOVE [31] and DEMONA experiments. Figure 4-1 shows the non-hygroscopic aerosol mass calculated for 1.8.2, 1.8.6, and 2.x, together with data from the AB-5 test. Note for this simple one volume calculation, the results have not changed noticeably since the early versions of the code. Similarly, the DEMONA test shows depletion of SnO_2 due to condensation on the non-hygroscopic aerosol. These examples demonstrate the version independence of such calculations.
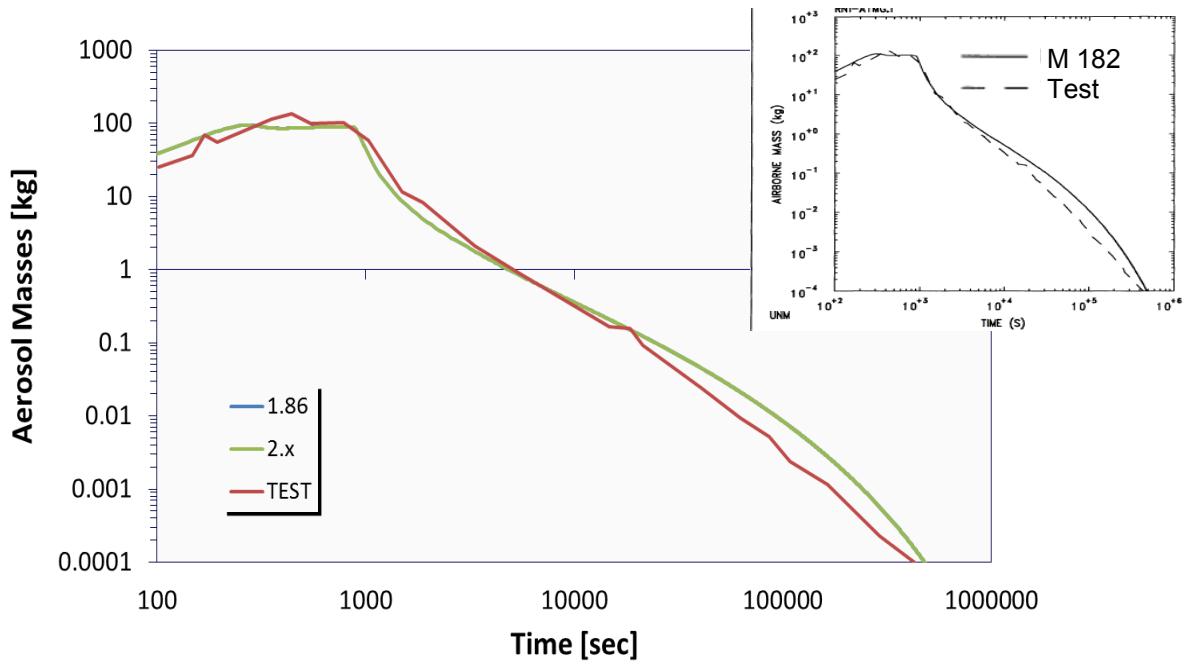
Figure 4-1   CSTF Airborne Mass Test AB5
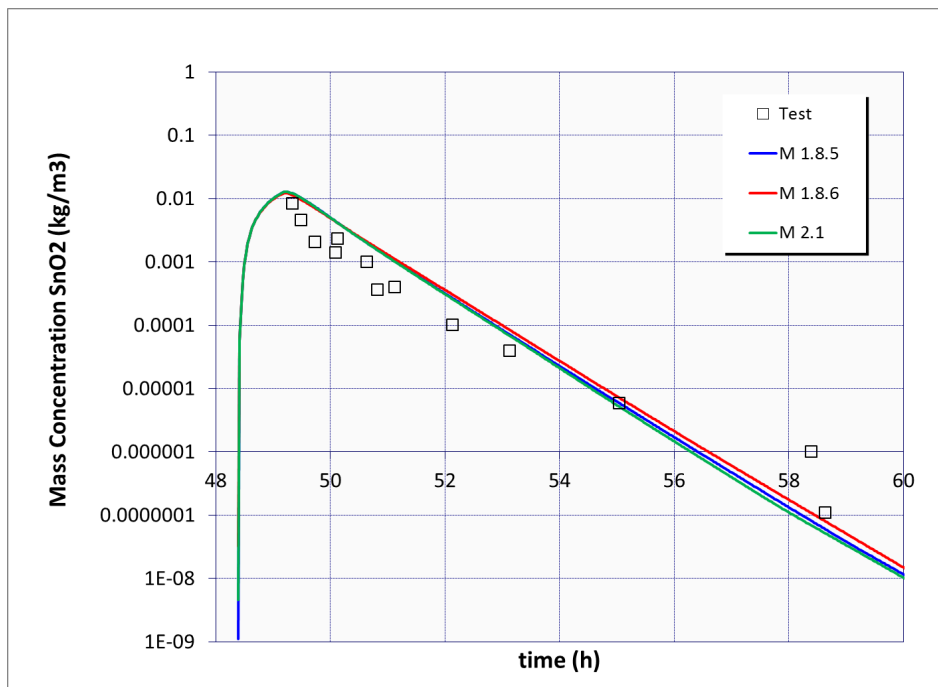
Figure 4-2   Depletion of SnO$_2$ in DEMONA-B3 experiment

4-7

4.3.2   Oxidation

Metal oxidation is calculated using standard parabolic kinetics, with appropriate rate constant expressions for Zircaloy and steel, limited by gaseous diffusion considerations if necessary. For the Zircaloy-H_2O reaction, the rate constant is evaluated using the Urbanic-Heidrich constants. Though these constants and equations have not changed since they were first implemented into the code, other changes to the code can lead to changes in clad temperature, surface areas, and oxidation thickness histories. Therefore, changes in results are not so much indicative of changes to the oxidation models as they are changes in the core heat-up and degradation modeling. Figure 4-3 and Figure 4-4 show the hydrogen generation calculated for the Phebus-B9+ and FPT-1 assessment cases [61] respectively, using MELCOR Versions 1.8.5, 1.8.6, and 2.1. Note that only minor differences are observed for these three code versions. There is a slight trend in the data showing that MELCOR Version 1.8.5 predicted higher hydrogen generation than MELCOR Version 2.1 and MELCOR Version 1.8.6 and that all three versions slightly over predict the cumulative hydrogen generation.
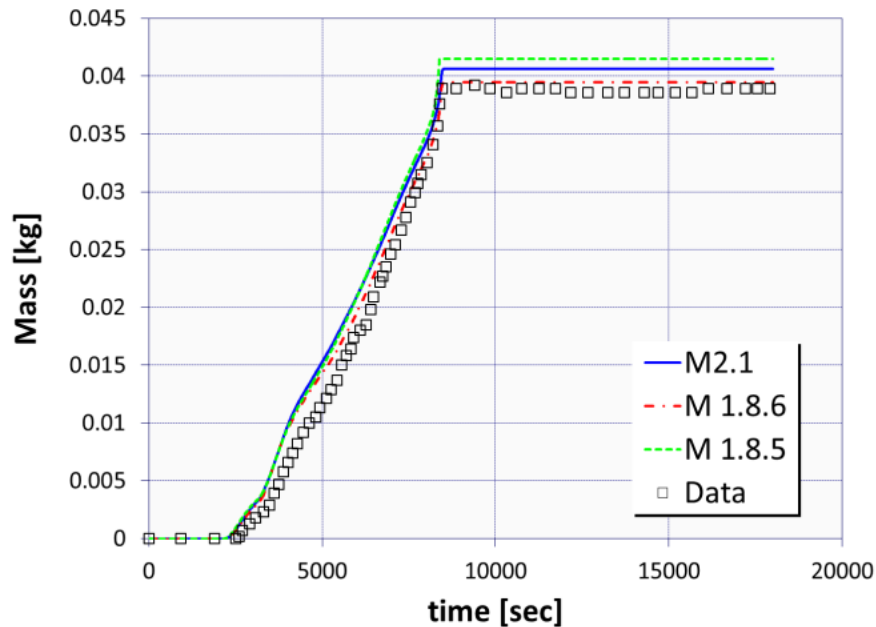
Figure 4-3   PHEBUS-B9+ hydrogen generation
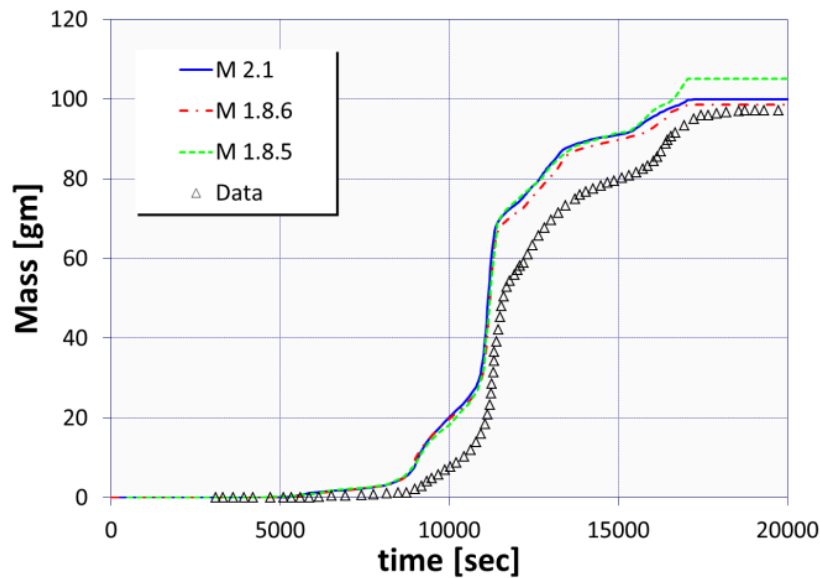
Figure 4-4   FPT-1 hydrogen generation

4.3.3   Hydrogen Stratification in Containment

Because of its lower density than surrounding air, hydrogen would concentrate in higher regions of the containment. It is important to be able to capture this stratification to predict local regions of flammability. The NUPEC M-8-1 [61] mixing test provides an excellent validation of MELCOR's capabilities for calculating stratification of helium in a large, compartmentalized containment. The MELCOR Version 1.8.5 input deck was converted to MELCOR Version 1.8.6 and then to MELCOR Version 2.1, using the Symbolic Nuclear Analysis Package (SNAP) as the converter. Though there are noticeable discrepancies between calculations and test data, it is important to observe that all three code versions give identical results. Overall, MELCOR does a reasonable job of capturing helium stratification for these tests.
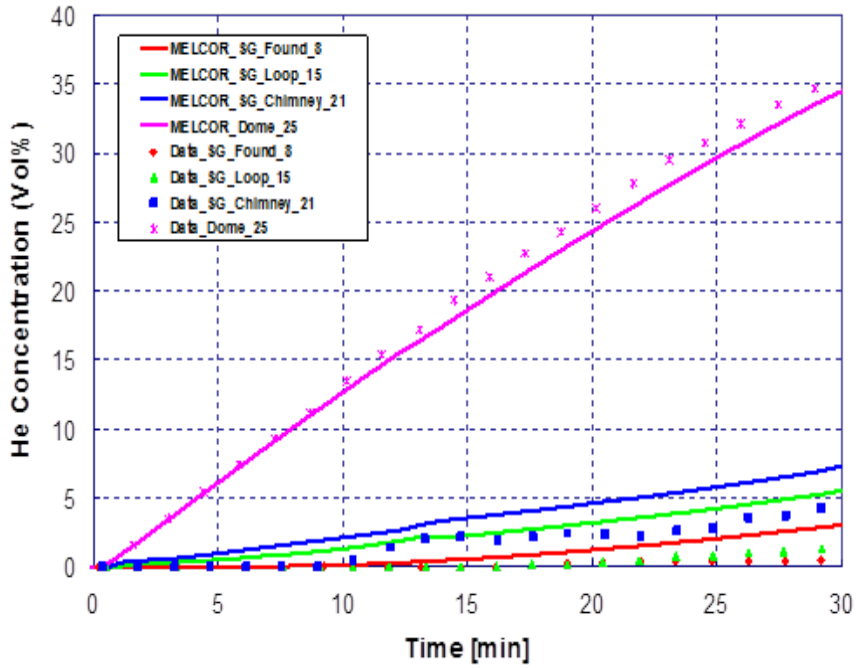
Figure 4-5   Helium stratification calculated for NUPEC M-8-1 for MELCOR 2.x
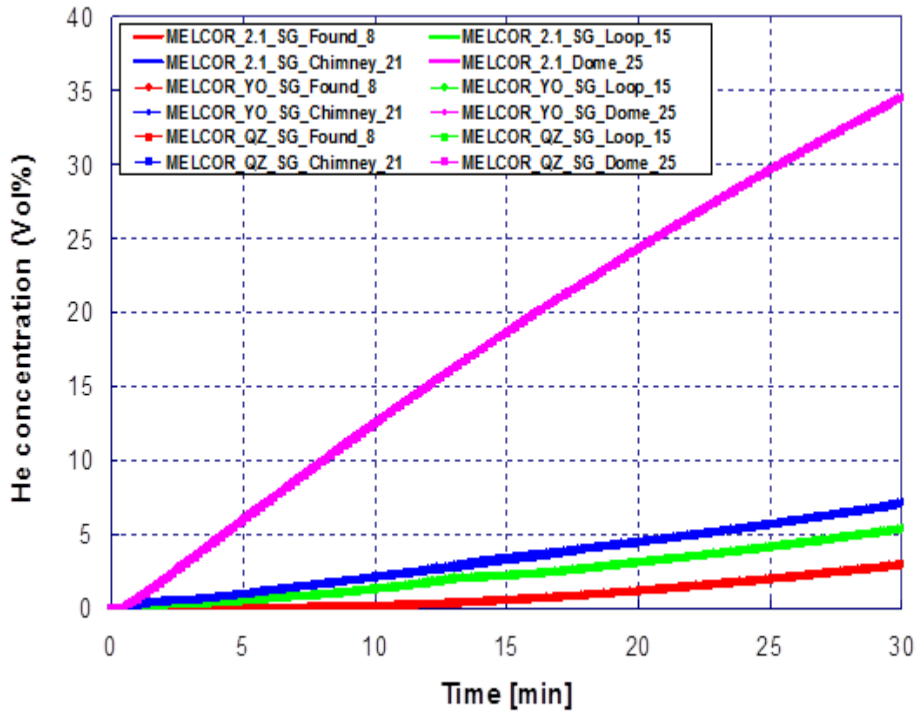
Figure 4-6   Helium stratification calculated for NUPEC M-8-1 for three MELCOR code versions

4.3.4   Combustion Modeling

MELCOR uses relatively simple models for burning of premixed gases without modeling the actual reaction kinetics or tracking the actual flame front propagation based on the HECTR 1.5 code; the models were implemented into the code before MELCOR Version 1.8.0. These models have a high level of maturity and only minor code corrections have been made to these models in recent code versions.

Table 4-3 through Table 4-5 show burn characteristics calculated for the NTS hydrogen burn tests. These tests were sponsored by the NRC and performed by the EPRI and were used as part of the MELCOR - CONTAIN parity study. No significant changes are observed among those tests included in the assessment study.

The MELCOR calculated burn times differ significantly from the experimental values. A likely explanation would be that the complexity of the flame propagation is not modeled. For example, if the first flame propagates upward and then down along the wall of the spherical pressure vessel, such behavior could not be captured in a lumped-parameter code. It should be noted however, that similar errors were obtained by analogous calculations performed with the CONTAIN code.

Table 4-3   Hydrogen burn completeness from experiment and MELCOR.

	Burn Completeness (%)			
Test	Experiment	M 1.8.5	M 1.8.6	M 2.1
NTSP01	32.0	36	35.67	35.67
NTSP12	58.0	74	72.94	72.94
NTSP15	100.0	100	100.0	100.0
NTSP20	100.0	100	100.0	100.0

Table 4-4   Hydrogen burn times from experiment and MELCOR.

	Burn Time (s)			
Test	Experiment	M 1.8.5	M 1.8.6	M 2.1
NTSP01	68.5	2.0	1.9	1.9
NTSP12	27.0	9.0	9.2	9.2
NTSP15	6.0	1.7	1.2	1.2
NTSP20	2.0	6.0	4.0	4.0

Table 4-5   Pressure ratio calculated with recent MELCOR code versions compared to test results.

Test ID and Initial H_2 & H_2O Concentrations			P(max)/P(initial)			
Test ID	H_2, v/o	H_2O, v/o	M 1.8.5	M1.8.6	M2.1	Test
Standard Tests						
NTSP01	5.3	4.2	1.71	1.70	1.70	1.48
NTSP15	9.9	4.2	4.11	4.08	4.08	3.61
Steam-Laden Tests						
NTSP12	6.9	28.3	2.37	2.36	2.36	1.831
NTSP20	12.9	27.8	3.97	3.95	3.95	3.87

4.3.5   Containment Pressure Response to Sprays

A series of experiments were conducted in the CSE vessel to evaluate the performance of aqueous sprays as a means of decontaminating containment atmospheres [33]. Measurements were obtained which provide a suitable basis for judging the ability of various mathematical models to predict spray performance in large nuclear power plant buildings. Assessments have been performed with MELCOR Version 1.8.3, 1.8.6, and 2.1 models for the A9 experiment.

The containment pressure response is shown in Figure 4-7 and Figure 4-8 for all modern code versions. These calculations indicate that the modeling of heat removal from sprays has not significantly changed in these recent code versions.
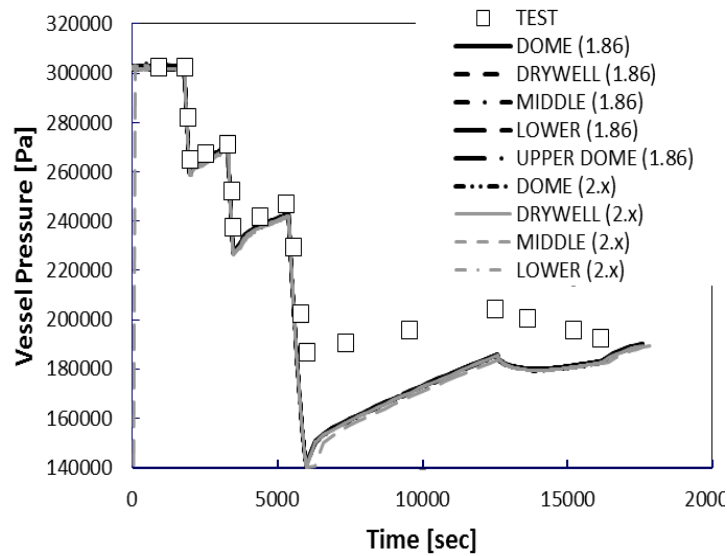
Figure 4-7   MELCOR 1.8.6 & 2.1 assessments of CSE A9
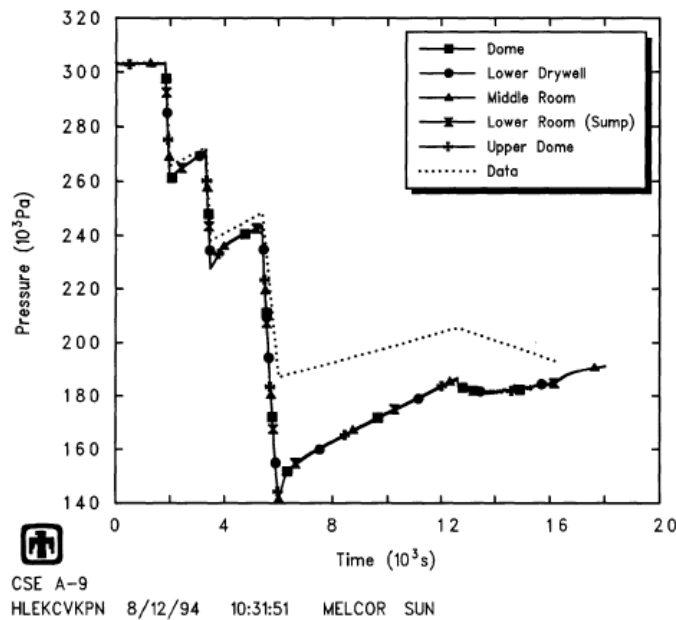
Figure 4-8   MELCOR 1.8.3 assessments of CSE A9

4.3.6   Fission Product Release

Fission product release rates are validated by comparison to several experimental series, principally the ORNL VI tests, Phebus FPT-1, and VERCORS-2 and 4. The release rates are set relative to Cs based on the VI tests. The releases were then adjusted based on FPT-1, which has the most complete data for the various fission products. The resulting release coefficients, termed "modified ORNL-Booth," were then compared to the VERCORS tests.

4-13

VERCORS-2 has data only on Cs release, and VERCORS-4 has some others also. The last comparisons to VI and VERCORS were done with MELCOR Version 1.8.5 and 1.8.6; comparisons to FPT-1 have been done with 1.8.5, 1.8.6 and 2.1. In general, differences observed were due to the switch to the modified ORNL-Booth release coefficients in 1.8.5 rather than to any version differences.

4.3.7   Molten Core-Concrete Interaction

The source term during the late phase of a severe accident is dominated by the molten debris – concrete interactions that occur in the reactor cavity. CORCON-MOD3 was implemented into MELCOR Version 1.8.3 and, aside from a few changes in default sensitivity coefficients, has largely remained unchanged. The SURC-1 test examines the one-dimensional ablation front from overlying core debris. Results of simulations for MELCOR Version 1.8.6 and 2.1 are shown in Figure 4-9. These results show that the CORCON models continue to give good results in predicting the ablation front for these tests. The MELCOR Version 2.1 assessment report will investigate more recent tests such as the Organization for Economic Co-operation and Development (OECD) MCCI tests.
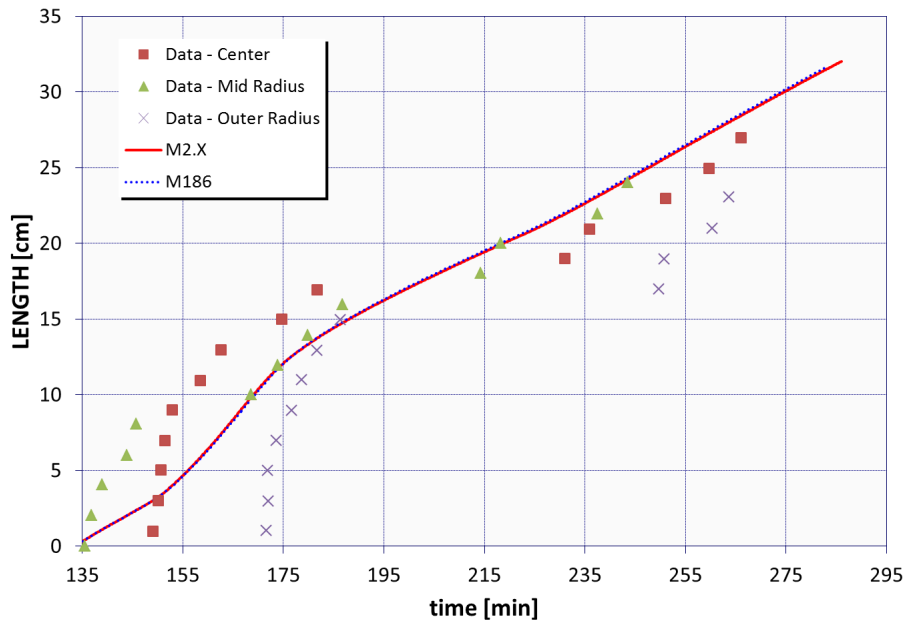
Figure 4-9   MELCOR 1.8.6 & 2.x assessments of ablation depth in SURC-1 Test

5. INSIGHTS

Conducting a state-of-the-art analyses project, such as the SOARCA project, provides an opportunity to investigate accident phenomena at a much greater level of detail than analyses performed in the past. Throughout the process, advanced knowledge and insights were gained that will benefit the PRA community in performing accident sequence analyses and the further refinement of branch probabilities. The methodology applied in the analyses established a framework for future applications and demonstrated that use of complex severe accident codes has advanced into risk informed application capable of evaluating response actions and timing to mitigate accident progression. The following insights were obtained during the SOARCA project. The general order of the presented insights is the authors' perception of importance, but many of the Surry ISLOCA insights were grouped as a matter of convenience for the reader.

1. In the Surry SBOs, the most likely first RCS failure occurs at the hot leg nozzle prior to significant in-vessel fuel damage. This leads to vessel depressurization, accumulator discharge, fuel cooling, and an interruption to the core heat-up. A new release pathway for radionuclide is established at the failed hot leg. The response of a TISGTR is also impacted by hot leg failure. The hot leg failure substantially decreases TISGTR flow due to the RCS depressurization and the introduction of the larger failure location as the primary fission product pathway from the vessel.

2. With regard to the ISLOCA modeling and the magnitude of predicted radionuclide releases to the environment, a key insight is the large amount of deposition of aerosolized radionuclides in the LHSI piping by means of turbulent deposition. Sustained high velocities in the LHSI piping during core degradation drive the importance of this phenomenon. A thorough representation of the LHSI piping is necessary to address turbulent deposition of fission product aerosols in the piping and revaporization of deposits.

3. The improvements to fuel degradation modeling and 2-dimensional core modeling show a delayed heat-up followed by accelerated oxidation. The accelerated oxidation phase ends following molten Zircaloy breakout. Without molten Zircaloy breakout, the subsequent heat-up is primarily controlled by decay heat. The best practice modeling of Zircaloy-oxide collapse creates a debris bed similar to TMI-2. The debris bed slows oxidation by creating blockages and inhibiting natural circulation. The debris bed gradually grows axially and radially, which eventually leads to core plate failure.

4. Upon core plate failure, the lower plenum debris response is consistent with experimental research and leads to delayed vessel failure versus the previously default 0-dimensional counter-current flow limiting models. The lower plenum debris cools as it transfers heat to the water and steel in the lower plenum. Once the water has evaporated, the debris bed heats the lower head towards creep rupture failure. Drain line, control rod drive penetration, etc. lower head failure modes are considered for the Peach Bottom reactor but could only be modeled parametrically and do not lead to significant changes in the source term magnitude.

5. Natural circulation processes substantially delay the heat-up of the fuel as heat is transmitted from the core into the vessel internals and to the steam generator in PWRs. The slower heat-up leads to high hydrogen production and more extensive transport of aerosols in the primary system.

6.   The failure of an in-core instrument tube leads to an early radionuclide release which does not impact the overall source term. A reviewer cited strong evidence of early noble gas releases through instrument tubes for the TMI-2 and Fukushima accidents. The approach is fully discussed in the NUREG/CR-7110, Vol. 1 and can be important for accident management and early release timing but less important for source term magnitude characterization.

7.   The inclusion of control rod materials and tin from the Zircaloy increases the aerosol density, especially at the start of the core degradation. The control rod and structural aerosols enhance in-vessel deposition by increasing agglomeration rates.

8.   The incorporation of structural, creep failure models for the core plate and enhanced in-core debris bed modeling leads to higher temperature debris relocating to the lower plenum. Following core plate failure, the application of the best practices demonstrates vigorous but not explosive interaction between the relocating debris and the lower plenum.

9.   Although the modified ORNL-Booth radionuclide release model has a slower release rate than the default CORSOR-M model, the new fuel degradation modeling leads to higher temperatures and a slower collapse than previous core degradation models. The net effect is essentially complete release of volatile fission products from the fuel.

10.   The BWR containment failure best practices include simultaneous consideration of multiple failure modes. Although each failure mode can have temporal significance, the impact on the source term is dominated by the liner melt-through failure.

11.   The potential of combustion failure of the PWR containment is significant in one scenario which included emergency containment sprays. While delayed combustion can lead to containment failure or increased leakage, the formation of combustible quantities can only occur through sustained spray operation that simultaneously captures radionuclides. Hence the impact is comparable to cases without delayed combustion-induced containment failure.

12.   For Peach Bottom, two modes of SRV failure were considered in the SOARCA project – failure due to excessive cycling (stochastic failure to close) and failure due to overheating (thermal failure to close). The best-estimate number of SRV cycles permissible before failing in an open position was taken as 270. The best-estimate temperature an SRV valve stem could withstand before seizing with the valve in an open position was taken as 900 K. Due to inclusion of these best-estimate failure mode values, the failure of the lowest set-point SRV occurs prior to the onset of core damage as a result of the excessive cycling criterion.

13.   For Surry, two modes of primary SRV and PORV failure are considered in the SOARCA project – failure due to excessive cycling (stochastic failure to close) and failure due to overheating (thermal failure to close). The 50th percentile number of SRV and PORV cycles permissible before failing in an open position was taken as 256 and 247, respectively. The best-estimate temperature an SRV or PORV valve stem could withstand before seizing with the valve in an open position was taken as 10 cycles above 1000 K for both valve types. Due to inclusion of these best-estimate failure mode values, the failure of the lowest set-point primary SRV occurs prior to the onset of core damage as a result of the excessive cycling criterion for the unmitigated LTSBO with late

RCP seal failure, the mitigated and unmitigated STSBO, and the mitigated and unmitigated STSBO with a TISGTR.

14. The formation of cesium-molybdate leads to a higher release of molybdenum, lower volatility of released cesium, and significantly different deposition and revaporization behavior. In the Surry ISLOCA analysis, the cesium release to the environment is strongly impacted by revaporization of radionuclide deposits formed in the LHSI piping. The majority of the cesium is in the form of cesium-molybdate, which is retained in the LHSI piping.

15. The necessity of modeling in detail the interconnected buildings into which the RCS would vent given an ISLOCA proved valuable and provided insights regarding the depth of the water pool formed in the buildings. The rupture in the Surry scenario was determined to be submerged in a pool formed from water leaked into the auxiliary buildings through the rupture. A key insight is that pool cooling of submerged LHSI piping sections strongly suppresses revaporization of radionuclide deposits in those sections and the pool scrubbing of radionuclides at the LHSI pipe rupture results in a meaningful reduction in release to the environment. Had the piping sections not been determined in the Surry scenario to be submerged, radionuclide releases to the environment would have been greater.

16. The degree of revaporization described above is strongly affected by to what extent gamma radiation emitted by the radionuclide deposits is transmitted through the LHSI pipe wall. In certain sections of the piping, including the gamma transmission or not meant the difference between not having and having revaporization, respectively.

17. The resuspension of radionuclide deposits formed in the LHSI piping is an important phenomenon that was not addressed mechanistically in the ISLOCA analysis. The phenomenon is important because of the large deposition in the LHSI piping predicted by MELCOR and the sustained high-velocity gas flow in the piping that can conceivably tear the deposits from the pipe wall and carry them along the piping and out the rupture. Resuspension is not addressed mechanistically because, while MELCOR includes modeling to predict deposition in the piping (turbulent deposition and impaction), it does not include modeling to predict resuspension. During the ISLOCA analysis, it was judged that that the deposits would likely break away from the pipe wall to some extent and be carried out the piping to buildings outside of containment, but that the material would be in a form difficult to aerosolize and so would not release to the environment. This is because the break is under water for the entire simulation time, and the aerosols generated by a melting core are very small since they are formed by vapor condensation but the aerosols formed by re-suspending the deposited materials by high speed vapor flow across the surface of the pipe are so large that the aerosols do not travel far downstream before re-depositing. The insight gained regarding the resuspension of deposited material in the LHSI piping is that a judgment regarding resuspension needs to be made when employing a tool such as MELCOR because the code models deposition but not resuspension.

18. Another fundamental insight gained from the ISLOCA analysis is that hydrogen deflagrations in the building(s) into which the RCS would vent (given an ISLOCA) were important because the resulting breaches in building boundaries were the ultimate paths of radionuclide releases to the environment. The best practices include pressurization and/or hydrogen deflagration failure logic for the BWR reactor building boundary. The

ineffective retention of fission products within the reactor building was confirmed by March 2011 events at Fukushima.

19. Aerosol (radionuclide, concrete, soot) deposition in the HEPA filters of the safety-related exhaust ventilation system serving the building(s) into which the RCS would vent was important to the Surry ISLOCA scenario. Deposition was determined to be high on the filters but not so high to suggest that the filters would fail or that the system would shut down because of excessive loading on the filters. This is insightful as the progression of the scenario (and the releases to the environment) would have been substantially different if the system shut down or if the filters failed but the fans continued to run.

20. The necessity of modeling in detail the filtered safety-related exhaust ventilation system serving the buildings into which the RCS would vent is another valuable insight gained from the ISLOCA analysis. Substantial amounts of fission products were captured in the filters of this system in the Surry analysis such that had the system not been represented, predicted releases to the environment would have been substantially greater.

21. A key insight from the ISLOCA analysis was the importance of operators completing certain critical procedural actions and the necessity of representing these actions in an ISLOCA simulation, see NUREG/CR-7110 [63]. At Surry, the timing of actions such as stopping the LHSI pumps, isolating the LHSI pump suctions from the refueling water storage tank, and stopping and/or throttling HHSI pumps to conserve RWST inventory, which strongly influence accident progression, were taken directly from operator response to the ISLOCA scenario in the control room simulator. With these actions accomplished in a timely manner, MELCOR predicts a slow progression to core damage; therefore, the operator responses and corresponding timings were of high importance in modeling the sequence. Analyses for individual sites should look closely at the timing of procedural actions as well as simulated response times, if possible.

6.   REFERENCES

[1]   U.S. Nuclear Regulatory Commission, "State-of-the-Art Reactor Consequence Analyses (SOARCA) Report," NUREG-1935, Washington, D.C.: NRC, 2012

[2]   Gauntt, R. O., Cash, J.E., Cole, R. K., Erickson, C. M, Humphries, L.L., Rodriguez, S. B., Young, M. F., "MELCOR Computer Code Manuals, Vol. 1: Primer and User's Guide, Version 1.8.6," NUREG/CR-6119, Vol. 1, Rev. 3, U.S. Nuclear Regulatory Commission, Washington, DC, 2005.

[3]   Bixler, N., et al., "MACCS Best Practices as Applied in the State-of-the-Art Reactor Consequence Analyses Project," NUREG/CR-7009, SAND2012-8500P, 2014.

[4]   Henry, R., Mohsen, K., Martin, R., Sanders, R., Sonnenkalb, M., State-of-the-Art Reactor Consequence Analyses (SOARCA) Project MELCOR Modeling Practices Review, Review Committee Report, ML062500079, U.S. Nuclear Regulatory Commission, Washington, DC, December 8, 2006.

[5]   U.S. Nuclear Regulatory Commission, "Technical Bases for Estimating Fission Product Behavior During LWR Accidents," NUREG-0772, 1981.

[6]   Ramamurthi, M., and M.R. Kuhlman, "Final Report on Refinement of CORSOR – An Empirical In-Vessel Fission Product Release Model," Battelle Report, October 31, 1990.

[7]   S.R. Greene, "MELCOR 1.8.2 assessment: comparison of fuel fission product release models to ORNL VI fission product release experiments," ORNL/NRC/LTR-94/34, 1995.

[8]   T. Nakamura and R.A. Lorenz, "A Study of Cesium and Krypton Releases Observed in HI and VI Tests Using a Booth Diffusion Model," Oak Ridge National Laboratory Research Paper, May 1987.

[9]   B.J. Lewis, et al., "Modeling the release behavior of cesium during severe fuel degradation," J. Nuc. Mat. (227), pp 83-109, 1995.

[10]   F.C. Iglesias, et al., "Fission product release mechanisms during reactor accident conditions," J. Nuc. Mat. (270) pp 21-38, 1999.

[11]   H. Manenc, P. Mason and M.P. Kissane, "The modeling of fuel volatilization in accident conditions," J. Nuc. Mat. (294) pp 64-68, 2001.

[12]   B.V. Dobrov, et al., "Kinetics of UO_2 oxidation in steam atmosphere," J. Nuc. Mat. (255) pp 59-66, 1998.

[13]   N.E. Bixler, "VICTORIA 2.0: A Mechanistic Model for Radionuclide Behavior in a Nuclear Reactor Coolant System Under Severe Accident Conditions," NUREG/CR-6131, SAND93-2310, 1998.

[14]   B. Clement and T. Haste, "Comparison report on International Standard Problem ISP-46 (Phebus FPT-1)," Note Technique SEMAR 03/021, Draft Final Report, April 2003.

[15] Annunziato, A., Magallon, D., et al., "Progress of the FARO/KROTOS programme," Cooperative Severe Accident Research Meeting, U.S. Nuclear Regulatory Commission, 1996.

[16] G. Ducros, et al., "Fission product release under severe accident conditions: general presentation of the program and synthesis of VERCORS 1-6 results," Nuc. Eng. And Des. (208) pp 191-203, 2001.

[17] V. Strizov, "MELCOR 1.8.5 Validation: Modeling of Fission Product Release," NSI-SARR-149-03, Russian Academy of Sciences, Nuclear Safety Institute, Dec. 2002.

[18] Soffer, L., et al., "Accident Source Terms for Light-Water Nuclear Power Plants," NUREG-1465, U.S. Nuclear Regulatory Commission, 1995.

[19] NUREG/CR-5582, "Lower Head Failure Experiments and Analyses," SAND98-2047, Sandia National Laboratories, 1998.

[20] M.T. Farmer, S. Lomperski, and S. Basu, "Results of Reactor Material Experiments Investigating 2-D Core-Concrete Interaction and Debris Coolability," Proc. Proc. Int. Conf. Adv. Power Plants, ICAPP'04, Pittsburgh, Pennsylvania, June 2004.

[21] Bayless, P.D., et al., "Severe Accident Natural Circulation Studies at the INEL," NUREG/CR-6285, INEL-94/0016, February 1995.

[22] Stewart, W.A., Pieczynski, A.T., and Srinivar, V., "Natural Circulation Experiments for PWR Degraded Core Accidents," EPRI Report NP 6324 D, 1989.

[23] Stewart, W.A., Pieczynski, A.T., and Srinivar, V., "Natural Circulation Experiments for PWR High Pressure Accidents," EPRI Report TR 102815, 1993.

[24] Boyd, C.F. Hardesty, K., "CFD Analysis of 1/7th Scale Steam Generator Inlet Plenum Mixing During a PWR Severe Accident," NUREG-1781, October 2003.

[25] Boyd, C.F., Helton, D. M., Hardesty, K., "CFD Analysis of Full Scale Steam Generator Inlet Plenum Mixing During a PWR Severe Accident," NUREG-1788, U.S. Nuclear Regulatory Commission, May 2004.

[26] Wagner, K. C., "MELCOR 1.8.5 Analysis of Natural Circulation Flow in the Westinghouse High-Pressure SF6 Experiments," Draft SAND Report, Sandia National Laboratories, June 2001.

[27] Fletcher, C. D., and Beaton, R. M., "SCDAP/RELAP5 Base Case Calculation for the Station Blackout Uncertainty Study," Letter report to D. M. Helton, US NRC, August 2006.

[28] Fletcher, C. D., and Beaton, R. M., "Evaluation of Uncertainties in SCDAP/RELAP5 Station Blackout Simulations," Letter report to D. M. Helton, US NRC, August 2006.

[29] Petrie, L.M et al., "Standard Composition Library," NUREG/CR-0200, Rev. 6, Vol. 3, ORNL/NUREG/CSD-2/V3/R6, Oak Ridge National Laboratory, September 1998.

[30] Downes, K.W., Beck, C.K., Cowan, F.P., Fleck, J.A., Kuper, J.B.H., McLaughlin, J., Singer, I., Smith, M., "Theoretical Possibilities and Consequences of Major

Consequences in Large Nuclear Power Plants," WASH-740, United States Atomic Energy Commission, March 1957.

[31]   Souto, F.J., Haskin, F.E., Kmetyk, L.N., "MELCOR 1.8.2 Assessment: Aerosol Experiments ABCOVE AB5, AB6, AB7, and LACE LA2," SAND94-2166, 1994.

[32]   Tautges, T.J., "MELCOR 1.8.2 Assessment: The MP-1 and MP-2 Late Phase Melt Progression Experiments," SAND94-0133, 1994.

[33]   Kmetyk, L.N., "MELCOR 1.8.3 Assessment: CSE Containment Spray Experiments," SAND94-2316, 1994.

[34]   Tills, J., Notafrancesco, A, Longmire, P., "An Assessment of MELCOR 1.8.6: Design Basis Accident Tests of the Carolinas Virginia Tube Reactor (CVTR) Containment (Including Selected Separate Effects Tests)," SAND2008-1224, 2008.

[35]   Tautges, T., "MELCOR 1.8.2 Assessment: The DFI-4 BWR Damaged Fuel Experiment," SAND93-1377, 1993.

[36]   Tautges, T., "MELCOR 1.8.3 Assessment: GE Large Vessel Blowdown and Level Swell Experiments," SAND94-0361, 1994.

[37]   Kmetyk, L.N., "MELCOR 1.8.2 Assessment: IET Direct Containment Heating Tests," SAND93–1475, 1993.

[38]   Kmetyk, L.N., "MELCOR 1.8.1 Assessment: LACE Aerosol Experiment LA4," SAND91–1532, 1991.

[39]   Kmetyk, L.N., "MELCOR 1.8.1 Assessment: LOFT Integral Experiment LP-FP-2," SAND92–1373, 1992.

[40]   Kmetyk, L.N., "MELCOR 1.8.1 Assessment: Marviken-V Aerosol Transport Tests ATT-2b/ATT-4," SAND92–2243, 1993.

[41]   Gross, R.J., "PNL Ice Condenser Aerosol Experiments," SAND92–2165, 1993.

[42]   Kmetyk, L.N., "MELCOR 1.8.1 Assessment: FLECHT SEASET Natural Circulation Experiments," SAND91-2218, 1991.

[43]   Kmetyk, L.N., "MELCOR 1.8.1 Assessment: ACRR Source Term Experiments ST-1/ST- 2", SAND91-2833, 1992.

[44]   "Reactor Safety Study, An Assessment of Accident Risks in U.S. Commercial Nuclear Power Plants," NUREG-75/014, U.S. Nuclear Regulatory Commission, October 1975.

[45]   Aldrich, D.C., Sprung, J.L., Alpert, D.J., Diegert, K.V., Ostmeyer, R.M., Ritchie, L.T., Strip, D.R., Johnson, J.D., Hansen, K., Robinson, J., "Technical Guidance for Siting Criteria Development," NUREG/CR-2239, U.S. Nuclear Regulatory Commission, Washington, DC, 1982.

[46]   Corradini, M.L. et al, "An Analysis of Containment Failure by Steam Explosion Following a Postulated Core Meltdown in a Light Water Reactor," Nuclear Engineering and Design, 66:287-298, 1981.

[47]   Theofanous, T.G., Yuen, W.W., "The Probability of alpha-mode containment failure," Nuclear Engineering and Design.155:495-473, 1995.

[48]   Turland, B., Fletcher, D.F., et al., "Quantification of the probability of containment failure caused by an in-vessel steam explosion for the Sizewell B PWR," Nuclear Engineering and Design 155:445-458, 1995.

[49]   Huhtiniemi, I., Magalon, D., Hohmann, H., "Results of recent KROTOS FCI tests: alumina versus corium melts," Nuclear Engineering and Design 189:379-389, 1999.

[50]   Huhtiniemi, I., Magallon, D., "Insight into steam explosions with corium melts in KROTOS," Nuclear Engineering and Design, 204:391-400, 2001.

[51]   Song, J.H., et al., "Experiments on the interactions of molten ZrO_2 with water using TROI facility," Nuclear Engineering and Design, 213:97-110, 2002.

[52]   Song, J.H., Park, I.K., Shin, Y.S., Kim, J.H., Hong, S.W., Min, B.T., Kim, H.D., "Fuel coolant interaction experiments in TROI using a UO_2/ZrO_2 mixture," Nuclear Engineering and Design, 222(1):1-15, 2003.

[53]   NEA/CSNI, "Technical Opinion Paper on Fuel-Coolant Interaction," NEA/CSNI/R(99), 2000.

[54]   Nuclear Regulatory Commission, "Severe Accident Risks: An Assessment for Five U.S. Nuclear Power Plants," NUREG-1150, U.S. Nuclear Regulatory Agency, Washington, DC, 1990.

[55]   Pilch M.M.; Yan, H., and Theofanous T.G., "The probability of containment failure by direct containment heating in Zion," Nuclear Engineering and Design, Vol. 164, Number 1. August 1996.

[56]   R. A. Lorenz and M. F. Osborne, "A Summary of ORNL Fission Product Release Tests with Recommended Release Rates and Diffusion Coefficients," NUREG/CR-6261, 1995.

[57]   Natesan, K. and Soppet, W. K. "Air Oxidation Kinetics for Zircaloy-4," Argonne National Laboratory, NUREG/CR-6846, July 2004.

[58]   Wright , A. L. and Arwood, P. C., "Summary of posttest aerosol code-comparison results for LWR Aerosol Containment Experiment (LACE) LA3", LACE TR-024, ORNL/M-492, June 1988.

[59]   Fauske & Associates, LLC, MAAP (Modular Accident Analysis program), http://www.fauske.com/pdf/MAAP.pdf

[60]   Gauntt, R. O., "Synthesis of VERCOS and Phebus data in Severe Accident Codes and Applications," SAND2010-1633, Sandia National Laboratories, April 2010.

[61]   Gauntt, R. O., Cole, R. K., Erickson, et.al., "MELCOR Computer Code Manuals, Vol. 3: Demonstration Problems, Version 1.8.5," NUREG/CR-6119 Rev. 0, U.S.SAND2001-0929P, Nuclear Regulatory Commission, Washington, DC, 2001.

[62]   US. NRC. "State-of-the-Art Reactor Consequence Analysis Project, Volume 1: Peach Bottom Integrated Analysis," NUREG/CR-7110, Volume 1, U.S. Nuclear Regulatory Commission: Washington DC, 2012.

[63]   US. NRC. "State-of-the-Art Reactor Consequence Analysis Project, Volume 2: Surry Integrated Analysis," NUREG/CR-7110, Volume 2, U.S. Nuclear Regulatory Commission: Washington DC, 2012

[64]   Gauntt, R. O., Cole, R. K., Erickson, et.al., "MELCOR Computer Code Manuals, Vol. 2: Reference Manuals, Version 1.8.5," NUREG/CR-6119 Rev. 2, U.S. SAND2000-2417/1, U.S. Nuclear Regulatory Commission: Washington DC, 2001.

[65]   US. NRC. "Research Activities FY2012-2014," NUREG-1925, Revision 2, U.S. Nuclear Regulatory Commissin: Washington DC, 2013.

Appendix A Other MELCOR Modeling Best Practices

Several user input options were enabled or adjusted for the SOARCA project that do not warrant detailed descriptions or justifications of their use. This Appendix presents these generic adjustments within Table A-1 as a reference for simple input options which readers may wish to review with consideration for implementation.

Table A-1   Standard MELCOR modeling practices, modeling parameters, and sensitivity coefficients for analysis of severe accidents

Item	Record	Field	Value(s) used in SOARCA	Description
1.	BUR000	IACTV	0 (Active)	Burn package activation
2.	BUR1xx (xx = CV)	IGNTR	86 for CVs where ignition is to be prohibited.	Apply to RCS control volumes to preclude combustion.
3.	BUR1xx (xx = CV)	TFRAC	1.0	Time fraction of burn before propagation to neighboring CV is allowed. Value of 1.0 means a flame must travel the radius of the control volume before propagating to its neighbor.
4.	FLnnn00	ZFM, ZTO	ZFM – ZTM != 0.0 (For vertical containment flow paths only)	To insure that MELCOR properly estimates vertical burn propagation in containment, and adjacent buildings, it is necessary to define "vertical" flow path "from" and "to" elevations with a small dZ. If the "from" and "to" elevations are set equal (which has been historical practice to ensure complete vertical pool drainage), the MELCOR burn package uses criteria for horizontal burn propagation.
5.	FLnnnFF	KFLSH	1	Calculate superheated pool flashing for all liquid LOCA connections to initially dry containment regions. KFLSH activates the model. Activate RN1Ikkk as needed for impact into specified heat structures.
6.	FLnnn02	IBUBF & IBUBT	-1 +2	Vapor heat transfer in pools for RCS FLs. SPARC scrubbing in pools for spargers, quencher, vents, and BWR downcomers.
7.	RN2FLTXX00	FPVAPOR	Various geometric values	MELCOR SPARC pool scrubbing model was modified to scrub all gaseous RN classes for
8.	COR00001	DRGAP	0.0	Thickness of gas gap between fuel pellets and cladding set 0.0 to account for swelling of operating fuel.
9.	COR00001A	ILHTYP ILHTRN	0 BWR =0, PWR =1	Lower head is a hemisphere Transition is at RCOR (BWR) or RVES (PWR)

Table A-2   Standard MELCOR modeling practices, modeling parameters, and sensitivity coefficients for analysis of severe accidents (continued)

Item	Record	Field	Value(s) used in SOARCA	Description
10.	COR00009	HDBPN HDBLH MDHMPO MDHMPM TPFAIL CDISPN	100 W/m^2-K 100 W/m^2-K 'MODEL' 'MODEL' 9999 K 1.0	This record activates the internal molten pool to lower head heat transfer models and provides reasonable solid debris to lower head heat transfer coefficient.
11.	COR00012	HDBH2O VFALL	2000 W/m^2-K 0.01 m/s	HTC in-vessel falling debris to pool (W/m^2-K) Velocity of falling debris (m/s).). Perhaps not correct for shallow pools and not necessary in deep pools since adoption of no 1-D CCFL limitation via the one-dimensional Lipinski model.
12.	CORCR0	IAICON	2	For PWRs only Activate control rod release model, 2 = Model is active, vaporization is allowed from both candling material and conglomerate.
13.	CORZjj01	PORDP	0.4	Porosity of particulate debris
14.	CORijj04	DHYPD	Core - 0.01 m LP - 0.002 m	Particulate debris equivalent diameter (LP values for DHYPD, HDBH2O, VFALL tuned to get appropriate end-of-pour debris temperature. 2mm based on FAERO fragmented debris size). Perhaps not correct for shallow pools.
15.	CORZjjNS	TNSMAX	1520 K 1700 K	Control blades failure temperature (BWR) Core top guide failure temperature (BWR)
16.	CORijjDX	FBYXSS	Calculated.	For BWRs only. Fraction of lower head COR cells normally displaced by control rod guide tubes should be 'excluded' from volume available to particulate debris. Volume recovered when tubes (as supporting structure) fails.
17.	SC-1132(1)	TRDFAI	2800 K	Fuel rod collapse temperature (addressed with CORijjFCL records)
18.	SC-1141 (2)	GAMBRK	0.20 kg/m-s	The maximum molten Zr breakout flow rate parameter adjusted to yield 2 mm/s as evidenced in CORA experiments
19.	SC-1701 (1)		0.01	Open volume fraction for subnode blockage criterion. This is the default setting.
20.	SC-4401(3)	XPASMX	15	Maximum number of iterations permitted before solution is repeated with a decreased (subcycle) timestep.

Item	Record	Field	Value(s) used in SOARCA	Description
21.	DCHNEMnn00	ELMNAM ELMMAS	Use ORIGEN results for core, if available.	Elemental fission product mass at shutdown for calculation of decay heat.
22.	DCHNEMnnnm	DCHEAT	Use pre-combined methodology for Cs, I, and Mo	Elemental fission product decay heat per unit mass (based on shutdown RN inventory). • Define specific decay heat for CsI (Class 16) as 0.51155 of value for Class 2 (Cs) plus 0.48845 of value for Class 4 (I). • Define specific decay heat for Cs_2MoO_4 (Class 17) as 0.7348 of value for Class 2 (Cs) plus 0.2652 of value for Class 7 (Mo). If ORIGEN results are not available for the core, perform an input deck with BE burn-up and cycle history. Redistribute RN mass as follows, • Class 2 initial mass represents the NUREG-1465 Cs gap mass not already included in Class 16. • Class 4 initial mass is empty (10^{-6} kg) • Class 7 initial mass is remaining Mo mass not included in Class 17. • Class 16 has all I and an appropriate amount of Cs mass for CsI stoichiometry. • Class 17 has the remaining Cs not included in Classes 2 and 16 plus Mo for Cs_2MoO_4 stoichiometry.
23.	DCHCLSnnn0, DCHCLSnnnm	RDCNAM, CLSELM	New RN definitions for Classes 1-12, 16-18	If ORIGEN results are available, synthesize ORIGEN data to define a single representative element for each class with decay heat data that reflects decay heat for all elements within the class (DCHNEMxxxx input.) Redefine each class to include only the representative element.
24.	DCHDEFCLS0	DEFCLS	13, 14, 15	Specifies that MELCOR DCH default classes are to be used.

Item	Record	Field	Value(s) used in SOARCA	Description
25.	DCHCLNORM	CLSNRM	'No' when ORIGEN results are available. 'Yes' when MELCOR is used to estimate initial inventories.	New ORIGEN input for elements/classes defines the total core decay heat. Otherwise, let MELCOR normalize the elemental decay heats to the rated power. Do not use RN1DCHNORM. Default behavior normalizes Class 10 (Uranium).
26.	HSccccc400 & HSccccc600	CPFPL CPFAL	See discussion	Minimum value of CVH pool fraction such that heat transfer is calculated to Pool/Atmosphere. For heat structures within the RPV, use 0.9. For PWR SG Tubes, use 0.1. All other structures modeled use default value of 0.5.
27.	HSccccc401 HSccccc601	EMISWL RMODL PATHL	0.27 EQUIV-BAND 0.1 m	Mean emissivity of SS type 316. Equivalent band radiation model. Nominal optical distance in steam (m). For SS heat structures within the reactor vessel and those being monitored for creep-rupture failure.
28.	HSDGccccc0	ISRCHS ISDIST GASNAM	HS # 1 SS	Heat structure for application of degas model. Degassing model requires 1 mesh. Name of released gas. For SS boundary structures modeled with the HS package that are coupled to the core.
29.	HSDGccccc1	RHOSRC HTRSRC TEMPL TEMPU	7930 kg/m^3 2.63x10^5 J/kg 1695 K 1705 K	Gas source density. Gas source heat of reaction. Lower temperature for degassing. Upper temperature for degassing. For SS boundary structures modeled with the HS package that are coupled to the core.

Table A-5 **Standard MELCOR modeling practices, modeling parameters, and sensitivity coefficients for analysis of severe accidents (continued)**

Item	Record	Field	Value(s) used in SOARCA	Description
30.	MPMATxxxx	MLT	2800 K 2800 K	Uranium-dioxide Zirconium-oxide Because of the interactions between materials, liquefaction can occur at temperatures significantly below the melt point. The interaction between ZrO_2 and UO_2 results in a mixture that is fluid at above about 2800 K (compared to the melting temperatures of 3113 K and 2990 K, respectively, for the pure materials). Similarly, although pure B4C melts at 2620 K, interaction with steel produces a mixture that is fluid at above about 1700 K.
31.	RN1001	NUMSEC NUMCMP NUMCLS	10 2 20 (PWR) 18 (BWR)	Default Default For BWR & PWR: 16 = CsI, 17 = Cs_2MoO_4 Now Class 17 includes default settings for Cs_2MoO_4.
32.	BWR structural tin release RN/DCH data for RN Class 18			For BWR: RN Class 18 = SnO_2 (non-radioactive) Define SnO_2 (DCHCLSnnn0) 18 = 'SnO2' SnO_2 decay heats (DCHNEMnn00) 0 W/kg (no decay heat) SC(7110) vapor pressures SnO_2: $Log_{10}(P(mm\ Hg)) = 15400/T + 8.15$ SC(7111) diffusion coefficients SnO_2: Sigma = 3.617, E/K = 97 SC(7120) elem./compound molecular weights Sn: MW = 150.7 kg/kg-mole

Item	Record	Field	Value(s) used in SOARCA	Description
33.	PWR control rod RN data for RN Classes 18, 19, and 20			For PWR RN Class 18 = Ag, 19 = In, 20 = Cd Define Ag, In, Cd (DCHCLSnnn0) 18 = 'Ag-CR', 19 = 'In-CR', 20 = 'Cd-CR' Ag, In, Cd decay heats (DCHNEMnn00) 0 W/kg (no decay heat) SC(7110) vapor pressures Ag: $Log_{10}(P(mm\ Hg)) = 1000/T + 1.26 \times 10^4 + 7.989$ In: $Log_{10}(P(mm\ Hg)) = 400/T + 1.27 \times 10^5 + 8.284$ Cd: $Log_{10}(P(mm\ Hg)) = 500/T + 5.31 \times 10^3 + 7.99$ SC(7111) diffusion coefficients Ag: Sigma = 3.48, E/K = 1300 In: Sigma = 3.61, E/K = 2160 Cd: Sigma = 3.46, E/K = 1760 SC(7120) elem./compound molecular weights Ag: MW = 107.8 kg/kg-mole In: MW = 114.8 kg/kg-mole Cd: MW = 112.4 kg/kg-mole
34.	RNCA100	ICAON	1 (Active)	Chemisorption model is active (default).
35.	RN1002	IHYGRO	1 (Active)	Hygroscopic model activation. (RNACOND set to default, 0 = condensation of water onto all aerosols.
36.	RNCRCLxx	ICRMT/ ICLSS/ FRAC	2 / 18 / 0.0145 3 / 18 / 0.0145	For BWRs, apply the non-fuel release model. Assign aerosol generated from Zr and ZrO_2 to RN Class 18 (SnO_2). The mass will be added as a non-radioactive mass to this class. The fraction of material mass available for release as an aerosol from these materials is 0.0145 (Sn fraction in Zirc-2 and -4.) Note: must also add input for the release rate (SC7103) for RN Class 18. Values should be identical to those used (default) for Class 12 (fission product Sn).
	SC7100	(2) Zr (3) ZrO2 (4) steel (5)steel ox. (6) B4C	0.1 1.0 0.0 0.0 0.0	Multipliers for various structural material types

Table A-7   Standard MELCOR modeling practices, modeling parameters, and sensitivity coefficients for analysis of severe accidents (continued)

Item	Record	Field	Value(s) used in SOARCA	Description
37.	RNFPNijjXX	NINP RINP1 RINP2	Use ORIGEN results, if available.	NINP = RN Class, RINP1 = mass, RINP2 = axial peaking factor. Distributes mass based on distribution developed with ORIGEN. If ORIGEN results are unavailable, NINP = 0, RINP1 = axial peaking factor, RINP2 = radial peaking factor. Where, $$\Sigma_i\Sigma_i\ RINP1_i * RINP2_i = 1.$$
38.	RNGAPijjnn	NINP RINP1 RINP2	1 (Xe) = 0.05 2 (Cs) = 1.00 3 (Ba) = 0.01 5 (Te) = 0.05 16 (CsI) = 0.05	Where, NUREG-1465 recommends the following gap quantities, • Xe = 5% • Cs = 5% • Ba = 1% • Te = 5%
39.	RN2FLTXX00	FPVAPOR	Various geometric values	For all flow paths entering pools via quenchers or spargers, specify the flow path to scrub all gaseous RN classes.

Appendix B   Updated Default Parameters

In review of the various input options that were modified for SOARCA applications, several user input options warranted a permanent adjustment to the default MELCOR value. This Appendix presents the new defaults, Table B-1, which reflect long term practices to better model severe accident phenomena, improve numerical robustness, or activate newer models.

Table B-1   Summary of Updated Default Parameters

#	Description	Parameter(s)	Field(s)	Value(s) used in SOARCA	Current Default Value(s)
1	COR package candling heat transfer coefficient.	COR00005	HFRZUO HFRZZR HFRZSS HFRZZX HFRZSX HFRZCP	7500 W/m^2-K 7500 W/m^2-K 2500 W/m^2-K 7500 W/m^2-K 2500 W/m^2-K 2500 W/m^2-K	1000 W/m^2-K 1000 W/m^2-K 1000 W/m^2-K 1000 W/m^2-K 1000 W/m^2-K 1000 W/m^2-K
2	COR package radiation heat transfer parameters	COR00003	FCELR FCELA	0.1 0.1	0.25 0.25
3	COR package min. porosity for flow and heat transfer	SC1505	(1) (2)	0.05 0.05	0.001 0.001
4	COR package min. CVH volume fraction	SC4414	(1)	0.01	0.001
5	COR package 1-dim. stress/strain distribution	SC1600	(1)	1.0	0.0
6	COR package min yield stress temperature	SC1603	(2)	1700.0 K	1800.0 K
7	COR package temp. for enhanced debris to lower head conduction	SC1250	(1)	2800.0 K	3200.0 K
8	CVH/FL direct versus iterative solution algorithm	SC4415	(1)	1.0	0.5
9	HS temperature convergence criterion	SC4055	(2)	0.5	5.0×10^{-4}
10	CAV package emissivity of oxide, metallic, and surrounding materials	CAVnnak	EMISS.OX EMISS.MET EMISS.SUR	0.9 0.9 0.9	0.6 0.6 0.6
11	Multipliers for surface boiling heat transfer and material (oxide/metallic) conductivity	CAVnnak	BOILING COND.OX COND.MET	10.0 (multiplier) 5.0 5.0	CORCON-Mod3 1.0 1.0
12	DCH package default classes – new default class 17 (Cs_2MoO_4)			* arrays initialized with 17 classes	* arrays initialized with 16 classes

Table B-2   Summary of Updated Default Parameters (continued)

#	Description	Parameter(s)	Field(s)	Value(s) used in SOARCA	Current Default Value(s)
13	RN class 17 physical properties	SC7120 SC7120 SC7170 SC7170 SC7170	(1,17) (2,17) (3,17) (4,17) (9,17)	351.75 kg/kg-mole 425.75 kg/kg-mole 0.67 kg/kg-H_2O 0.67 kg/kg-H_2O 4030.0 kg/m^3	28.97 kg/kg-mole 28.97 kg/kg-mole 0.0 kg/kg-H_2O 0.0 kg/kg-H_2O 1000.0 kg/m^3

Appendix C   MELCOR Validation Test Suite

A list of the assessment analyses performed for the MELCOR severe accident analysis code is presented below. The MELCOR assessment is comprised of analyses performed to simulate test series, integral and separate effects, as well as the TMI accident to demonstrate sufficient characterization of the relevant phenomena.

- ABCOVE: AB5 & AB6 [31]
  - General Description:
    - Simulation of the dry atmosphere conditions of a liquid metal fast breeder reactor containment with a sodium fire, i.e., sodium combustion product aerosols. AB6 modeled fission product aerosols, sodium iodide, in the presence of sodium combustion product aerosol.
  - Important Physics:
    - Agglomeration behavior of two aerosol species (hygroscopic and non-hygroscopic), condensation of water vapor
  - Results and Findings:
    - MELCOR adequately predicts deposition of the sodium combustion, NaO_X, aerosols.
    - MELCOR over predicts aerosol depletion of sodium iodide in AB6, possibly due to lack of resuspension modeling.

- ACRR: MP1 & MP2 [32]
  - General Description:
    - Tests investigated late phase core melt progression and examined material interactions and rod degradation for an intact rod / dense $Zr-UO_2$ crust / rubblized debris bed geometry.
  - Important Physics:
    - Heat transfer in a degraded core geometry, core degradation, material interactions

- AHMED: AMMD
  - General Description:
    - A series of hygroscopic aerosol experiments were conducted at the AHMED Test Facility by injecting NaOH in aerosol form into an atmosphere with controlled humidity.
  - Important Physics:
    - Hygroscopic effects under differing humidity conditions and the impact on aerosol masses available for release

- Bethsy-6.9c (ISP-38)
  - General Description:
    - The purpose of the Bethsy test was to study the accident transient following the loss of the RHR during mid-loop operation with the primary circuit open at the pressurizer and steam generator outlet plenum manways. The Bethsy facility is a three-loop PWR core and primary circuit, with the elevations scaled 1:1 and the volume scaled to 1:100.
  - Important Physics:
    - Entrainment and retention of water in the pressurizer caused by steam flow through the pressurizer manway
    - Low pressure pool boiling

- Level swell in the upper head
- Expulsion of water through the steam generator manway
- Level of pressurization
- Reflooding of the core from the gravity and forced emergency core cooling water injection

- CORA-13 (ISP-31) [61]
  - General Description:
    - CORA-13 permitted analysis of the heat-up and meltdown phases of a PWR type fuel element in the CORA test facility. The CORA facility consists of a fuel rod bundle with heated and unheated rods under controlled thermal-hydraulic boundary conditions with a steam supply to provide superheated steam and a quench capability.
  - Important Physics:
    - Oxidation/hydrogen generation, fragmentation of rods, relocation of core materials, formation of blockages, forced convection, conduction, radiation, and fluid-structure heat transfer
  - Results and Findings:
    - MELCOR was unable to predict significant hydrogen production during the quench phase. MELCOR does not have any models to simulate quench-induced fracturing of the otherwise protective oxide layer on the cladding surface. Some experiments in the QUENCH facility suggest that such fracturing can result in high transient oxidation rates owing to the exposure of fresh metallic Zircaloy following cool-down fracturing of the oxide layer.

- CSE-A9 [33]
  - General Description:
    - Eight experiments have been performed in the CSE containment vessel to evaluate the performance of aqueous sprays as a means of decontaminating containment atmospheres.
  - Important Physics:
    - Cesium and uranium aerosol and iodine vapor washout by sprays. aerosol depletion by gravity, thermal-hydraulic response to containment sprays
  - Results and Findings:
    - MELCOR does an adequate job of predicting the thermal/hydraulic response to the spray injection with differences explained by the fundamental assumptions of fully mixed spray and that the droplets fall through a volume atmosphere at rest. This leads to a slight overestimation of steam condensation.

- CVTR: Test 3, 4, and 5 [34]
  - General Description:
    - Design basis simulation of a postulated main steam-line break (MSLB) inside a large dry PWR containment was performed. The Carolinas-Virginia Tube Reactor (CVTR) facility is a decommissioned reactor containment building.
  - Important Physics:
    - Multi-component gas compression/expansion, thermal/hydraulic response to containment sprays, atmosphere cooling by fan cooler, jet-plume gas

interaction, buoyancy/stratification, 1-D heat transfer to HS, free convection, forced convection

- DEMONA: B3
  - General Description:
    - Investigation of the transport and deposition behavior of aerosols in the containment was performed. The test was performed in the Battelle model containment (total volume 640 m^3) using an open (quasi one-room) geometry and condensation aerosols from a plasma torch generator.
  - Important Physics:
    - Effects of steam condensation on aerosol settling

- DF: DF4 [35]
  - General Description:
    - The purpose of the Damaged Fuel, or DF, series of experiments was to investigate core melt progression. This experiment investigated the behavior of BWR-type fuel materials and configurations in a high-temperature oxidizing environment typical of the conditions during a LOCA.
  - Important Physics:
    - Eutectic interaction between the control poison material (B_4C) and the stainless steel control blade sheath and tubes, and the oxidation of Zircaloy in the cladding and canister

- FALCON: 1 & 2 (ISP 34)
  - General Description:
    - Heating of a bundle of six fuel specimens and six absorber specimens in steam-helium environment containing boric acid was performed. The ISP provided information concerning deposition along a controlled thermal gradient tube and containment structure.
  - Important Physics:
    - Physical and chemical behavior of fission products under simulated severe accident conditions and multi-component aerosol effects, vapor-aerosol interactions, thermophoretic deposition

- FLECHT-SEASET (Natural Circulation) [42]
  - General Description:
    - The facility design is scaled to a typical Westinghouse PWR on a 1:307 volume basis, with prototypic full lengths and full heights. The loop piping consists of two flow paths representing the unbroken, or intact, three loops and the broken loop of a 4-loop PWR. However, for the natural circulation tests the broken loop is not connected to a containment tank, simulating a break, but is connected to the downcomer extension to provide a normal, uninterrupted, flow path from the upper plenum through the steam generator, the loop pump seal and the cold leg to the downcomer.
  - Important Physics:
    - Pool boiling in core, natural circulation, steam condensation and reflux

- FPT1 (ISP 46)
  - General Description:

- The FPT-1 system consisted of an in-pile fuel bundle assembly and upper plenum region, an external circuit including a steam generator U-tube and connecting lines, and a containment section. The objective of the fuel bundle assembly was to assess fuel degradation and fission product release from a degraded fuel assembly. In the circuit, the objective was to determine fission product transport and deposition in steam generator tubes.
    - Important Physics:
        - Thermal modeling was assessed from thermocouple responses and temperature profiles
        - Oxidation (thermocouple responses and measurements of hydrogen generation)
        - Material relocation (thermocouple and radiography and transmission tomography for the end state)
        - Fission product release, transport, and deposition (Emission tomography of the fuel bundle and steam generator as well as measurements of activity along the external line to the containment)
    - Results and Findings:
        - Fuel and clad temperatures very close
        - Hydrogen generation rate close
        - Fission product release timing and amount close (Xe, I, Cs)
            - Modified CORSOR-Booth model
        - Fission product deposition in hot leg also close (new Ag-In-Cd control rod poison release model)

- GE Mark III Suppression pool
    - General Description:
        - Purpose of test was to obtain validation data for Mark III suppression pool vents during DBA.
    - Important Physics:
        - Vent clearing times, pressures in drywell/wetwell, LOCA DBA conditions

- GE Level Swell [36]
    - General Description:
        - A number of blowdown tests were conducted, some with blowdown occurring near the top of the vessel (vapor blowdown) and others with blowdown occurring near the bottom of the vessel (liquid, two-phase, vapor transient). These experiments were conducted in the "large blowdown vessel" (4.5 m^3).
    - Important Physics:
        - Vessel blowdown, level swell, critical flow
    - Results and Findings:
        - Level swell is better predicted by a single control volume than from a finely subdivided stacked volume
        - Blowdown flow and vessel depressurization are strongly dependent on the break discharge coefficient used
        - Discrepancies in top blowdown calculations due to maximum allowed pool bubble fraction, C4407(11)

- SNL/IET: IET-1, 3, 6 [37]
    - General Description:

- Series of experiments performed at the Surtsey test facility at Sandia (1:10 linear scale) and in the corium-water thermal interactions (CWTI) test facility at ANL (1:40 linear scale), to evaluate the effects of high pressure melt ejection (HPME) on DCH.
  - o Important Physics:
    - High pressure melt ejection, DCH, oxidation and hydrogen generation, hydrogen combustion

- RTF (ISP41) [61]
  - o General Description:
    - Objective was to develop data on the behavior of iodine in reactor containment pools. The experiment consisted of a pool in a stainless steel vessel with a radioisotope dose source and aqueous iodine provided by adding CsI to the pool. The pool pH was controlled during the experiment by adding acid and base chemicals to the pool.
  - o Important Physics:
    - Speciation of iodine in the aqueous and gaseous phases, effect of radiation on H_2O_2 and H_2 concentrations, adsorption/desorption of iodine on surfaces

- Quench-6 (ISP45)
  - o General Description:
    - The objective of the Quench-6 test was to assess the capability of severe accident codes to simulate delayed reflood situations in which a pre-oxidized LWR fuel rod bundle is quenched by water inserted from the bottom.
  - o Important Physics:
    - Oxidation of metallics, bottom reflood cooling

- JAERI Spray Tests: PHS-1, 6
  - o General Description:
    - Pressure suppression spray tests were conducted in Japan during the late 1970s in a 700 m^3 steel vessel (20 m high, 7 m in diameter). PHS-6 was a single nozzle test where PHS-1 was a 6 nozzle test. Vessel walls are hot so that droplets contacting walls are vaporized, degrading spray effectiveness.
  - o Important Physics:
    - Containment pressure reduction by sprays
  - o Results and Findings:
    - Comparison of single cell and multi-cell models confirm appropriate treatment of spray droplets falling through stacked volumes.
    - Calculation sensitive to assumed spray/vessel contact.

- LACE Turbulent Deposition: LA1 & LA3
  - o General Description:
    - The LACE LA1 and LA3 tests experimentally examined the transport and retention of aerosols typical of LWRs through pipes with high speed flow and in containment volumes during rapid depressurization. Specific objectives of these tests were to provide validation data that would expose important dependencies in modeling deposition. The effects of gas velocity, aerosol composition and aerosol size were considered.

- o   Important Physics:
    - ▪   Turbulent deposition of aerosols in pipes and deposition of aerosols in pipe bends

- •   LACE: LA4 [61]
    - o   General Description:
        - ▪   The purpose of the experiment was to determine the disposition of aerosols in the containment building under conditions of high steam concentrations. Of particular interest was the difference in aerosol disposition between hygroscopic (water-soluble) aerosols such as CsOH and nonhygroscopic aerosols such as MnO in a high steam concentration.
    - o   Important Physics:
        - ▪   Hygroscopic effects, deposition of aerosols on surfaces, heat transfer to surfaces, steam condensation on surfaces
    - o   Results and Findings:
        - ▪   Calculates pressures very well but slightly over predicts pool temperature
        - ▪   Aerosol removal of hygroscopic CsOH well calculated until late in test
        - ▪   Prior to venting aerosol removal of non-hygroscopic MnO well-predicted, however after, MELCOR under predicts aerosol removal
        - ▪   Early in the calculation, the dynamic film tracking overestimates film drainage from heat structures. The quasi-steady thickness provides a better calculation of pool mass.

- •   LOFT: LP-FP-2
    - o   General Description:
        - ▪   Experiment LP-FP-2 models the V-sequence accident, defined as a rupture in a low pressure injection system line outside the containment with simultaneous failure to isolate the system. The experimental subsystems include the reactor vessel, the intact loop, the broken loop, the blowdown suppression tank system, and the emergency core cooling system.
    - o   Important Physics:
        - ▪   Heat conduction/convection (temperatures and pressures measured), hydrogen generation (hydrogen mass measured), fission product release, flow blockage in degraded core, break flow, choked flow

- •   MARVIKEN: ATT-4 [40]
    - o   General Description:
        - ▪   Test ATT-4 studied fission product transport in the presence of a structural aerosol simulant; in addition to the fissium aerosol, a "corium" aerosol was produced that was composed of Ag and Mn. Corium vapors were mixed with vaporized fissium and steam in the lowest portion of the reactor vessel to form aerosols which were transported through the simulated large-scale primary piping.
    - o   Important Physics:
        - ▪   Thermal hydraulics of a PWR, aerosol and vapor transport and deposition

- •   MARVIKEN Blowdown Tests: CFT-21 & JIT-11
    - o   General Description:

- Large scale tests intended to provide data for analysis of critical flow from vessel blowdown were performed at the Marviken facility. The CFT-221 test was designed for validation of subcooled and two-phase flow through a discharge nozzle whereas JIT-11 tested a saturated steam flow.
  - o Important Physics:
    - Vessel blowdown, critical flow of vapor, subcooled liquid, and two-phase flow
  - o Results and Findings:
    - Vapor critical flow well calculated by MELCOR (sonic flux as minimum section)
    - Subcooled liquid critical flow well calculated by Henry-Fauske critical flow model
    - Moody model predicts a larger flow rate than observed for two-phase flow

- NEPTUN: 5006 & 5007
  - o General Description:
    - The NEPTUN experiments were designed to measure the rate of boil-off and additionally, the heat-up of fuel rods during two-phase uncovery of the core in a severe accident.
  - o Important Physics:
    - Boil off, fuel rod heat-up, level swell
  - o Results and Findings:
    - Level swell calculated for stacked control volumes highly dependent on nodalization (see also General Electric (GE) Level Swell)

- NTS Burn: NTSP01, NTSP12, NTSP15, NTSP20
  - o General Description:
    - Premixed hydrogen combustion experiments with hydrogen concentrations ranging from 5 to 13% (by volume) and steam concentrations from 4 to 30% were performed.
  - o Important Physics:
    - Combustion burn completeness, burn time, vessel pressurization
  - o Results and Findings:
    - MELCOR slightly over predicts the burn completeness for oxygen limited tests, likely because it is assumed a homogeneous mixture in a single control volume. Consequently, MELCOR predicts slightly higher peak pressures and temperatures, for these cases.
    - Because MELCOR is a lumped parameter code, it does not predict burn times and flame propagation well

- NUPEC: M-8-1, M-8-2 [61]
  - o General Description:
    - The tests explored the response of a 1:4 scale containment to steam injection and containment spray actuation (M-8-2) with helium as a surrogate for hydrogen gas.
  - o Important Physics:
    - Pressure response, temperature distribution and stratification, and hydrogen mixing
  - o Results and Findings:
    - Without sprays, MELCOR calculation predicted higher pressures (10%) and temperatures in dome

- Tracked helium concentrations in the dome and upper compartments well
- In lower compartments, calculation predicted decreased mixing after 15 minutes where data showed strong mixing throughout test

- PBF SFD: 1-4
  - General Description:
    - The Severe Fuel Damage (SFD) tests were performed at the Power Burst Facility (PBF) to investigate fuel rod and core response as well as the release of fission products and hydrogen generation during degraded core accidents.
  - Important Physics:
    - Fission product release
    - Oxidation and hydrogen generation

- PHEBUS: B9+ (ISP 28) [61]
  - General Description:
    - The B9+ test was designed to provide data principally on fuel degradation. It consists of a driver reactor core to provide neutronic heating to the test bundle, a fluid supply system to inject steam and helium into the test bundle, and associated cooling systems for the bundle and driver core.
  - Important Physics:
    - Heat conduction/convection (temperatures measured), hydrogen generation (hydrogen mass measured), and fuel degradation (no direct measurement)
  - Results and Findings:
    - Excellent agreement with thermocouple data
    - Excellent agreement with hydrogen generation
    - Improvements with MELCOR Versions 1.8.6 and 2.1

- PNL Ice Condenser: 11-6 & 16-11 [41]
  - General Description:
    - A series of large-scale experiments conducted at the High Bay Test Facility at Pacific Northwest Laboratory (PNL) to investigate the extent to which an ice condenser may capture and retain air-borne particles. In Experiment 11-6, the low flow rate induced a natural circulation flow between the diffuser outlet and the ice condenser. Experiment 16-11 was performed with every compartment full of ice and was a high flow test with no recirculation.
  - Important Physics:
    - Aerosol deposition, heat transfer in ice condenser containment, natural circulation, ice phase transition
  - Results and Findings:
    - MELCOR captured well, the thermal response of the experiment
      - The HS characteristic length should reflect the physical diameter of a typical ice cube in the condenser.
      - HS heat transfer coefficient is design specific
      - Because the model is not a moving boundary model, it is recommended that only 2 nodes are modeled
      - Model must be nodalized to capture natural convection

- TEMPL should be set to 274 K (rather than 273.15 K) to avoid numerical problems with CVH when temperatures are near freezing
  - MELCOR adequately captured the limited data for aerosol retention
    - Aerosol retention calculated is extremely sensitive to particle density

- STORM: SR-11 (ISP 40)
  - General Description:
    - The Simplified Test of Resuspension Mechanisms (STORM) test SR-11, was intended for examining aerosol deposition and resuspension in pipes and included two distinct phases: (1) the aerosol deposition by thermophoresis and eddy impaction, and (2) aerosol resuspension under a stepwise increasing gas flow. MELCOR does not have a resuspension model and the second phase was not modeled.
  - Important Physics:
    - Aerosol deposition from thermophoresis and eddy impaction as well as resuspension (not modeled in MELCOR)

- SURC: SURC-1 & SURC-2
  - General Description:
    - The Sustained Urania-Concrete (SURC) experiments were designed to measure and assess releases due to interactions between core materials and concrete in containment structures.
  - Important Physics:
    - Ablation of concrete, release of reactant gases, temperature response
  - Results and Findings:
    - Reasonable prediction of concrete ablation front

- MCCI: CCI-1 & CCI-2
  - General Description:
    - The CCI Phase 1 experiments were designed to measure concrete ablation with different types of concrete.
  - Important Physics:
    - Ablation of concrete, release of reactant gases, temperature response
  - Results and Findings:
    - Reasonable prediction of concrete ablation front

- TMI-2
  - General Description:
    - Though not an experiment, the TMI-2 accident serves as an excellent resource for code validation.
  - Important Physics:
    - The accident conditions stress the capabilities of the code for predicting core degradation, formation of a debris bed in the upper core, formation of a molten pool in the core, relocation of molten corium to the lower plenum, the response of the lower head, and reflood and quench of the degraded core.

- VANAM: M3 (ISP 37) [61]
  - General Description:

- The objectives of the VANAM-M3 test was to provide data on containment-building response to severe accident conditions with particular emphasis on characterizing the depletion rate of hygroscopic aerosol under varying humidity and thermal-hydraulic conditions.
  - Important Physics:
    - Multi-compartment geometry, stratified atmosphere, atmosphere mixing by forced convection loops, thermal energy balance, structural heat transfer, steam condensation effects, and aerosol behavior
  - Results and Findings:
    - Calculated room temperatures indicated code's ability to correctly capture the forced and natural circulation patterns that occur at different times in the test
    - Calculated pressure behavior demonstrated the ability of the code to calculate the response of a multi-room building to sources and sinks of steam and air
    - Aerosol depletion results demonstrated adequacy of aerosol growth modeling, aerosol transport, and depletion from gravitational settling

Appendix D   MELCOR Code Version Progression Overview

The discussion regarding the validation history for MELCOR was focused solely on the experimental comparisons between various MELCOR versions as well as side-by-side comparison between MELCOR versions to demonstrate evolution in models or consistency during the MELCOR development. As development progressed, MELCOR has received various updates which were not presented directly alongside with the validation discussion. This Appendix presents a summary of the major modification made to MELCOR for the major version milestones since MELCOR Version 1.8.2.

MELCOR 1.8.3
- CORCON-MOD3 (including VANESA) was added to MELCOR to replace the separate CORCON-MOD2 and VANESA models.

MELCOR 1.8.4
- Previous versions of MELCOR were known to predict too-early collapse of reactor cores. A model for retention of molten metals behind oxide shells (particularly, molten Zircaloy on fuel rods), with ultimate failure by another mechanism was added to correct that behavior.

- A creep rupture model was added for the lower head, together with the capability to model external cooling of the lower head in a flooded cavity.

- A "flow blockage" model was added to account for redistribution of flow through a reactor core as a result of changed flow resistance when intact geometry is lost and a debris bed or pool forms.

- A capability was added to calculate radiative heat transfer between pairs of heat structure surfaces.

- Models were added for the behavior of hygroscopic aerosols and for the chemisorption of Cs onto the surfaces of heat structures.

- The SPARC 90 pool decontamination model replaced a previous "preliminary" version of SPARC (SPARC 87). In addition to other improvements, the new model includes removal of iodine vapor.

MELCOR 1.8.5
- A diffusion flame model was added to calculate the combustion of hydrogen flowing through flow paths during direct containment heating.

- Previous versions of MELCOR required the use of a single component (called "Other Structure", OS) to represent all support structures, control structures, and miscellaneous structures in the core in addition to fuel rods and BWR canisters. This approach had serious deficiencies, and none of the structures could be realistically represented. New components referred to as "Supporting Structure" (SS) and "Non-supporting Structure" (NS) were introduced. Both parametric and mechanistic, load-based, failure models were added for SS, which can support other core components. NS is subject to simpler failure models, but these have sufficient flexibility to represent BWR control blades, PWR control rods, and structures such as filler rods in experiments.

- Optional models were added for convective heat transfer to water pools from the top and bottom surfaces of SS plates, and for radiative heat transfer between the bottom of such a plate and the water pool or lower head below it.

- Previous versions of MELCOR did not properly differentiate between debris in the channel and debris in the bypass of a BWR. This was resolved by introduction of a "Particulate debris in the Bypass" (PB) component. After failure of the fuel canisters in a BWR that separate PD from PB, the two debris fields were allowed to mix and equilibrate. A debris exclusion model (with flexible user control) was implemented to control the relocation of particulate debris (PD and/or PB) based on the presence or absence of intact structures that could prevent it (for example, solid debris cannot, as a general rule, enter the small spaces between fuel rods.)

- The flow blockage model was much improved as a result of the ability to distinguish particulate debris in the channel of a BWR from that in the bypass, and a model was added to allow the opening of a flow path on failure of a channel box (canister).

- Improvements were made to the implementation of candling and debris slumping models and to those for conductive, radiative, and candling heat transfer.

- Cesium iodide was added as a default class.

- Substantial improvements were made in the model for hygroscopic aerosols.

- A model for the chemical behavior of iodine in water pools was added to MELCOR. It includes models for pH, including transport of nitric and hydrochloric acid formed by radiolysis off air and plastic in cables, respectively. The effects of different surface coatings on containment structures are also modeled.

MELCOR 1.8.6
- Flexibility was added to allow the user to enhance quenching of ejected debris through conductivity multipliers.

- New LM-CREEP and PIPE-STR CF types were added to make it far less difficult for users to model pipe ruptures.

- Modeling of the lower plenum and head was heavily revised. The curvature of the head and its effect on lower plenum volumes can now be consistently modeled (this was not possible in previous versions). The head can take the form of a cylinder, hemisphere, or hemispherical segment. Heat transfer and failure models were improved. Because the new model contains all of the capabilities of the separate BH package, this package was eliminated.

- Models were added for formation of stratified molten debris pools, both in the core and in the lower plenum. These include circulation-driven convective heat transfer in the case of coherent pools.

- A core periphery model was introduced for PWRs to allow proper modeling of the core baffle (shroud) and core formers, and the bypass region between the baffle and the core support barrel. Such modeling was impossible in previous versions of MELCOR.

- A model was added for quenching of core structures by reflood of water from below. A model was also added to evaluate oxidation of the submerged but unquenched surfaces that could be predicted by this model.

- More realistic models were added for behavior of control poison in a PWR. One involves oxidation of B4C control poison, the other models release of AgInCd control poison, including formation of aerosols.

- The local fluid temperature model (also known as "dT/dz" was improved to reduce problems with small stagnant volumes that had forced falsification of geometry in some previous input decks.

- Treatment of support structures modeling columns was modified to allow better representation of the support in a typical PWR. The package now allows user-defined "flavors" of support structures, allowing further flexibility.

- A model was added to calculate breakaway oxidation of Zircaloy in air.

- The default modeling of collapse of BWR canisters was modified; previous code versions predicted survival to unreasonably high temperatures.

- The previous approach to specification of the inner and outer areas of BWR canisters did not always allow a correct representation; these areas may now be directly input.

- Current best practices for modeling reactor cores involve reducing the melt temperatures used for ZrO2, UO2, and B4C from handbook values to account for the fact that they do not typically appear as pure materials. Redefinition of all the tables and other MP input is tedious and time consuming, particularly if one is interested in the effects of changes in these reductions. So-called "interacting materials", ZRO2-INT, UO2-INT, and B4C-INT were added to the MP package. Their properties differ from those of the pure materials only in the melt temperatures. Initialization in MELGEN uses the modified melt temperature to generate complete and consistent properties tables from those of the pure materials; the melt temperature of any of these materials can be modified from its default value with a single input record.

- Creep data have been added to the MP package.

- The user can now specify (via Control Functions) the failure criteria for COR components and add arbitrary heat sources in and heat transfer paths between them.

- A new fuel collapse model was added to allow a user to supply a time at temperature lifetime failure table to determine rod collapse. Fuel collapse was previously specified by a failure temperature.

- The user has more control over the flow resistance calculated from the Ergun equation in the flow blockage model to account for phenomena such as fuel swelling.

- New sensitivity coefficients are available to modify the surface emissivities used in the radiation model.

- A new, optional model was added to treat flashing of superheated water entering a volume, either through a flow path or from a volume source. It improves the partition of mass and enthalpy of the water between the volume pool and atmosphere, and includes the formation of water aerosols.

- Previous versions of MELCOR could exhibit unphysical behavior if the volume of either hydrodynamic field (pool or atmosphere) in a volume became very small or was absent. A new thermodynamic model has been added to better model these situations.

- Heat structure surfaces may be partially covered by a water pool. In previous code versions, a rising pool surface acted as a "squeegee", increasing the film thickness by maintaining its total mass rather than subsuming the covered portion of the film. This was corrected in MELCOR 1.8.6.

- Mechanistic models are used for draining of thick films from surfaces that are involved in a "film tracking network", but previous versions of MELCOR used a simple maximum film thickness to remove water from too-thick films on other surfaces. The mechanistic treatment is now used universally, replacing the maximum limit on isolated structure surfaces. In effect, an isolated structure surface is treated as if it form a film tracking network of length one.

- A new version of the CORSOR Booth release model corrects an obvious error in the previous implementation based on published material from Battelle Columbus.

- The algorithm previously used to interpolate aerosol agglomeration and deposition kernels could lead to significant errors if a calculation spanned a wide range of temperatures and/or pressures. A much-improved interpolation algorithm has been implemented.

- The aerosol filter model was extended to allow specification of decontamination factor by particle size as well as by class. Each decontamination factor may now be defined by either a constant or a control function.

- A model was added to calculate deposition of water from a jet impacting on the surface of a heat structure.

- New turbulent deposition models were added along with bend impaction model.

2. TITLE AND SUBTITLE	3. DATE REPORT PUBLISHED	
MELCOR Best Practices as Applied in the State-of-the-Art Reactor Consequence Analyses (SOARCA) Project	MONTH August	YEAR 2014
	4. FIN OR GRANT NUMBER	

5. AUTHOR(S)	6. TYPE OF REPORT
Kyle Ross, Jesse Phillips, Randall O. Gauntt, Kenneth C. Wagner	Technical
	7. PERIOD COVERED (Inclusive Dates)

8. PERFORMING ORGANIZATION - NAME AND ADDRESS (If NRC, provide Division, Office or Region, U. S. Nuclear Regulatory Commission, and mailing address; if contractor, provide name and mailing address.)

Sandia National Laboratories
Albuquerque, New Mexico 87185
Operated for the U.S. Department of Energy

9. SPONSORING ORGANIZATION - NAME AND ADDRESS (If NRC, type "Same as above", if contractor, provide NRC Division, Office or Region, U. S. Nuclear Regulatory Commission, and mailing address.)
Division of System Analysis
Office of Nuclear Regulatory Research
Washington, DC 20555-0001

10. SUPPLEMENTARY NOTES

11. ABSTRACT (200 words or less)
The modeling approach used in the State-of-the-Art Reactor Consequence Analyses (SOARCA) project to characterize the release of radionuclides to the environment accompanying a postulated severe (core damage) accident is based on plant-specific applications of the MELCOR computer code. This document describes the specific manner in which MELCOR modeling capabilities were used to represent important, and in some cases uncertain, aspects of severe accident behavior in the SOARCA project. This description includes choices made among alternate modeling options offered through code input, changes to selected input parameters from those offered as 'default' values, and in some cases, user-generated 'models' to represent features of plant response to a severe accident that are not directly available in MELCOR. Collectively, these features represent the "SOARCA best practice" guidance for using MELCOR to calculate severe accident behavior in operating nuclear power plants.

12. KEY WORDS/DESCRIPTORS (List words or phrases that will assist researchers in locating the report.)	13. AVAILABILITY STATEMENT
SOARCA state-of-the-art reactor consequence analyses MELCOR Best Practices severe accident modeling	unlimited
	14. SECURITY CLASSIFICATION
	(This Page) unclassified
	(This Report) unclassified
	15. NUMBER OF PAGES
	16. PRICE

Printed
on recycled
paper

Federal Recycling Program

NUREG/CR-7008

MELCOR Best Practices as Applied in the State-of-the-Art Reactor Consequence Analyses (SOARCA) Project

August 2014